

University of Central Florida

College of Optics and Photonics

College of Engineering and Computer Science

EEL 4915L – Senior Design II

Final Document

Instructors: *Dr. Lei Wei, Dr. Chung Yong Chan, Dr. Aravinda Kar*

Authors: *Tamara Nelson (PSE), Kara Semmen (PSE), Misael Salazar (CpE),
Jarolin Jimenez Vasquez (EE), Miguel Daboin (EE)*

(Team #3)

Project Mentor:

Dr. Stephen Eikenberry, CREOL's Astrophotonics Research Group

Review Committee:

Dr. Stephen Eikenberry, Dr. Mike Borowczak, Dr. Sonali Das, Dr. Stephen Kuebler

December 8th, 2023



Table of Contents

1. Executive Summary	1
2. Project Description	2
2.1. Motivation and Background	2
2.2. Goals and Objectives	3
2.2.1. Basic Goals	3
2.2.2. Advance Goals	3
2.2.3. Stretch Goals	3
2.2.4. Objectives	3
2.3. Prior Related Work	4
2.4. Engineering Specifications	6
2.5. Diagrams	6
2.5.1. Overall Diagram	7
2.5.2. Software Flowchart	9
2.5.3. Optics System Flowchart	10
2.5.4. Optics System Schematic	11
2.5.5. Previous Hardware Block Diagram (SD1)	12
2.5.6. Hardware Block Diagram (SD2)	13
2.6. House of Quality	14
3. Research	16
3.1. Technology Comparison and Selection	16
3.1.1. Frequency Comb	16
3.1.2. Hollow Cathode Lamp	19
3.1.3. Tunable FPI	20
3.1.4. Multichannel Spectrograph	21
3.1.5. Solar Tracking System	22
3.1.6. Software technology	25
3.2. Part Comparison and Selection	29
3.2.1. Optical System	29
3.2.1.1. Dispersive Element	29
3.2.1.2. Gratings	33
3.2.1.3. Lenses	36
3.2.1.4. Detector	38
3.2.1.5. Optical Fiber	38
3.2.1.6. Mirrors	41
3.2.1.7. Broadband Sources	44
3.2.2. Hardware System	48
3.2.2.1. Power Supply	48
3.2.2.2. Weather Station	52
3.2.2.3. MCU	55
3.2.2.4. DC Motors	60
3.2.2.4.1. Stepper Motors	60

3.2.2.4.2. Weather Protection Motor	62
4. Standards and Design Constraints	69
4.1. Optical Standards	70
4.2. USB Standard	76
4.3. Manufacturability Constraint	79
4.3.1. Deadline	79
4.3.2. Dimensions	80
4.3.3. Accuracy	80
4.3.4. Fabry-Perot Etalon Precision	80
4.4. Maintenance and Reliability Constraint	81
4.4.1. Solar Tracker System	81
4.5. Sustainability Constraint	82
4.6. Social Constraint	83
4.7. Risk	83
5. Comparison of ChatGPT with Similar Platforms	85
5.1. Definition and Introduction	85
5.2. Questions and answers comparison	86
5.3. Software (model types) comparison and limitations	87
6. Optical Design	90
6.1. Spectrograph Design	90
6.2. Fabry-Perot Etalon Design	101
7. Hardware Design	106
7.1. Initial Design and Related Diagrams	106
7.2. External Power Supply AC/DC	108
7.3. DC/DC Converters	109
7.4. Power Supply PCB Designs	109
7.5. DC Motor / Driver	114
7.5.1. Weather Protection System Motor	115
7.6. iOptrom CEM70 Mount	115
7.7. Weather Station	116
7.8. Light Sensors PCB Design (Layer-1)	118
7.9. SolarMEMS Sensor (Layer-2)	121
7.10. Camera	123
7.11. Weather Protection Box	123
7.12. Main-Components Platform	124
8. Software Design	125
8.1. Software Design Principles and Patterns	125
8.2. System's Software	128
8.3. Motor Software	130
8.4. Weather Station and Camera	131
8.5. Rain Prediction	132
8.6. USB Communications	134
8.7. Software Control Flow	135

9. System Fabrication/Prototype Construction	137
9.1. Optical Fabrication and Prototype Construction	137
9.1.1. Spectrometer Fabrication and Prototype Construction	137
9.1.2. Fabry Perot Etalon	137
10. System Testing	139
10.1. Optical Testing	139
10.1.1. Spectrograph Testing	139
10.1.2. Fabry-Perot Etalon Testing	141
10.2. Hardware Testing	143
10.2.1. Electrical Parts for PCB	143
10.2.2. Power Supply PCB v3 Load	144
10.2.3. Wind Speed Sensor	144
10.2.4. Rain Sensor	144
10.2.5. Linear Actuator DC Motor	145
10.2.6. Light Sensors PCB v2	145
10.3. Software Testing	145
10.3.1. Unit Testing	146
10.3.2. Integration Testing	147
10.3.3. System Testing	148
10.3.4. Test-Driven Development	149
11. Administrative Content	150
11.1. Budget estimate	150
11.2. Bill of Materials	150
11.3. Milestones	152
11.4. Work Distribution	154
12. Conclusion	155
Appendix A – reference	157

1.0 Executive Summary

Throughout the course of time the fascination and interest for the studies of out of space has grown tremendously. It started even before the Apollo 11 mission, under commander Neil Armstrong on July 16, 1969. A great example of this fact is when in 1959, the Soviet Union sent their spacecraft to the moon. Now to go even earlier in life, in the late 1609 Galileo Galilei was studying the moon and he discover that the Moon had mountains and valleys, just like we have here on earth. Many aircraft since then have been sent out of space for further investigation, exploration, and research. We all these facts in consideration, it is ok to say that the studies of out of space seem important and relevant for quite some time now.

The moon is just one of the stars that we humans have studied. Lots of studies have been done for the star that gives us light during the day and natural vitamin C with just been exposed to it. The sun was first studied during the 17th century after the invention of the telescope. And once again Galileo was the first one to start been curious about the sun and started studying it, around the same time he was studying the moon. As the survival instincts that humanity has always have, it has been in our best interest to study out of space just for the research of finding any living thing other than us, or resources that we could exploited. The millennials do not stay behind as far as the study of out of space goes. The Astrophotonics department at UCF has been doing research about the sun. They have asked us to be part of this research by asking us to create a prototype of a device that can track the sun. This device is to be used on top of the building roof of the Astrophotonics department. This device is a part of a bigger product that collects data of the sun's redshift that can be used to analyze the wobbling of the sun.

The Astrophotonics research group can study properties of the sun such as radial velocity and the spectrum's absorption lines. This can be achieved through the development of a single mode astronomical spectrograph to observe the spectrum from sunlight. Our group has two optics students, so one of us is working predominantly on this spectrometer. Our second optics student is utilizing the anticipated results of the spectrograph to design a broadband Fabry-Perot etalon to act as a calibration method for the spectrograph. This is a low-cost option to realistically achieve results in the timeline of senior design. Utilizing a separate continuum broadband source to illuminate the etalon produces a relatively stable spectrum that can act as a "ruler" or reference for the drift in the sunlight's spectrum. Our device needs to be autonomous, need to track the sun from sun rise to sundown. As it is tracking the sun, our device needs to be able to take images of the sun every 10 seconds so that does images get sent to a computer to the office of our sponsor for further analysis. The device should be able to move to a certain degree according to the seasons change. The up and down movement of it is significantly gradually smaller, while the side-to-side movement is more significant and that is the wobble movement that we need to be able to measure.

2.0 Project Description

In this section, we discuss the motivation that prompted our project, as well as important background information and current related work. Our goals for the single mode autonomous solar spectrometer, as well the objectives to reach them are listed as well, followed by a description of our requirements and specifications.

2.1 Motivation and Background

Throughout many millennia humankind has survived by assessing dangers and engineering new solutions. As ocean levels and the human population rise, the Earth's natural resources are slowly depleted, which poses real risks for our future generations. While many work tirelessly to ensure the survival of planet Earth through sustainable practices, others look to the stars, searching for other planets like our very own. These surveys of space have been an ongoing project for several international institutions, including NASA (National Aeronautics and Space Administration). A potentially habitable planet would need to have temperatures like Earth's, a habitable atmosphere containing carbon dioxide and oxygen in the system, the presence of water, and satisfy various other specific requirements. In the distant future, Earth-like planets may be the saving-grace for humanity, either as an alternative home, or as a treasure-trove of resources. One primary cause for humanity's negative impact on our own planet is the massive strain of 8 billion people on Earth's resources. We could potentially save the Earth by outsourcing many of these needs. If the damage is irreversible, an Earth-like planet could serve as the new home for humankind.

Exoplanets are those not in our solar system and which orbit their own star(s). Studying them is important to understanding how the Earth functions and to finding potentially habitable planets. A key step towards finding exoplanets is to study sun-like stars in the universe. But that begs the question, how do we find a star like our own? How do we even spot it with our telescopes? To study such stars, we must first be able to compare their characteristics with that of our own sun. A common method used to observe the sun is to measure its redshift. As a star moves away from us, the light emitted by the star becomes stretched out, resulting in light with a longer wavelength. Since the longest wavelengths our eyes can detect correspond to red, this effect causes the light to appear shifted closer to the red end of the spectrum, thus we get the name "redshift". Astronomers use this redshift to find the velocity of the star. Since the sun is made up of gas and plasma, it rotates at varying speeds across different regions: the equator takes approximately 24 days to make a full rotation, while the poles take about 30 days. As a planet rotates around its star, the star wobbles slightly around the center of gravity of the entire system. Due to the gravitational pull of our solar system's planets as they orbit, our sun also wobbles slightly. This results in a small amount of redshift. If we can measure the redshift (and therefore the velocity) of our own sun, then we can

look for the same redshift-signature in far-off stars. However, constant changes in the magnetic field cause sunspots that block redshift which results in less precise velocity measurements. To account for the unpredictable nature of the sun, our project was proposed by the Astro-photonics research group in CREOL to implement a method of continuously monitoring the sun. This is the goal of our system, to measure our own sun's redshift.

2.2 Goals and Objectives

For this section we touch base on the goals and objectives that we have for our project. As far as the goals are concerned, we will be setting some basic, advance and stretch goals for ourselves to see which of them we will be able to achieve.

2.2.1 Basic Goals

Our basic goals were to have two aligned telescopes on a platform with automated sun tracking and weather protection. One primary goal was for the system to be completely autonomous. This system must be connected to a spectrometer that outputs the spectrum of light from the sun. The spectrographs collected were to be calibrated using a broadband Fabry-Perot Etalon. The Fabry-Perot Etalon should have an implemented thermally stable design. Additionally, the system needed to have a solar imager that captures one of our advanced goals which is to be able to make the system run on solar energy instead of wired power source (AC power).

2.2.2 Advance Goals

One of our advanced goals was achieving higher precision and more accurate calibration of the Fabry-Perot Etalon. Another advanced goal was to implement cross-dispersion in the spectrometer. An additional advanced goal was buying all the weather and light sensors separately instead of a built-in weather station and develop a system to integrate/control each sensor. Our last advance goal was to be able to run the entire system in solar power instead of AC power, by creating a build in system that can store energy during the times the sun is out so that it can work continuously even if there is not sun providing power to the system.

2.2.3 Stretch Goals

The stretch goals for this project included a fiber connection from the second telescope to a second research laboratory for future use. A second stretch goal was to integrate our design into a pre-existing, full-scale observatory which is already equipped with single-mode technology for other purposes. Finally, a third stretch goal was to design a laser frequency comb to be used in place of the Fabry-Perot Etalon.

2.2.4 Objectives

One of our objectives was to have precise single mode fiber alignment from a single telescope into the spectrometer, which would output a spectrum with distinct function lines. This improves the system's resolution when compared with a

multimode fiber. The Fabry-Perot interferometer must be able to filter broadband light into a stable comb-line pattern. The pattern is fed through the spectrograph system, resulting in the comb-like pattern overlapping the spectrum resulting from the sun's input light. A comparison of the pattern with the spectrum will allow researchers to see any disturbances to the system in real time, and achieving our goal for system calibration. In order to achieve our stretch goal of improving the Fabry-Perot's stability, incorporated a thermostable design and implemented an insulated environment. We also explored the use of fiberglass triangular stands to minimize acoustic vibrations. The spectrograph and reference data are sent to an appropriate network, to be viewed in real time by the researchers. Another one of our objectives was to make the system autonomous, so that it can track the sun's movement consistently from sunrise to sundown. The final objective was for the system to have a weather-protection system, which consists of sensors monitoring weather conditions and motors to cover the optical system. These were to be connected to a computer system programmed to respond to various weather conditions, such as incoming rain and high winds.

2.3 Prior Related Work

There are observatories around the world that study the sun using multimode fiber spectrometry. Our system uses single mode fibers that will collect light from micro solar telescopes previously designed by the Astro-photonics research group. The single mode fiber causes more dispersion of the light from the fiber into the spectrograph. This results in a significant improvement of the system's resolution.

A previous study from 2010 titled, "The solar gravitation redshift from HARPS-LFC Moon Spectra: a test of the general theory of relativity" has the same end-goal as our project (i.e., to measure the redshift of our sun for use in locating other earth-like planets in the universe). The paper utilizes a similar approach to our own, with one major difference being that rather than measuring the light coming directly from the sun, this group collected their data using the sun's reflection off the moon (moonlight). While imaging the moon allows for less excess noise to fill the system, the amount of light measured is drastically decreased. When the detected signal is small, unwanted light in the surrounding environment can heavily skew the results. Because our system will be on the roof of a university campus building, it would be better for our system to image the sun. Additionally, this study employs a laser frequency comb (LFC) rather than a Fabry-Perot interferometer (FPI) to calibrate the device. Utilizing a frequency comb allows the system to measure with far better accuracy and precision. It is, however, a drastically more expensive system. This expense may have been necessary when measuring dim moonlight to minimize data-skew from external noise but is unnecessary for our purposes.

A system, titled the Spectrometer for Sky-Scanning Sun-Tracking Atmospheric Research (4STAR) was developed to measure the spectrum of the sun. This project was not created with the intent to measure the redshift of our sun, but to better understand the composition of gases that make up the sun. This system

utilizes two spectrometers, and a multimode fiber. As discussed previously, our system uses a single mode fiber to yield a higher resolution. While our system consists of an etalon and a spectrometer rather than two spectrometers, the etalon performs the same function as the first spectrometer in the 4STAR, acting as a calibration mechanism for the second spectrometer.

On the topic of an interferometer calibration system, there have been studies that test broadband Fabry-Perot etalons as an alternative to Hollow-cathode lamps and frequency combs (as previously mentioned). Hollow-cathode lamps (HCL) produce emission lines as atoms collide with the carrier gas, excite, and drop to the lowest energy level. For decades, this method has acted as a calibration standard, though it produces irregular line distribution and limited reference lines. Since Fabry-Perot etalons are an inexpensive and reliable alternative to frequency combs, HCLs have been used to increase the precision of broadband FPIs by cross checking the spectrums. This was proved through calibration of a HARPS Echelle spectrograph, in which the combined technique overcame distortion of 50 m/s (Bauer et al., 2015).

In addition to the prior research conducted on spectroscopy, we also found various products which offered similar functionality to what we are looking to accomplish. When searching through hobby astronomy forums, we discovered that there were online stores selling personal observatories. These observatories are much larger than what our project demands, typically being 8 feet in diameter and over 200 pounds. However, when looking at these products, we saw how their designs differ from each other and provided insight on the constraints that could impact our design. For example, all the observatories we looked at had a round dome, a feature intended to protect it from the environment. For our design, we designed a weather resistant observatory platform, so it might make sense to use a classic domed canopy. The online stores also offer insightful documentation for their observatories, and some even have open-source code available. Their schematics have also informed our understanding of the hardware and sensors we need to operate our own observatory.

From the solar tracking system perspective, prior research shows that an active tracking system would be the most recommended for this project. A previous article from 2019 titled, "Review of dual axis solar tracking and development of its functional model," (Mpodi et al., 2019) categorizes active tracking systems as Electro-optical based tracker, auxiliary bifacial solar cell, and chronological tracker. This article mentions the Electro-optical based tracker as the most popular one. We found that a chronological tracker could cause big error margins since it uses time and data to determine the position of the sun which means that the device must be adjusted accordingly to the specific location it is placed. Also, auxiliary bifacial solar cell requires a solar panel which would increase the dimensions of our proposed project. Hence, an Electro-optical based solar tracker could simplify our design and provide more accuracy when tracking the sun.

In another research study from 2018 titled, "Recent advancements and challenges in Solar Tracking Systems (STS): A review," (Nsengiyumva et al., 2018) from the

mechanical engineering point of view, they classify solar trackers as single-axis, dual-axis, and multiple-axis solar trackers. The research compares active and passive solar tracker systems and mentions that active solar tracker systems with dual-axis reach 60% more energy from the sun than single-axis ones. On the other hand, they conclude that a dual-axis solar tracker suffers from energy losses due to dual-motor operation, auxiliary units and moving joints.

2.4 Engineering Specifications

Our system incorporates different components and characteristics. We have categories that cover the hardware, software, and optical portion of the design. For our design to work and meet the expectations of the sponsor there are several engineering specifications that we needed to follow and try to meet. These specifications need to be in alignment with our objectives and final goals. Below we have a table that provides the specifications needed with the description and the measurements that the design meet.

For the software design we needed the system to detect the weather so that when severe weather or drastic changes of the weather occur, the sensor can get a reading to have the weather machine close so the system can be protected, if it hits IP66 the weather machine needs to close. We also needed to have our MCU program to tell the motors to move a certain angle every season change to keep accurate track of the sun. We also needed to have our software program to record information of the spectrum taken continuously, for at least every 10 seconds. Lastly it needed to be programmed so that the start-up time is approximately 1 minute.

For the hardware design we needed to focus on the size of the system. The dimensions of the design requested by the sponsor are approximately the size of a laptop, that we ended up deriving to be a 15x15x15 inches. It can be heavier than 30 lbs. Our goal is to have a power consumption of not more than 100 W. The motor step angle that will be mounted to our system platform needs to be at a 2.0-degree angle maximum.

For our optical design, we needed to meet the criteria for the spectrograph determined by a combination of customer requirements and calculations. This includes a resolving power of 100,000, with a resolution element of 6 GHz. To properly calibrate a spectrograph, the Fabry-Perot etalon has a mode spacing that is 3-5 times the spectrograph's resolution element and a linewidth that is one half to one tenth the resolution element. This results in the specifications tabulated for the etalon's FSR, linewidth, and finesse with a mirror reflectance of 99%. The resolution of the solar imager taking the pictures that are sent to the sponsor office needed to meet a 12 megapixel per resolution. The image frequency cannot exceed 10 seconds.

Description	Specifications
Spectrograph Resolving Power	100,000
Spectrograph Resolution Element	6e9 Hz
Etalon Linewidth	< 0.6 – 3 GHz
Mirror Reflectivity	98%
Free Spectral Range of Etalon	18 – 30 GHz
Finesse	> 100
Total Cost	< \$5000
Start-up Time – Door Opening	<1 minute
Weather Resistance	IP66 equivalent
Weather Model Accuracy	> 50%
Power Consumption	< 100W
Rain sensor door-closing response	<1 minute
Wind speed door-closing response	<1 minute
Camera Resolution	12 megapixels (MP)
Image Frequency	10 seconds
Dual-axis motors accuracy (step angle)	< 2.0°
Weather protection door closing	<40 seconds

Table 2.4.1 Engineering Specifications

2.5 Diagrams

This chapter contains a series of diagrams for various aspects of the system including the overall diagram, software flowchart, optical system flowchart, and hardware system block diagram.

2.5.1 Overall Diagram

Below is a diagram depicting the plan of the system. Here we highlight the work distribution of each of our group members. It depicts the overall system when connecting our hardware design, software design, and optical design. The hardware and software design consists of a weather protected platform with a solar tracking system. The weather protection system keeps all the core components and main electrical/hardware components safe from rain and extreme weather conditions. It has a servo motor that serves the closing door of the weather protection case using predictive logic and the data from the weather station. The solar tracking system autonomously tracks the sun using a dual-axis mount with stepper motors guided by a solar MEMS detector and light sensors. The platform houses two mini telescopes and a solar imager. The optical system includes a broadband Fabry-Perot etalon and a spectrometer. A single mode fiber connects one of the telescopes on the platform to the spectrometer. The output of the solar

imager and spectrometer are sent to the appropriate server for the Astrophotonics research group.

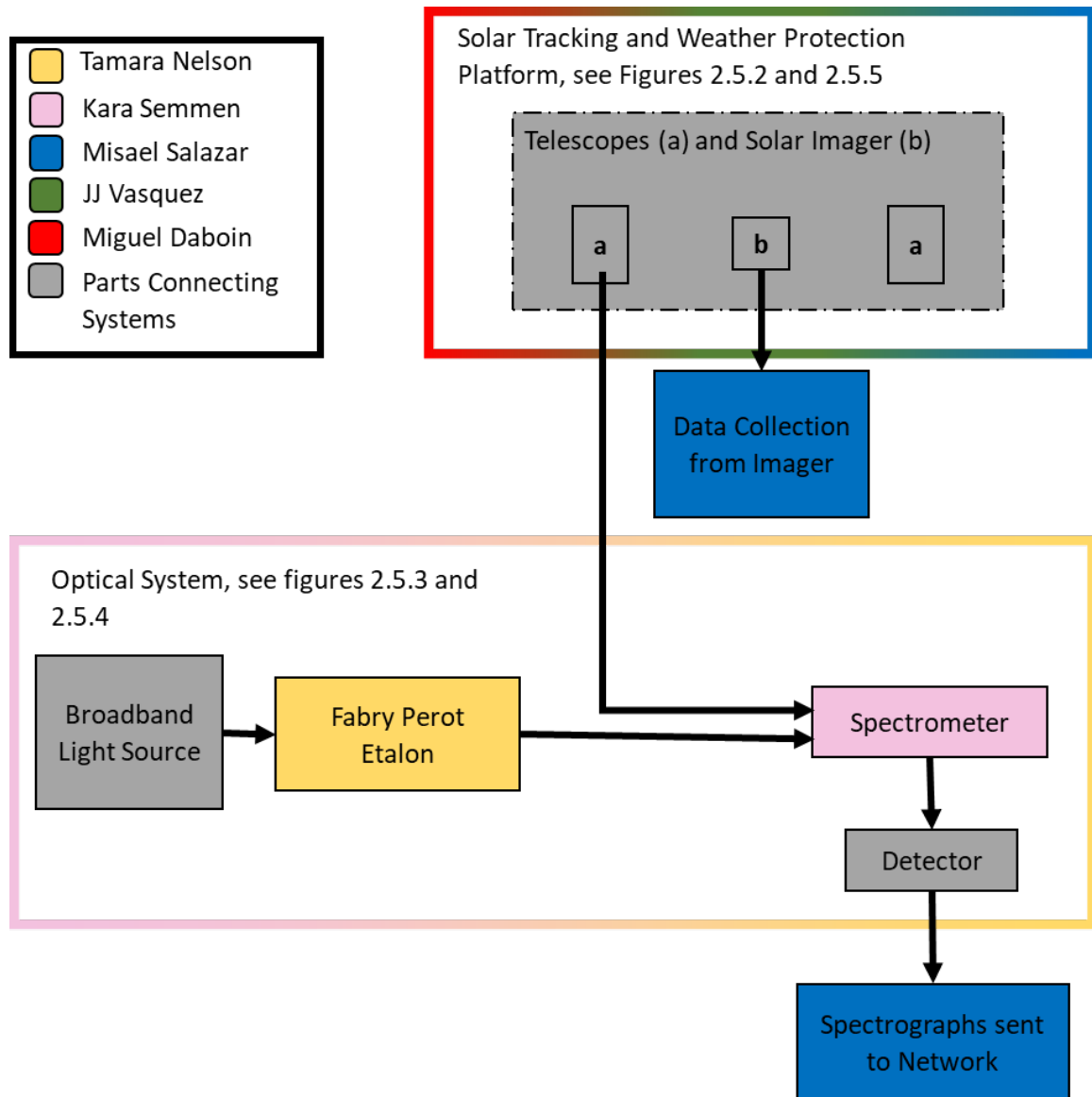


Figure 2.5.1 Overall block diagram of system

2.5.2 Software Flowchart

In this flowchart we are able to depict our design as far as the software components of the system go. It shows all of the program's processes that are going to be integrated in our software and the logic that it needs to follow. From the reading of the weather detection to the reading of the sensors depicting the rain or bad wind. Shows the reading of a clear day so that the observatory can open to detect the light and be able to read the sun redshift and take the desired data, as well as the pictures.

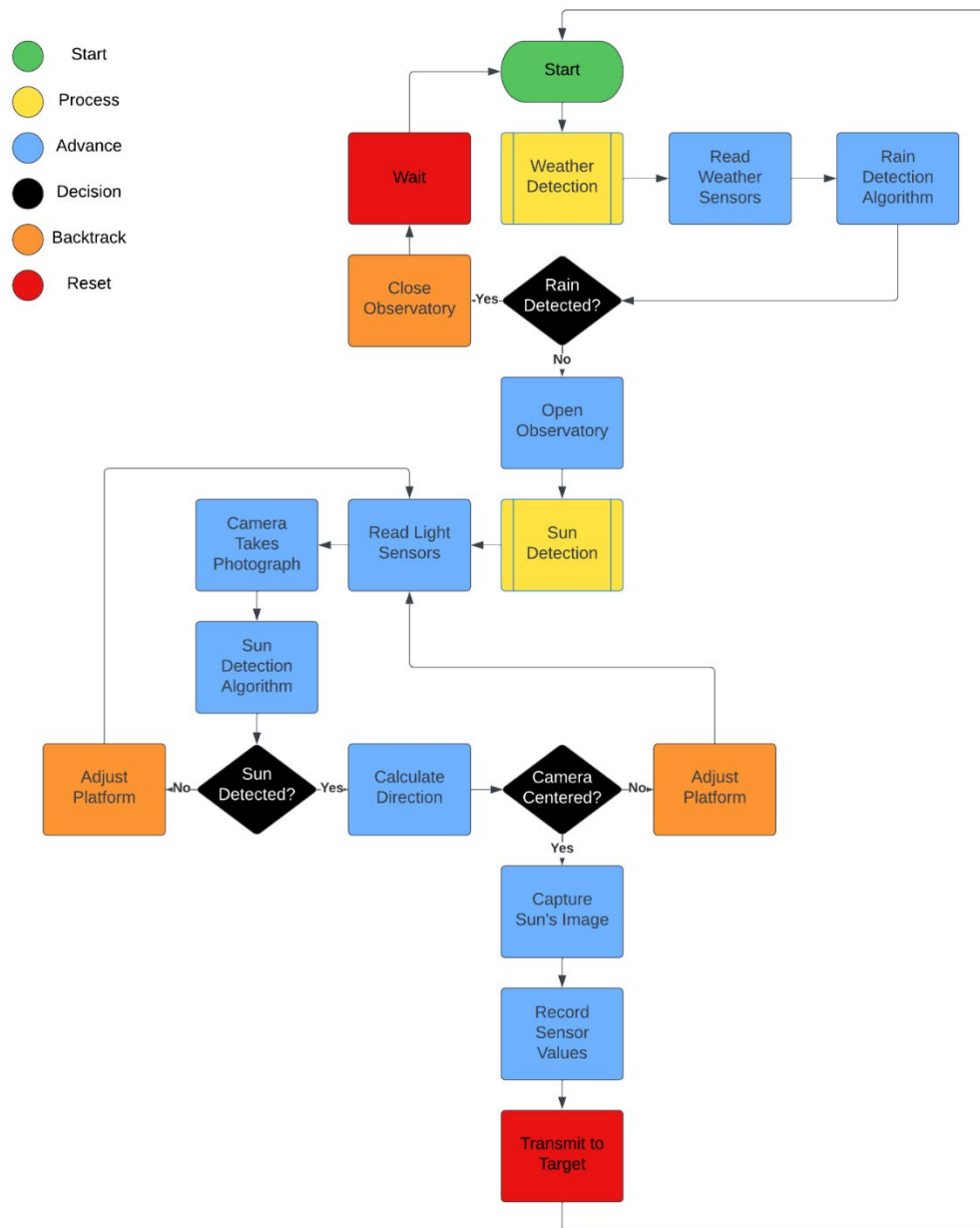


Figure 2.5.2 Software Flowchart

2.5.3 Optics System Flowchart

The following flowchart depicts the design of the optical part of the system.

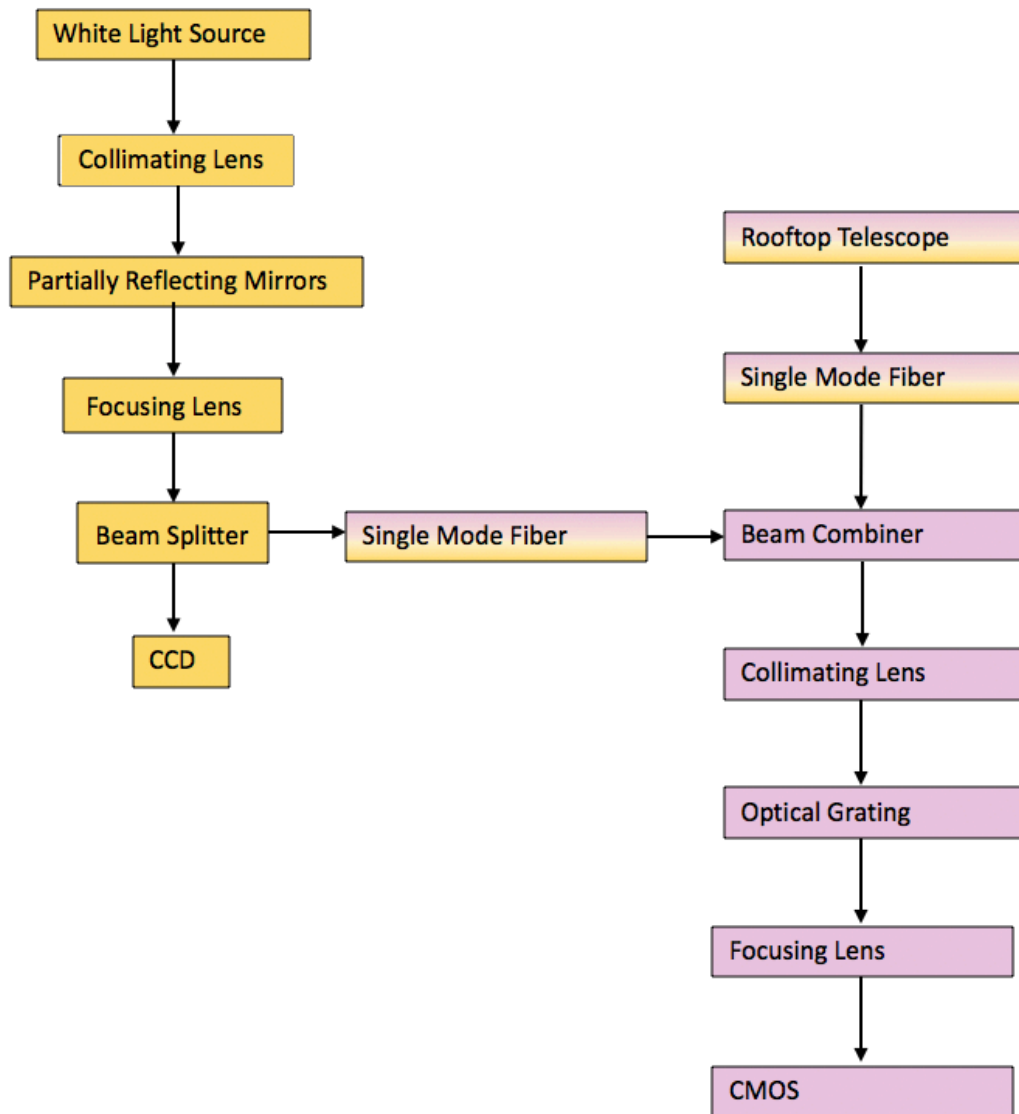


Figure 2.5.3 Optics System Flowchart

2.5.4 Optics System Schematic

This section contains a detailed schematic of the spectrometer and Fabry-Perot etalon, with their respective input of sunlight and a separate continuum broadband light source. Important distances between components are also included. Work distribution is not highlighted in this diagram because the focus should be on the position and addition of the components used in the optical system design.

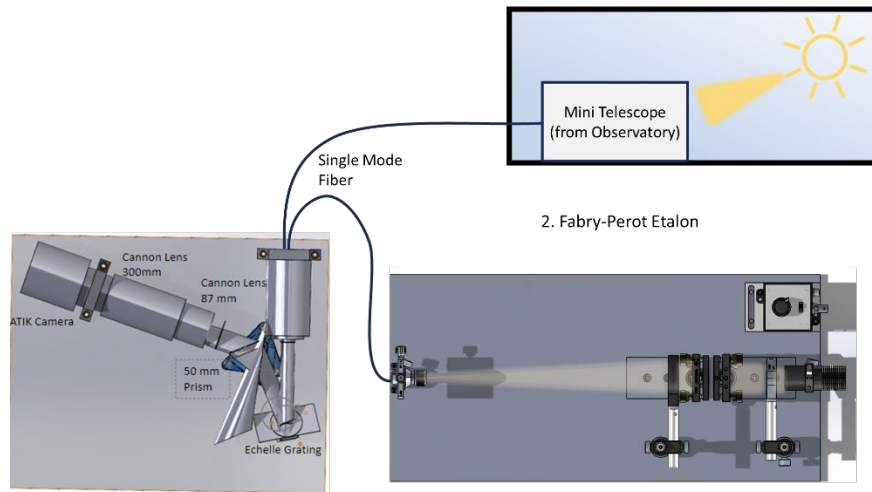


Fig. 2.5.4 Schematic of optical system

2.5.5 Hardware Block Diagram of the Solar tracking system

Here we are depicting the way we are planning to implement the hardware of our system. With color coded work distribution, we are depicting each component that will be integrated into our system and who is responsible for it. As we can see below, for our SD1 diagram, we planned to have two stepper motors that were going to be the ones in charge of moving the whole platform with respect to the solar-tracking system (refer to block diagram 2.5.5.1 below). Due to a request from our sponsor and, in order to get a very high accuracy on dual-axis motor step angle and keep all the solar spectrometry equipment balanced, we replaced the stepper motors for a center-balance equatorial mount iOptrom CEM70 (refer to diagram 2.5.5.2 below). Then we have one other motor to integrate our weather protection system. The diagram below shows the full hardware plan of our system (2.5.5.2).

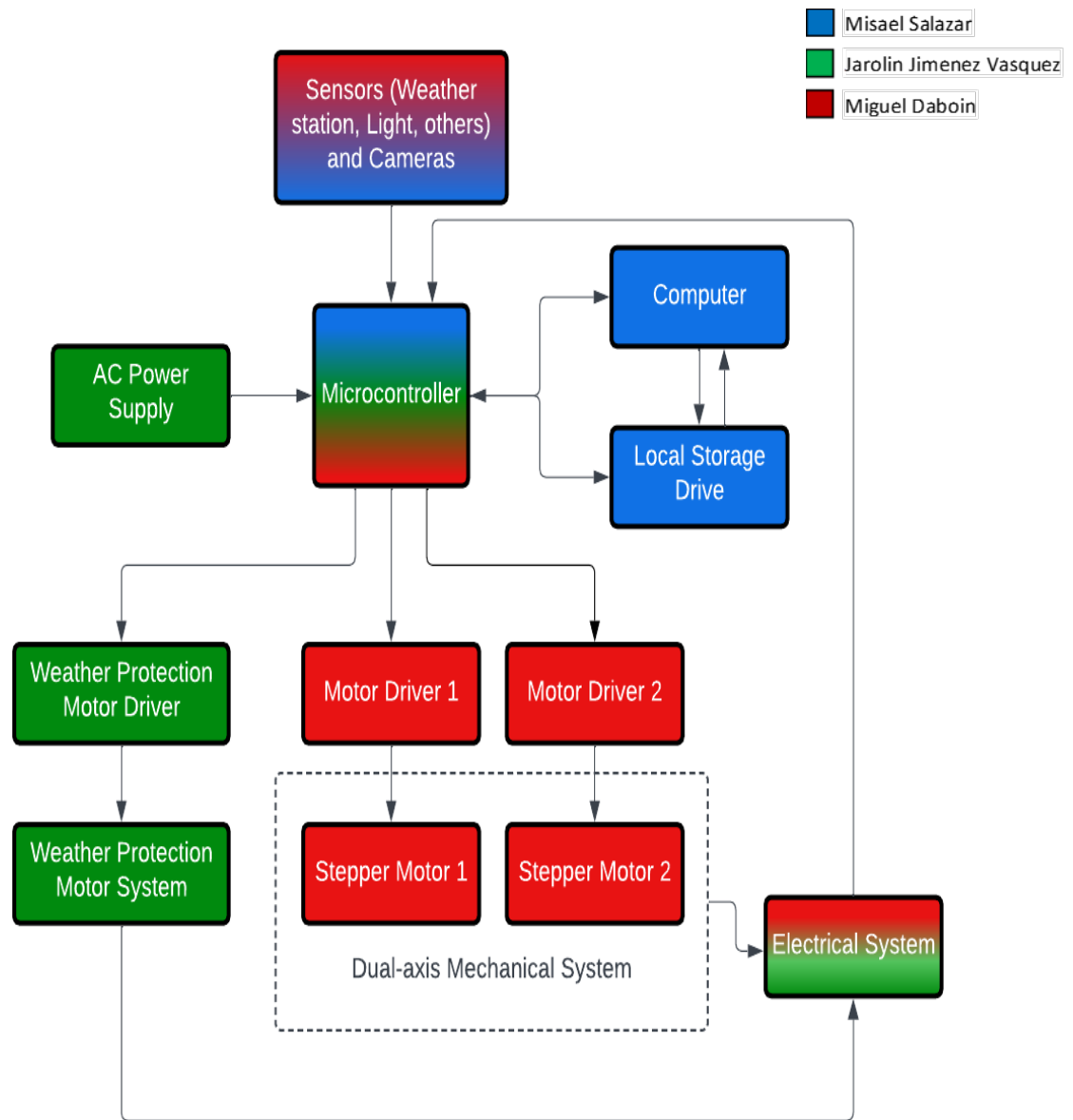


Figure 2.5.5.1 Previous Hardware Block Diagram of the Solar tracking system (SD1)

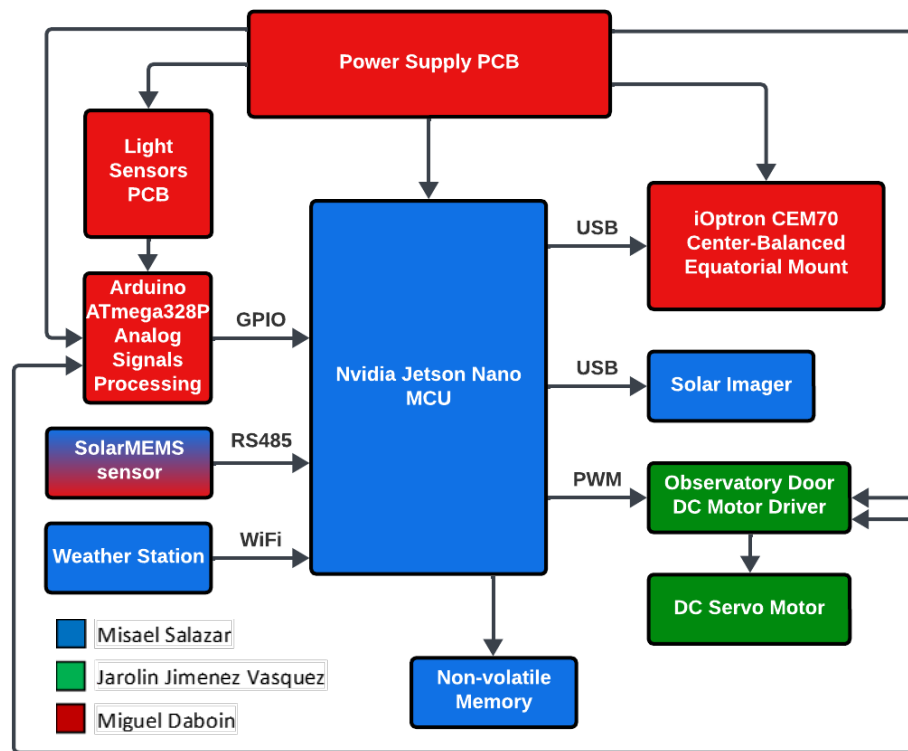


Figure 2.5.6 Hardware Block Diagram of the Solar tracking system version 2 (SD2)

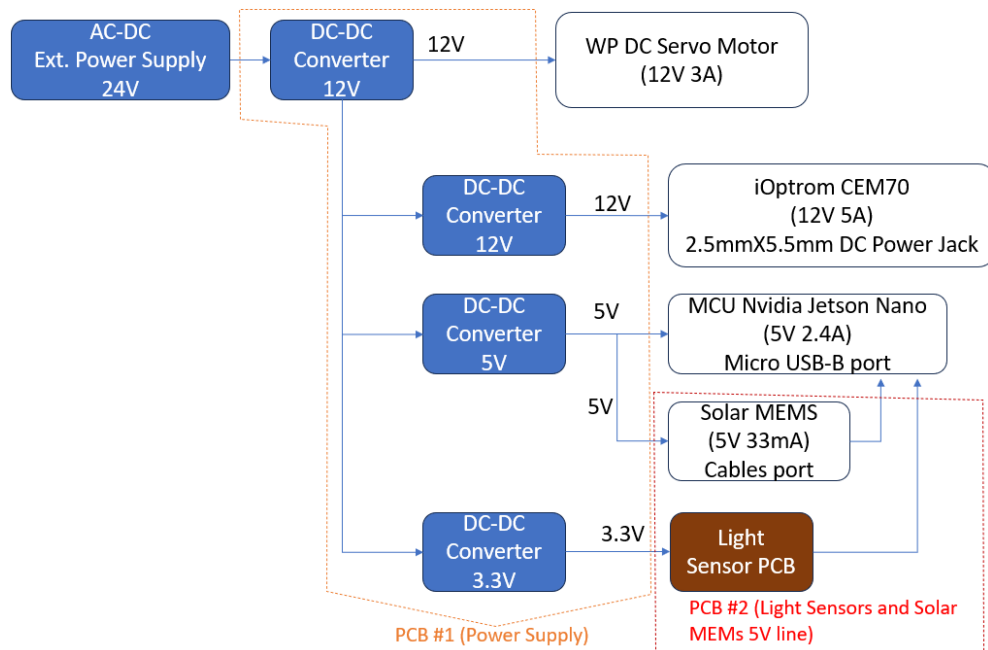


Figure 2.5.6.1 Power Supply PCB Block Diagram (SD2)

2.6 House of Quality

For this section of our project, we integrate the house of quality. This is the diagram that shows the market requirements the sponsor or customer prefer in the product they are paying to have in relation to the engineering requirements. This diagram helps us show the characteristics that were required to be able to satisfy both the engineering requirements as well as the customer/sponsor specifications. We were able to use this diagram to analyze the tradeoffs that we would be able to be fulfilled or not fulfilled.

The market requirements that we needed to fulfill with our spectrometry system highlights the size of the system, the clearness of the images being taken, the reliability of the recorded data, the range on cost that we need to stay on, the power consumption of the system, the weight, as well as how well the system can resist to the different weather conditions. For the side of the engineering we incorporated the relevant requirements that we could meet to fulfill the market requirements, we focused on the dimensions we want the system to have to be able to have the compact size the sponsor want us to meet, the accuracy of how the weather station protects the system as well as the record data continuously, the efficiency of the weather station, and the resolution that we needed to meet for the images, the weight of the system so that it can support all the components needed it but meet the size requirements.

The rest of the engineering requirements that we incorporated was the harmonic portion of the system so that we could set the desired frequency of the imager to the desired value by the sponsor. One more specification taken into consideration was the cost effect of the design. Even though the sponsor was kind of flexible as far as money expenditure was concerned, since some parts can be found and used by us in the optic department the set goal was not to exceed a certain amount. Power consumption was another one of the specifications to be followed, although is a system that will be in the roof tracking the sun the actual mechanism does not use the energy of the sun to track it, it will be using AC power, so we needed to make sure to not exceed a power consumption of 100 watts.

For our dimension we were to build the system as a 15x15x15. We preferred it to be less the 30 lbs. of weight. The desired resolution was of 12 megapixels. With a maximum cost of \$5000.00 dollars. Reaching an efficient movement of 0.6 degrees. To be able to consume less than 100 watts of power. With a resolution of 10^5 from the imager. with a frequency of every 10 seconds for data recording. All of these specifications and requirements are depicted in the table below as a house of quality diagram.

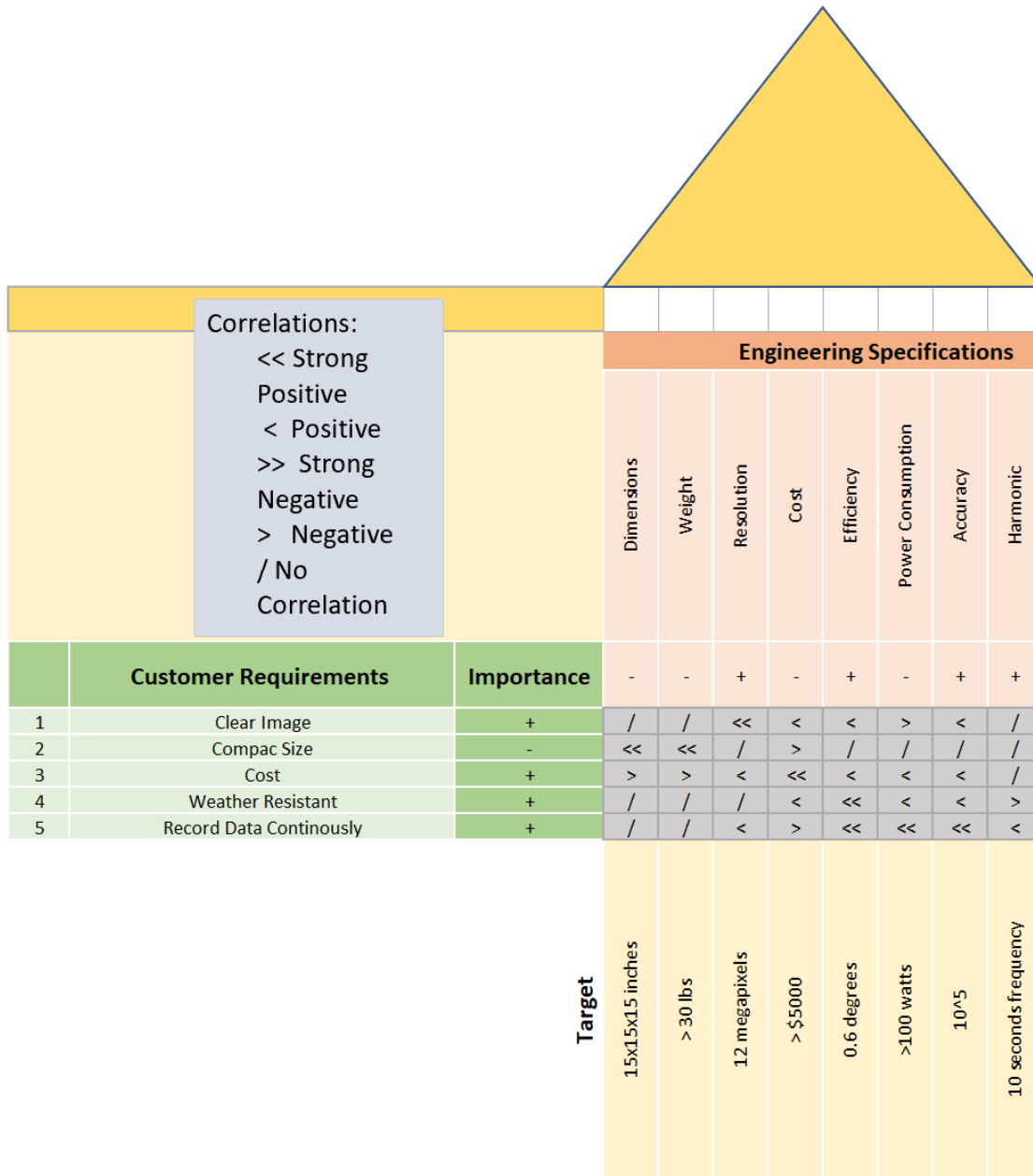


Fig. 2.6.1 House of Quality

The plan was to be able to get all the work needed done on a timely basis. With this in mind we have divided the workload evenly since the requirement is to have 30 pages per member. The way we did the work distribution was based on the member's experience and field of expertise, as well as the engineering department they are enrolled in. We all been working collaboratively with each other but do have different parts for each member to focused on. most of the flowcharts and diagrams above depict what each member has been assigned to work on as well as a table below that shows basic primary and secondary parts that each member was assigned to.

3.0 Research

In this chapter, we discuss current technologies that contribute to our goals. There is also an in-depth comparison of various components so that we could make well-informed design decisions.

3.1 Technology Comparison and Selection

In this section, we compare alternate technologies to our project that are currently being implemented. Alternatives to spectrograph calibration include frequency combs, hollow cathode lamps, tunable Fabry-Perot etalons, and solid etalons. Current astronomical spectroscopy is done with multi-channel spectrometers. Comparison of solar tracking methods and software technology is also covered in this section.

3.1.1 Frequency Combs

Instruments for measuring the radial velocity have been researched and improved upon for decades. The most advanced and precise method for astronomical spectrograph calibration is laser frequency combs, also referred to in this context as astrocombs. At least seven telescopes across the world use optical frequency combs to calibrate their spectrographs. A frequency comb produces a mode-locked spectrum with discrete, equally spaced frequency lines, typically from a mode-locked laser. The modes produced are phase coherent and harmonically related. Two important factors of frequency combs include repetition rate (mode spacing) and laser offset frequency. The offset frequency is directly related to the pulse's carrier phase (Fortier & Baumann, 2019). A significant contributor to higher stability and precision of LFC calibration is the capability to stabilize these factors to an atomic clock resulting in traceable and well-known frequencies (McCracken et al., 2017).

For astrocombs to properly calibrate, a required spectral coverage is needed and the comb spacing must match the resolving power of the spectrograph (typically $>10,000$) (Chih-Hao et al., 2008). Implementing spectral broadening can improve the coverage and a Fabry-Perot etalon can filter out modes to achieve the desired repetition frequency which would be otherwise unobtainable from femtosecond laser systems (McCracken et al., 2017). A basic frequency comb has been implemented in which the output of the source comb is directly filtered to attain the required mode spacing, however, this restricts the calibration range of the spectrograph, decreasing the spectral coverage (Fortier & Baumann, 2019). This has been alleviated by either frequency doubling or spectrally broadening the laser output before filtering.

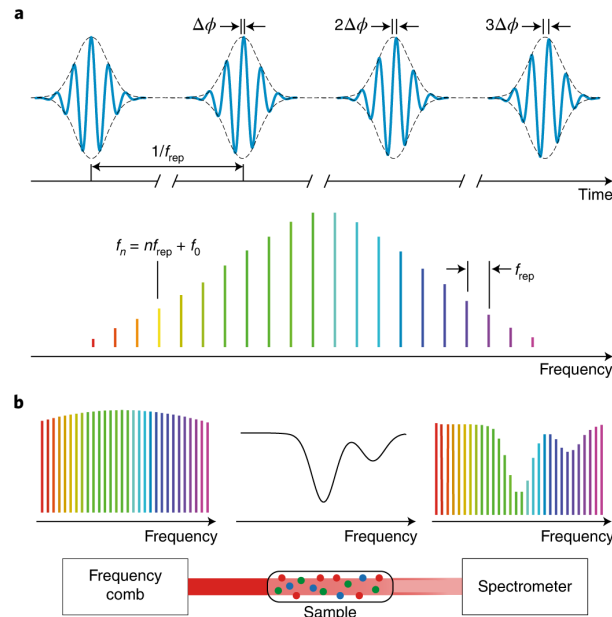


Fig 3.1.1.1 (a) The laser's output in the time domain and the spectrum of lines in the frequency domain and (b) an example of the spectrum going a spectrometer, where the dip corresponds to absorption from the sample. Reproduced with permission from Springer Nature (Picqué & Hänsch, 2019).

There are various configurations implemented in observatories across the world that have improved the precision of frequency combs, solid state lasers, electro-optically modulated combs, and fiber combs. Solid state lasers with a GHz repetition rate are commercially available, providing a sufficient frequency comb source. They have shorter pulses and provide a higher initial power, preventing the need for amplification. The pulse energy emitted is also sufficient for coherent spectral broadening. However, this system is prone to noise from its free-space environment and long-term drift. Electro-optically modulated frequency combs are produced from a narrow-line continuous wave pump laser that is phase modulated to produce sidebands set by the modulation frequency. In this case, the pump can be stabilized to an atomic clock, minimizing unwanted drift, though the coverage range has been restricted to a 1–2-micron band and there is a decrease in long-term stability. Fiber-based laser frequency combs offer long-term stability, but they have a narrow spectral coverage that requires a form of broadening or wavelength shifting to account for it. The repetition rates are limited, meaning that the comb modes require filtering. Amplification would be needed to achieve this, causing unwanted third-order dispersion, sideband amplification, and potentially component damage. Another option for frequency combs is microcombs, which operate by optical pumping of a micro-optical cavity. The line spacing resulting from this method is determined by the pump power, so both the laser and the power must be stabilized. Microcombs have a large line spacing that eliminates the need for filtering. Characteristics of the various configurations implemented by observatories are listed below.

Comparison of Frequency Comb Calibrators

Table Content from (Fortier & Baumann, 2019; McCracken et al., 2017)

	Pros	Cons
Solid State	Shorter pulses	Less developed automation
	Higher average powers directly from oscillator	Noise factors due to free space architecture
	No need for amplification stages	Long term performance drift
	Reduces demands for FP filtering	
	Supplies sufficient pulse energies for coherent spectral broadening	
	GHz repetition rate Ti: sapphire lasers are commercially available	
Electro-optically modulated	Enables comb stabilization without spectral broadening	
	No Fabry-Perot etalon	Decreased long term stability.
	Absolute traceability by stabilizing the pump laser to an atomic reference.	Increased modal position uncertainty
	Prevents wavelength shifts	Lack of full automation

The resulting spectral lines are narrow with stability and accuracy that exceeds astronomical spectrograph requirements. Bright spectral lines improve the signal to noise ratio, but the line intensity varies across the bandwidth. Laser frequency combs have been reported to have a precision of 1 cm/s. The LFC must have mode spacing that can be resolved by the spectrograph, requiring a laser with a high repetition rate or the addition of Fabry-Perot filter cavities to remove the excess lines. It also takes intensive maintenance to remain operational.

Although laser frequency combs have been proven to be precise and reliable, the development is extensive and expensive, especially with the more complex configurations. It is commonly only done for larger facilities. A broadband Fabry-Perot Etalon may not be as precise, but it is lower in cost and manageable to produce results for a smaller scaled project in a limited time frame. A Fabry Perot Etalon would still produce a clear spectrum across the visible wavelength, with expected precision to distinguish a drift of 600 MHz. The stability can be improved depending on the environment of the system. The purpose of this project was not meant to be as precise as professional observatories, so the Fabry-Perot is

sufficient to demonstrate the system's spectrograph capabilities for future applications.

3.1.2 Hollow Cathode Lamps

Hollow cathode lamps, designed with a metal cathode, anode, and a noble gas at a set pressure, were the standard for calibrating astronomical spectrographs. Various HCL element combinations enable customization for calibration. HCLs emit many spectral features, and most commercially available fulfill the standards for calibration. Researchers have created wavelength databases for the emitted spectral lines of various HCLs. This was achieved through Fourier transform spectrographs (Lovis & Pepe, 2007). The emitted wavelengths are from both the cathode material and the buffer gas. The spectral lines have a drastic difference in intensity because the majority are metallic lines which grow in intensity far quicker than that from the buffer gas. The key to using HCLs for calibration is to have high accuracy and precision of the emitted wavelengths.

A common choice for Hollow Cathode Lamps is Thorium and Argon. As time has passed, the quality of ThAr lamps has decreased as growing restrictions have been placed on the use of Thorium, decreasing the availability of pure Thorium. Instead, HCLs typically have a cathode made of thorium-oxide (Sarmiento et al., 2018). The impurities produce unwanted emission lines in high resolution measurements. Thorium is known to emit fewer lines at the near infrared range, so the use of Uranium has been explored. A study was conducted demonstrating that Uranium lamps produce a larger number of spectral lines than Thorium and that the Uranium Neon lamp had fewer strong long lines. A line list was produced for the range 500-1700nm, which is beneficial to calibrating high resolution spectrographs across a broader range. The use of HCLs results in unevenly distributed lines, varying intensities, and line blending (Schwab et al., 2015). Improving the spectral lines can also be complicated and time consuming. This method has been implemented by the High Accuracy Radial Velocity Planet Searcher (HARPS) with a precision of 20 cm/s.

	Frequency Comb	Hollow Cathode Lamp	Broadband Fabry-Perot Etalon
Precision and Stability	< 5 cm/s Potential for atomic clock stabilization	< 1 m/s	Dispersion shifts Sensitive to temperature and environment
Price, Availability, and Development	Expensive	Relatively Inexpensive Readily available	Inexpensive Easier development to match most spectrograph specifications since the FSR is a function of the cavity width
Spectral Range	Visible-Infrared	Visible-Infrared	Visible
Spectral Lines	Densely packed (spectrographs resolving power not high enough) More narrow wavelength coverage than spectrograph	Narrow lines Limited number of reference lines Irregular line distribution Undesirable spectral features from impurities Blending	Dense grid with uniform intensity over entire spectral range

Table 3.1.2.2: General Comparison of Spectrograph Calibrators

3.1.3 Tunable and VIPA Fabry-Perot Etalons

A Tunable Fabry Perot Etalon (TFPE) system is designed to so that it can be tuned for wavelength. By adjusting either the refractive index or the distance between the two mirrors with very fine accuracy, the wavelength can be varied over a wide bandwidth. A common method for this device is to utilize a piezo-electric stage

which moves the two mirrors. By moving the mirrors apart by one half of a wavelength, the transmission peak moves by one free spectral range. However, systems like this require highly sensitive equipment, which drives up the cost. This system has challenges when used in far infrared region as well. Also, this system can be somewhat sensitive to temperature changes in the surrounding environment.

Another type of Fabry Perot system is known as the VIPA (Virtually Imaged Phase Array) Etalon (*Virtually Imaged Phase Arrays* | *LightMachinery*, n.d.). This is a Fabry Perot design which brings incoming light into the cavity without passing through the first mirror. This strategy allows the first mirror to have 100% reflectivity, increasing the resolving power of the system. A VIPA is composed of three coatings. These are: 1) an Antireflective coating (AR), 2) a partially reflective coating, and 3), a 100% reflective coating. The AR coating is on a very small section of the first mirror. The rest is coated with a 100% reflective coating. The opposite side, which is where the light exits out of, is coated with a partially reflective coating. This is designed so that the light can be entered through the small AR coated section, and the system will be angled in such a way that the incoming light will then bounce between the two surfaces without ever returning to the AR piece of the substrate, always striking the 100% reflective surface. VIPA etalons are generally solid etalons (meaning the two etalons are separated by something that is not air), but they can be air etalons as well. Fused silica, silicon, and calcium fluoride have been used as materials for these systems. Solid etalons tend to be more sensitive to temperature changes, although solid etalons are more difficult to misalign (as it is a block and not two separate surfaces). This system produces higher resolution than your classic Fabry Perot system. However, due to manufacturing costs it tends to be more expensive (Tayebati et al., 1998).

3.1.4 Multi Channel Spectrograph

In a similar project to our own, a system built to perform UV spectroscopy on the sun was built, titled the Ultraviolet Coronagraph Spectrometer (UVCS) at the Solar and Heliospheric Observatory (SOHO). This system is much like a classic spectrometer, utilizing a reflection grating, mirrors, an entrance slit, and a sensor. This design mechanically scans around the edge of the sun by rotating the mirror, as the goal for this project is to conduct spectrometry on the solar disk. This system, to increase the overall bandwidth of the system, is a multi-channel spectrograph. The light is guided and split into multiple channels. Each channel is optimized for a specific bandwidth. This allows scientists to study a much larger variety of spectral characteristics from just one system. Each channel operates as its own small spectrograph system. The light is guided into the telescope through the overall entrance slit. It is then split and guided into the channels, each of which has its own entrance slit, diffraction grating, and detector. Each individual channel can be adjusted for resolution, bandwidth, and wavelength, providing endless opportunities for spectral measurements. These systems boast hundreds of

channels working simultaneously, taking both hyperspectral and spectral measurements.

This system could have been quite useful for our goals, as a multi-channel spectrograph would increase the number of absorption lines that could be tracked at once. Rather than designing purely for the visible spectrum and planning to shift to measure the near infrared in the future, this system would save time and therefore money. The system also presents very high precision. However, one must always be aware of the drawbacks. The most obvious being that the system is significantly more expensive, as it basically consists of many spectrometers in one. The brightness of any one signal will be greatly diminished as well, as the light must be divided between the channels.

3.1.5 – Solar Tracking System

The solar tracking mechanism plays a very crucial role when designing the Single Mode Solar Autonomous Spectrometry due to the several requirements and capabilities that are needed to guarantee and maximize its efficiency and performance. In order to track the movement of the sun accurately and optimally, the equipment needs to be positioned correctly so the sun disk is always in the middle and inside of the camera frame and the telescopes aiming in the right direction. Also, one of the challenges is that the sun's position in the sky changes throughout the year due to the tilt of the Earth's axis and its elliptical orbit around the sun. This causes some variations in the length of days, the angle of sunlight, and the height of the sun in the sky. It is very important for the efficient functioning of the solar tracking system to be able to track these variations during the year. According to Schroeder et al., the sun follows different paths at different seasons/times of the year, most northerly at the June solstice and most southerly at the December solstice. At the equinoxes, the sun moves around the celestial equator. The sun drifts leftward by about one degree per day (Schroeder, 2010-2011); see figure (3.1.5a) below for a similar illustration from a public domain website.

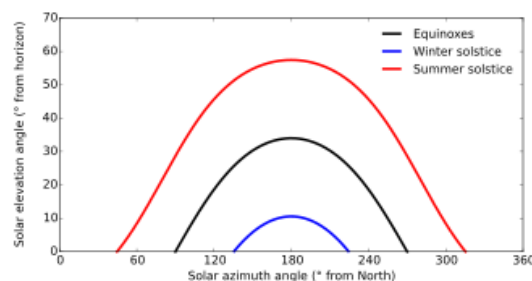


Figure (3.5.1a). Declination of the Sun as seen from Earth (Wikipedia, 2023)

The sun's path also changes during the time of the day approximately at 15° per hour from east to west. These sun's paths both yearly and daily clearly represent one of the most important requirements of the system to be able to track the disk sun during all the year. According to Bikos, K., (2019) the horizontal coordinate

system, also known as the Altitude/Azimuth system, is a method for describing the exact position of objects in the sky, such as planets, the Sun, or the Moon. Azimuth represents the horizontal angle measured clockwise from a reference direction, usually the north, to the object of interest (It ranges from 0° to 360° , with 0° corresponding the north, 90° to the east, 180° to the south, and 270° to the west). Altitude represents the vertical angle measured from the observer's horizon to the object in the sky. It ranges from 0° (on the horizon) to 90° (directly overhead or the zenith) (Bikos, 2019).

This horizontal coordinate system is needed to calibrate, obtain data, and accurately position the solar tracker system in the right direction depending on the type of technology that will be used. C. Jamroen et al., proposes a pseudo-azimuthal system of tracking system and compares it to the horizontal coordinate system. A three-dimension unit vector (S) is used to represent the sunlight incident to the observer. Its axes can be determined by using the altitude (α) and azimuth (β) angles. The azimuth angle is the difference angle of north-south and the altitude angle is used to follow the daily path of the sun from east to west. The author represents the coordinate axes of the sun position with the following formulas (Jamroen et al., 2020):

$$S_x = \cos(\alpha)\sin(\beta) \quad (1)$$

$$S_y = \cos(\alpha)\cos(\beta) \quad (2)$$

$$S_z = \sin(\alpha) \quad (3)$$

$$S = (\cos(\alpha)\sin(\beta), \cos(\alpha)\cos(\beta), \sin(\alpha)) \quad (4)$$

For the pseudo-azimuthal system proposed by C. Jamroen et al., the unit normal (N) of the PV-module or platform should be equal to the sun position (s) in Eq. (4). The author establishes two coordinate systems: XYZ-O and IJK-O systems as follows (ϵ = daily angle; ρ = elevation angle) (Jamroen et al., 2020):

$$N = S \quad (5)$$

$$N_{IJK-O} = (\sin(\epsilon), \cos(\epsilon), 0) \quad (6)$$

$$N_{XYZ-O} = (\sin(\epsilon), \cos(\epsilon)\sin(\rho), \cos(\epsilon)\cos(\rho)) \quad (7)$$

$$\epsilon = \tan^{-1} (\cot(\alpha)\sin(\beta)) \quad (8)$$

$$\rho = \tan^{-1} (\cos(\alpha)\cos(\beta)) \quad (9)$$

This system type explained above could potentially improve the detail of the solar tracker system by providing effective position coordinates that can assure an improved accuracy of our Single Mode Autonomous Solar Spectrometry. Several research studies have explored various solar tracking technologies with the purpose of guaranteeing the accuracy, cost-efficiency, and reliability of the system. In a research article by A.Z. Hafez et al., (2018) a historic overview of the solar tracking systems is discussed as follows (Hafez et al., 2018):

Inventor/ Developer	Year	Main System Details
McFee (Hafez et al., 2018), (Ferdaus et al., 2014)	1975	An algorithm is used to calculate the total power in a central receiver of a solar power system. Error tolerance of the position of the sun between 0.5° to 1° (microprocessor-based, electric-optical sensor-based and time methods)
Zogbi and Laplaze (Hafez et al., 2018), (Zogbi & Laplaze, 1984)	1984	Dual-axis tracking system with two angles (azimuth and elevation). Four electric-optical sensors placed in four-quadrant formed using two rectangular plans with cross one another in a line. The two tracking motors operate using the signal received and the system would reset at the beginning of the night. The motor is operated by an amplifier when the output of one of the sensors is greater than the threshold
Rumala (Hafez et al., 2018), (Rumala, 1986)	1986	Close loop control tracking system depending on the shadow method. Four photoresistor sensors are placed on a rigid platform. The control circuit is a signal conditioning circuit using a low pass filter (feed an amplifier) that sends signals to drive a servomotor for tracking and aligning the system.
Poulek (Hafez et al., 2018), (Poulek, 1994)	1994	Passive tracking system using shape memory alloy (SMA) based on axis actuators where SMA deformed at low operation temperatures range (below 70°C), and when it is heated above a certain specific temperature, SMA returns to its original shape. Disadvantages: low efficiency, mostly used for the equator sun's position, not accurate, and the system depends on thermal expansion process.
Kalogirpu (Hafez et al., 2018), (Kalogirou, 1996)	1996	Single-axis tracking system using three light dependent resistors (LDR). LDR1 detects the focus state of the collector while LDR2 and LDR3 discriminate the information between day and night and detect the presence or absence for shadowing. Low speed 12V DC motor that receives signals from LDRs
Khalifa and Al-Mutawalli (Hafez et al., 2018), (Khalifa & Al-Mutawalli, 1998)	1998	Dual-axis solar tracking system on a parabolic concentrator to improve thermal. Designed to track the sun every 3 mins with respect to horizontal plane and 4 min with respect to the vertical plane

Table (3.5.1c). Historic Overview of Solar Tracker Systems (Hafez et al., 2018)

It is notable that solar tracking systems have evolved during the last years based on different applications, available technologies, and system types. On the other

hand, A.Z. Hafez et al., reviewed many research studies and concluded the following (Hafez et al., 2018):

Solar tracker system type	Advantages	Disadvantages
Single axis	Simplicity, lower cost, and lower energy consumption	Lower efficiency, energy gain
Dual axis	Higher efficiency, more accuracy, easier to adapt to sun paths on each season	Higher cost, higher energy consumption

Table (3.5.1d). Most useful solar tracker system types (Hafez et al., 2018)

Understanding the seasonal variations in the sun's position is crucial for accurately predicting the sun's coordinates and optimizing the solar tracking system so the telescopes and cameras point out in the right direction in a very efficient way. At the same time, using a very highly efficient solar tracker system, like the dual-axis one, could potentially improve the quality of data obtained from the device although it will mean a higher cost and energy consumption.

3.1.6 Software Technology

When we began researching software technologies it immediately became clear that the focus of our research should be on finding a suitable algorithm for predicting incoming rainfall. The ability to predict incoming rain is critical to our project's success because our observatory's functionality relies on remaining dry to protect sensitive components. It turns out that predicting the future is a rather hard thing to do. Modern weather forecasting relies on the synthesis of various observation technologies such as radar, satellite imaging, and ground or aerial sensors to get a complete image of the current conditions(*Forecast Process*).(). Then, those readings are run through numerical weather prediction models. These models use the current weather data to run complicated simulations of the atmosphere by which they can predict future conditions(*The Forecast Process - Forecasting the Future*). These kinds of models require far more computational power than we can achieve on an embedded platform, and they model the behavior of the whole atmosphere, which is irrelevant to our desired prediction of incoming rainfall. For these reasons, we could not rely on conventional weather modeling to predict incoming rain, we needed a model that could run on the limited data our weather station collects (temperature, atmospheric pressure, wind speed/direction, etc.) and be light enough to run efficiently on an embedded system.

The most intuitive approach would be to use a machine learning algorithm to build a model based on the sample data we collect. Machine learning is a branch of artificial intelligence that focuses on the collection and use of data to develop algorithms that can improve themselves over time(*What is machine learning?*). In

order to choose an algorithm that best suits our needs, we needed to understand how different algorithms work and what advantages or disadvantages each one has. Before we can begin looking at these algorithms, we first needed to collect some data.

How do we collect weather data? In the United States, the National Oceanic and Atmospheric Administration (NOAA) offers free access to NCDC's archive of global weather and climate data(*Climate Data Online*). This archive includes several datasets of different weather measurements and most importantly to us, they have a dataset containing historical 15-minute precipitation observations. This dataset offers a granular look at precipitation trends across the U.S. which we can leverage to achieve more accurate rainfall predictions. Having free access to this data gives us a huge advantage because we can be sure that we have reliable high-quality training and testing data for whichever algorithm we implement.

Now let's introduce the different algorithms we had available at our disposal before taking a deeper look at a few of them. One of the simplest algorithms available is linear regression. Linear regression is a method of statistical analysis that predicts the value of an outcome as a linear combination of its inputs(*What is linear regression?*). In our case, we would be using a multiple linear regression to consider multiple input variables in order to predict a single output variable. Then there is the decision tree, a supervised learning algorithm for classification and regression tasks. This algorithm starts with a root node, which then branches to decision nodes and continues branching until it reaches a leaf, or terminal node(*What is a Decision Tree?*). Naïve Bayes classifiers are algorithms that work based on Bayes' Theorem, by applying certain assumptions we can apply probabilities to certain events and classify outcomes based on those probabilities(*What are Naïve Bayes classifiers?*). The assumptions naïve bayes makes are that each feature in the data set is independent of each other and they all contribute to the outcome equally(**Singh Chauhan**, 2022). These assumptions allow naïve bayes methods to solve classification tasks efficiently. Naïve bayes methods are less complex than other classifiers, the scale well and can handle more variables. The K-nearest neighbors algorithms uses the proximity of a given data point to its neighbors to classify that data point(*What is the k-nearest neighbors algorithm?*). Classification labels are given based on a majority vote, which allows the algorithm to solve classification problems. The K-nearest neighbors' algorithm is limited by its inability to scale efficiently to larger data sets. Long short-term memory (LSTM) networks are a kind of recurrent neural network(Lheureux, 2023). Unlike standard neural networks, these models are 'recurrent' because they have feedback connections. They are called long short-term memory networks because they can predict based on variables held in long term memory(Saxena, 2021). This makes LSTM models ideal for problems that are concerned with the long-term behavior of sequences. When we try to predict incoming weather, we have plenty of algorithms at our disposal.

Now let's take a closer look at some of the viable machine learning models for our project. The first and simplest model we described was linear regression. We

mentioned previously that linear regression is a model of one dependent variable on one or more other independent variables as a linear dependence function(Sharapov, 2022). The linear dependence function is the following:

$$y = b + w_1x_1 + w_2x_2 + \dots + w_nx_n$$

Where y is the resulting dependent variable, b is the y-intercept, x_i is the independent variable measured, and w_i is the coefficient of x_i or the change in y with respect to x_i (Akua Opoku). Sometimes this equation also includes an error term θ (Sharapov, 2022). Since the model is based on this equation, it makes linear regression a simple model to implement, and a good choice for testing our computer system's capabilities. The simplest way to implement a linear regression model is using the ordinary least squares algorithm. We found evidence that shows linear regressions have been successful when applied to weather forecasting. One study using linear regression to predict the upcoming temperature forecast was able to show an average absolute error is about 1.5 degrees(Sharapov, 2022). While not exceptionally accurate, this suggests that linear regressions are in fact capable of making meaningful weather predictions. One of the issues with linear regression is that it will not give us a 'prediction' of whether it will rain or not, instead it will give us an output value of the expected amount of rainfall in a given time frame. One solution then, is to use a logistic regression model. Logistic regression is a modified form of the linear regression model, where outcomes are binary events (either they happen, or they don't happen). Thus, logistic regression gives us a probability for the possibility of an event occurring. The logistic regression has been used successfully to predict the probability of rainfall with forecasts up to 90% accurate.

The next model we'll look at is the decision tree. The decision tree model consists of a tree where each branch represents a decision being made, and the outcomes are the resulting leaf nodes. There are a few different types of decision tree algorithms, but in general they share the same properties. Decision trees are easy to understand, they require little data preparation, and are useful for both classification and regression tasks. The disadvantages of decision trees are that they are prone to overfitting, can be highly variable, and may take longer to train than other algorithms. One way to get around the overfitting issues is to use a modified model called a random decision forest, or just random forest. The random forest is a model made of multiple decision trees with each tree made with a sample of the data. Then for a regression task the individual trees are averaged, and for a classification task a majority vote is taken. Random trees reduce the overfitting tendencies of decision trees, but they often take longer to train due to their use of many decision trees. A 2018 comparison of three different regression techniques, Support Vector Regression, random forests, and decision trees found that when applied to rainfall predictions, random forests performed and predicted more accurately than the other models.

The last modeling technique we're interested in is the long short term memory (LSTM) network. Over the past decade, the use of artificial neural networks to

forecast incoming rain has become a point of interest for researchers. Of the neural network models currently available, recurrent neural networks (RNNs) have the most potential for their ability to model time series. A time series is a sequence of observations $\{\phi_1, \phi_2, \dots, \phi_t\}$ recorded over time. Recurrent neural networks are well suited to problems that require modeling time series because unlike regular neural networks, they have feedback loops that allow the network to include information from previous nodes into the current node's calculations. However, this presents a problem, as in traditional RNNs the contribution of that feedback 'vanishes' over time, which means that the network will show a recency bias, not really considering the long-term data it trains on. This issue is solved by the LSTM network due to its unique architecture.

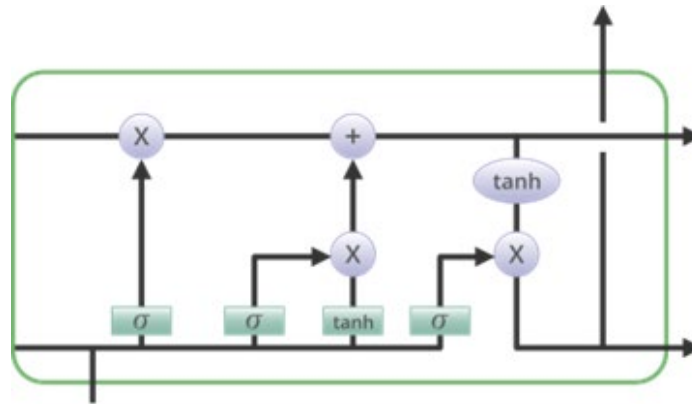


Figure 3.1.6: Internal Architecture of a LSTM memory block, source:
<https://www.geeksforgeeks.org/deep-learning-introduction-to-long-short-term-memory/>

LSTM networks are composed of these memory blocks which can contain one or more memory cells. This design allows LSTM networks to capture long term dependencies, which enables the model to remember significant context. The disadvantage is that these models are more computationally expensive due to their complexity, which means that training can take longer and require more data.

Many neural network models have been applied to the study of weather forecasting. Among the first uses of neural networks in rainfall prediction was the PERSIANN algorithm. This model applied a recurrent neural network to satellite data of the atmosphere in order to predict incoming rainfall at a given area. The researchers were able to successfully apply their rainfall prediction model across two different sites in the state of Florida. Another research paper applied a LSTM based rainfall prediction model to estimate rainfall in Jimma, Ethiopia. Their model achieved 99.72% accuracy in estimating average rainfall over a time period of 60 days. The use of LSTM models has been a very popular and successful area of exploration in recent years.

For our project's ideal weather prediction algorithm, we would use an LSTM neural network. When considering the possible constraints we will face, it would make the

most sense to implement a simpler model first, before moving on to try to develop a neural network. This means that we will likely apply a simpler model such as a logistic regression, which will give us an easy way to predict the weather so that we may test our system's functionality. Once the system is fully functional, we may upgrade the predictive model to a more complex approach such as the LSTM network.

3.2 Parts Comparison and Selection

In this section, we compare various components and parts of the optical and hardware systems.

3.2.1 Optical System

The optical portion of the system is comprised of the spectrometer and the Fabry-Perot etalon. The etalon has a broadband source and two parallel partially reflective mirrors. Mirror coating and shape play a vital role in Fabry-Perot etalon design, so they are emphasized in this section.

Like many systems, the spectrometer had many designs to choose from. These designs range from high to low price and vary by purpose. There are four primary components of the spectrometer. They are: 1) the guiding optics, 2) the dispersive element, 3) the input opening, and 4) the sensor. All three of these affect the resolution of the spectrometer. Here, we delve into the primary methods used for each of the three categories and compare the pros and cons of each method. The driving factors of our design are resolution, bandwidth, and peak wavelength.

3.2.1.1 Dispersive Element

Let us begin with the dispersive element of the spectrometer. There are two noteworthy options utilized within a basic spectrometer: the prism and the grating. These vary by price, spectral resolution, and bandwidth. There are many systems utilizing only prisms, only gratings, and a combination of the two, known as grisms. Whether a grating or prism is used, the other general elements of a spectrometer (guiding optics, slit opening and sensor) remain the same, however the focal lengths of lenses and size of the sensor may have to vary to accommodate for a difference in resolving power between the two dispersive elements. The resolving power of a system is determined by the following equation:

$$R = \frac{\lambda_o}{\Delta\lambda}$$

Where λ_o is the peak wavelength measured, $\Delta\lambda$ is the minimum resolvable change in wavelength, and R is the resolving power.

The prism is a classic method, utilizing dispersion, which causes the optical path length in a medium to vary by wavelength. The image produced by a prism is relatively bright, as the input light is limited simply by the size of the input beam and the prism itself. Prisms are also quite affordable. However, the spectral resolution depends primarily on the refractive index of the prism (which can only go so high), limiting the resolving power capabilities of a prism-based system. In prism spectroscopy both the shape as well as the material of the prism vary based on the area of the spectrum one is attempting to measure, as well as the spectral resolution goals of the system. The choice of material depends heavily on the absorption and transmission characteristics of the materials. BK7 and flint glasses (such as F2) are utilized when measuring the visible spectrum, infrared spectroscopy generally calls for zinc selenide, silicon, or germanium, crown glass and for the UV region we look for fused silica or quartz. For our system, if we were to utilize a prism, we would choose from the first list for visible light, as this is what we aim to measure. Antireflective coatings can be added to prisms to increase contrast and resolution. A common method for increasing the resolution of a prism-based system is to place multiple prisms in consecutive order, thereby increasing the total angle of diffraction experienced by the incoming light. There are a variety of configurations, the most notable of which includes the double Amici prism design, which increases the diffraction angle, and manages to refract the center wavelength at the same angle as the incidence beam. This design allows for greater design flexibility. The double amici prism consists of two triangular prisms, the first of which has a lower refractive index than the latter. Common materials for this design include crown glass and flint glass. A variation in the number of prisms as well as their indices of refraction have been found to greatly increase the angle of dispersion, thrilling many who seek prism systems for their high optical throughput and lower cost. Despite the many geometries, materials, and coatings to choose from which solve for the initial issues presented by prisms for spectroscopy, there are still many downsides. The primary con for our project is that a prism-based spectroscopy system is very difficult to adjust for wavelengths. As of now, our group aims to measure visible light. However, it is possible in the future that the group may want to study the infrared spectrum of the sun. A prism-only spectrometer will be far more difficult to adjust to a new area of the spectrum, requiring a complete switch-out and realignment of the system (Sasian, 2000).

There is however a method which utilizes two dispersive optics: one to disperse the light, and one to cross disperse in this design we delve into a cross-dispersion configuration. This system utilizes both a grating as well as a prism. The grating disperses the light, and the prism then takes the light, dispersing it at a 90-degree angle to the grating's dispersion. The result is a spectrum where each order of diffraction is assigned to a specific wavelength. This system gives us a higher resolution while maintaining bandwidth. For this design, we must choose a type of prism as well as the material it should be made out of. We have already concluded

that the material will be either a crown or a flint glass, as these are the best with visible wavelengths. We will therefore be choosing between F2 and BK7 glass. There are many different prism configurations, which include equilateral, right angle, and more, which can be used as reflectors, beam redirectors, polarizers, and dispersive elements. For our purposes, equilateral triangles provide the best fit. This is because we want the prism to provide as little of a beam path change as possible. The equilateral triangle will still change the angle of the beam path, but in the least amount in comparison to the other prisms. The most common material for use in a dispersing equilateral prism is the F2 material.

Gratings disperse light by the method of light interference. A grating is made out of periodic changes in the refractive index in a substrate. As the light strikes the grating, the light waves interfere with the periodic function of the grating. The result is a new wave that is equal to some sum of the two periodic functions (grating wavelength + light wavelength). This results in the light being separated into each distinct wavelength, as the exit angle will be slightly different for each angle. The angle that the light will exit at from a simple transmission grating can be determined by the following equation:

$$a \sin \theta = m \lambda$$

Where a is the groove period, λ is the peak wavelength, and m is the order of diffraction. Because we are dealing with an interference pattern, there are many modes, where the dispersed spectrum repeats itself. As the mode number rises, the resolution does as well. However, as usual the tradeoff for high resolution is reduced throughput. There are a very large number of options when it comes to selecting a grating. Here, we will compare the following important categories to consider when selecting a grating, and then we will table existing gratings on the market to compare their compatibility with our system: Coating, reflection vs. transmission, ruled vs. holographic, and number of grooves/mm. Let us begin with coatings. When utilizing a reflection grating, there are three primary coatings that we are evaluating: gold, silver, and aluminum. If we were to use a transmission grating, a decision which will be discussed next, we would be more concerned with the types of antireflection coatings. These coatings on the other hand are developed to provide maximum reflection in the area of the spectrum that one is searching to examine. Gold coatings are generally utilized for the IR side of the spectrum, as it has reflectivities of 95 to 99% from 700 nm and up, but dips below 90% in the visible region. Gold is also a more expensive option. Silver also has very good reflectivity for the infrared spectrum and maintains above 90% until around 300 nm. Aluminum, while dipping slightly at around 800 nm, maintains around 90% reflectivity throughout the visible band. As we are aiming for a peak wavelength of 550 nm, this could be the best option. Despite silver fitting our requirements for over 90% reflectivity in the visible band, aluminum provides a better bandwidth and price. Silver, gold, and aluminum can also be. Below we see

the spectral relativity curves of aluminum, gold, and silver. This graph shows the reflectivity of the bare elements, as well as “enhanced” and “protected” coatings. These have been enhanced to either have a wider bandwidth, with the “protected” silver having a better reflectivity in the visible and infrared regions. It is clear from the graphs that protected silver will provide us with the best reflectivity and bandwidth. However, as we are only concerned with the visible range, and silver coatings add greatly to the price of the grating, aluminum is still a possible candidate for our grating.

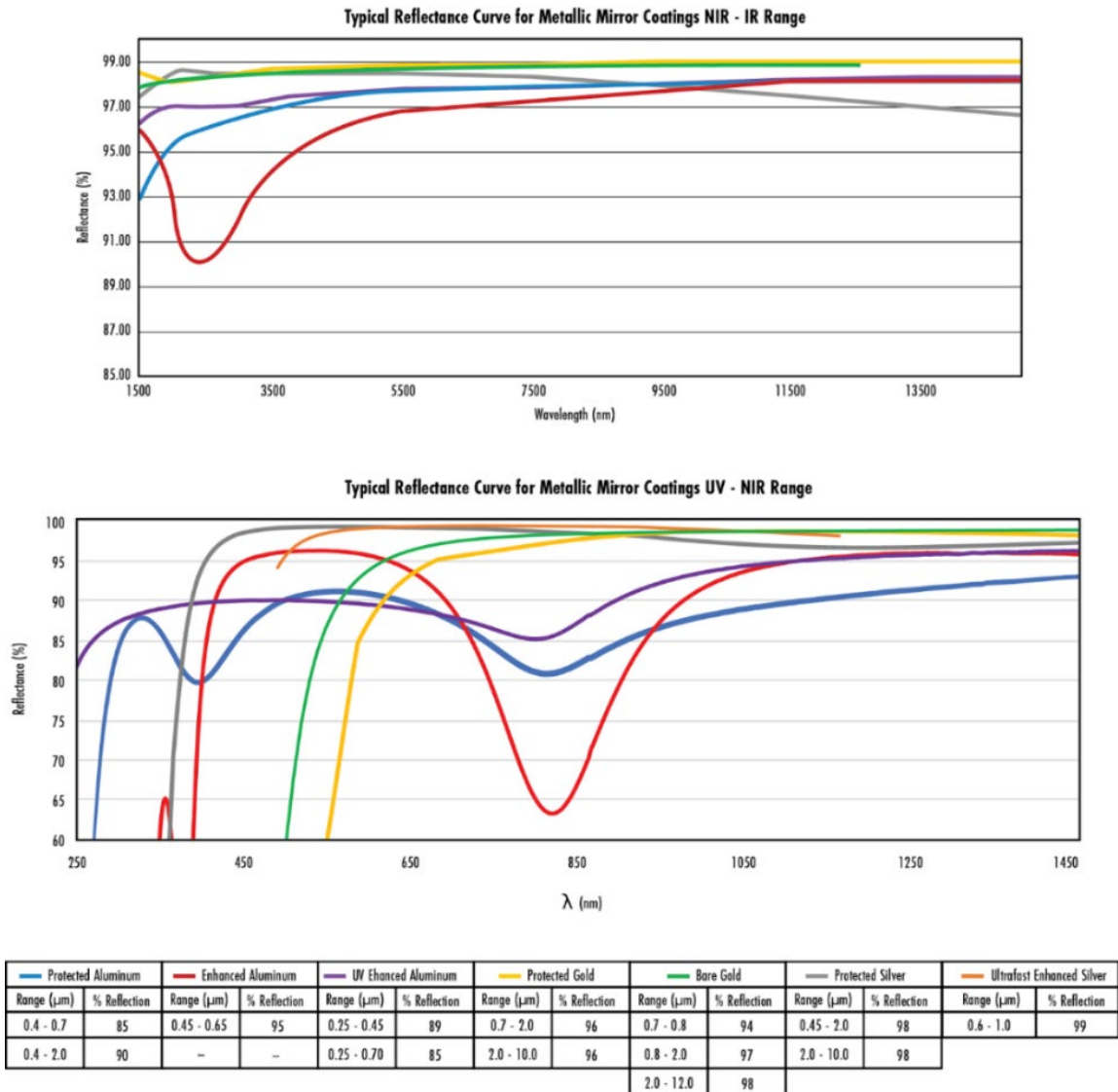


Figure 3.2.1.1: Spectral characteristics of optical coatings (*Off-Axis Parabolic Mirror Selection Guide | Edmund Optics, n.d.*)

These coatings are all in reference to the reflective gratings. What if we were, however, to utilize a transmission grating? In this case, the grating becomes a part

of the optics, where a big problem is unwanted reflections. This is solved with anti-reflective coatings, usually made using magnesium fluoride if operating in the visible spectrum.

3.2.1.2 Gratings

Transmission vs. Reflection Gratings

The two primary methods for making periodizing changes in either the light path or the refractive index of the grating are by either making tiny slits into the substrate through which light passes (transmission grating), or by etching reflective grooves into a substrate off of which light reflects (reflective gratings). The choice of gratings determines the geometry and focusing optics of the system (*Spectroscopy: Diffraction Grating*, n.d.). Reflection gratings are much more common for spectroscopy because: 1) reflection gratings allow the system to be “folded” rather than “inline” (reducing the size of the system), 2), reflection gratings have much higher resolving power than transmission gratings, 3), transmission gratings have a lower maximum diffraction efficiency (due to absorption, reflections, and material dispersion), and 4), there are certain parts of the spectrum that cannot be measured utilizing a transmission grating, as the loss would be too great regardless of the coating (Weisberg, 2023). This is mostly referring to the UV spectrum, which is not a concern for us, as we are dealing with the visual and, perhaps in the future, the near infrared. Transmission gratings may however be useful, as a simple spectrometer can be designed with a transmission grating and a simple camera by inserting the grating between lenses. Transmission gratings also display consistent diffraction efficiency across a large bandwidth, making the designs and calculations of the system much simpler. Regarding the higher resolving power of a reflective grating, we can utilize two more equations to better understand transmission (left) and reflection (right) grating angles of dispersion. Where m is the mode, λ is the peak wavelength, a is the spacing between the grooves, θ_i is the input angle of the light and θ_m is the output angle of mode m .

$$m\lambda = a(\sin\theta_m - \sin\theta_i) \text{ and } m\lambda = a(\sin\theta_m + \sin\theta_i)$$

Ruled vs Holographic Gratings

There are two methods of fabricating a diffraction grating, both of which can be either a transmission grating or a reflective grating. These are called ruled and holographic gratings. Ruled gratings are made by mechanically etching grooves into the substrate. Holographic gratings on the other hand are made by interfering with two beams onto the substrate. The constructive interference fringes etch the grooves. The method of fabrication has a noticeable effect on the grating's operation. Ruled gratings have sometimes produced an effect known as “ghosting”, where stray light is also diffracted onto the sensor. This is an issue which is greatly diminished with holographic lenses, due to a decrease in

irregularities, which provides a significantly better signal to noise ratio (SNR). Ruled gratings can be made at a “blaze” angle, where the grooves are etched at an angle to the surface. This can be done to maximize the signal of a specific mode, and to operate at a specific peak wavelength, known as the “blaze wavelength” (*All about Diffraction Gratings | Edmund Optics*, n.d.). Due to this blaze angle, ruled gratings generally display a higher efficiency than holographic gratings. The efficiency of a grating is the ratio of the input light to the amount of light diffracted into a certain order. However, efficiency decreases dramatically as one gets further from the blaze wavelength, resulting in a lower overall bandwidth. Holographic gratings are characterized by their peak wavelength rather than their “blaze” wavelength and have a flatter spectral efficiency curve (*Differences between Ruled and Holographic Gratings*, n.d.)

An important note concerning gratings is that they can be extremely delicate. The handling of gratings should be done very carefully and with gloves, as touching the grating with bare hands will rub off the coating from the grating.

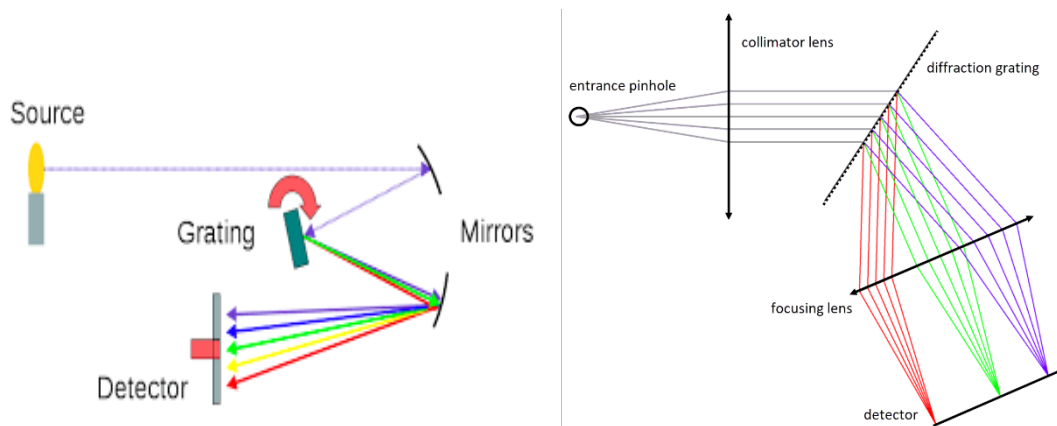


Figure 3.2.1.2 Czerny-Turner Spectrograph and Transmission Grating Spectrograph (Wikipedia, 2023)

Echelle Gratings

There is a specific type of ruled grating, known as the Echelle grating. This is a ruled grating with very coarse grooves, meaning there are far fewer grooves than one would find on most gratings. These grooves are made to have a very high blaze angle. This maximizes the brightness of a specific order. These gratings are popular amongst astronomy-based spectrographs due to the high resolution these result in. The downside of these spectrographs is that, as usual, the light throughput as well as the bandwidth of the system is dramatically decreased to provide this high resolution. When designing an echelle-based system, the system is usually initially designed in the Littrow configuration. This configuration provides the highest resolving power. The Littrow configuration is characterized by the output light exiting at the same angle as the input light. When using a transmission grating

this can be the final design, however when using a reflection grating, the design must be made into a Quasi-Littrow configuration. This is done by tilting the grating in a different axis, so that the grating is still tilted at the blaze angle to the incoming light, but still aims the light away from the incident beam (Zang, 2022).

Below is a table of a few ruled gratings on the market, noting important characteristics and prices.

	Groove density	size	Blaze angle	Price
Transmission Grating Edmund Optics	1800 grooves/mm	12.7x12.7 mm	NA	
Echelle ruled reflective grating	31.6 grooves /mm	50x25 mm	63.9 degrees	\$284
Echelle ruled reflective grating	79 grooves/mm	50x25 mm	63.9 degrees	\$284

Table 3.2.1.2.1: Ruled Gratings

Holographic Gratings Comparison	Edmund Optics Stock #54-512	Edmund Optics Stock #43-216	Edmund Optics Stock #15-746 Blaze wavelength=700	Edmund Optics Stock #55-264
Groove Density (grooves/mm)	500	1200	1200	1200
Wavelength Range	400-700 nm	400-700 nm	400-1200	400-700
Dimensions (mm)	50.8x50.8	25x25	25x25	12.3x12.3
Coating	Not Given	Bare Aluminum	Aluminum	Bare Aluminum

Type	Transmission Diffraction grating	Reflective Diffraction Grating	Reflective Diffraction Grating	Reflective Diffraction Grating
Peak Efficiency	Not Given	73%	Not Given	73%

Table 3.2.1.2.2: Holographic Gratings

Below is a figure of an Echelle grating. This clearly depicts the blazed angle of the diffraction grating, and the reflected wavelengths.

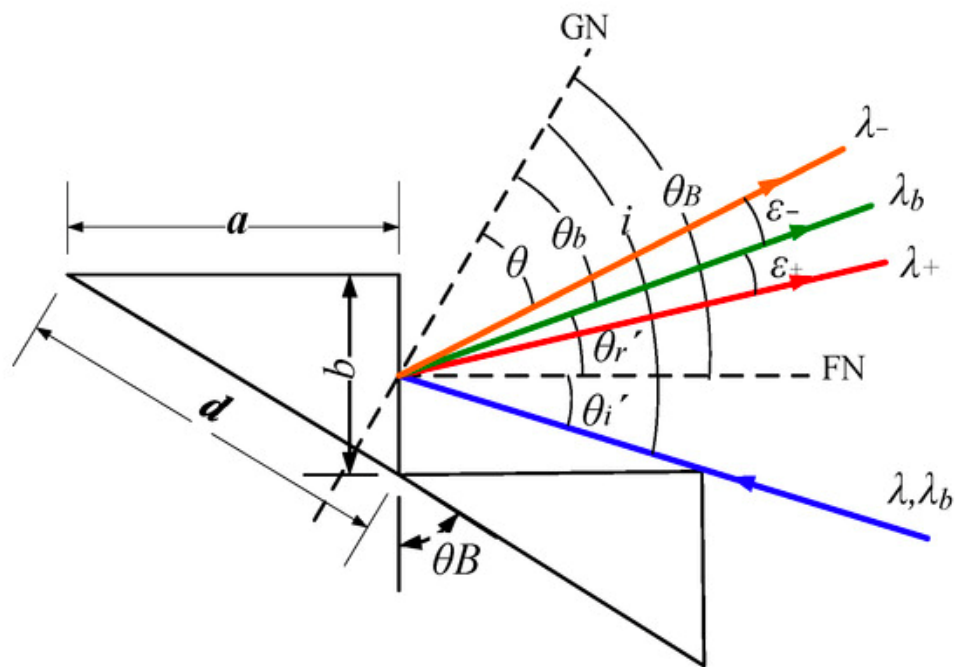


Figure 3.2.1.2.3: A close look at an Echelle grating (Zang, 2022)

3.2.1.3 Lenses

Our lenses must be chosen based off of the grating used in the final system. We will see in the design section of this paper for the spectrograph how we come to find the necessary focal length and numerical aperture of the lenses. Here we will simply discuss the choice of the type of lens. In our case, all lenses chosen will be achromat lenses. This is vital to decrease chromatic dispersion. Chromatic dispersion will directly affect the system's eventual purpose, as the spectrometer readings must be capable of reading very minor shifts in the spectrum. Even small amounts of chromatic aberration must be avoided to the best of our ability. Here, we compare the lenses that we can use for the system including the focal length, Diameter, price, and material. The highlighted rows are the lenses chosen for the

actual system. We can see from this table that increasing the diameter of a lens will increase the price. This factor comes into play with the overall design of the spectrograph, as we seek to minimize the price of our optics while we try to avoid decreasing the light throughput or overall optical resolution of the system. The maximum diameter we will choose is 50mm, which means that the beam spot size when it reaches this lens should be no larger than 50 mm to avoid cutting off light throughput. In the end, the system was designed in two different formats: Once for a collection of custom lenses which is optimized in Zemax for minimal aberrations, and once for pre-made lens systems which reduces the cost and time scale of the project. Due to the cost and time that the custom lens system requires, this project utilizes a pre-made lens system, which are Cannon telephoto lenses.

Lenses	EFL	CA	Diameter	Price
Canon F/4-5.6 III	75-300 mm	60 mm	65 mm	\$199
Collimating	85mm	24 mm	25 mm	\$114
Camera	300 mm	73.5 mm	75 mm	\$341
Canon F/4-5.6 III	75-300 mm	60 mm	65 mm	\$199
Camera	300 mm	39 mm	40 mm	\$173
Camera	300 mm	29 mm	30 mm	\$139

Table 3.2.1.3.1: Lens Selection

Mounting components play an important role in the design of the system. The size of the mounts will affect the angle that a reflective grating will be placed at, to ensure vignetting is minimized. The optical mounts which will have the lenses placed inside of them must be made to have the same clear aperture as the lens chosen. The mounts for this system are custom designed in solidworks. This system is very alignment sensitive. For this reason, the traditional alignment method of using a breadboard and adjustable mounts is a much more challenging approach to achieving perfect alignment and light throughput. Instead, the zemax ray trace of the spectrometer system is exported into solidworks. Using this ray trace, the height, angle and placement of each mount can be pre-determined and the mounts can be accordingly designed. The mounts holding the grating and prism are 3-D printed, while the mounts holding the cannon lenses and sensor are custom machined with aluminum metal. The lens mounts cannot be 3-D printed because the weight of the lenses and sensors require sturdy, load-bearing mounts with custom threads. These characteristics are not easy to achieve via 3-D printer, so the machining route was taken.

3.2.1.4 Detector

There are two different types of detectors that most spectroscopy systems use: CMOS (complementary metal oxide sensor) and CCD (charge-coupled device). CMOS detectors have a rolling shutter, capturing each pixel one by one. CCDs on the other hand capture the entire field of view at once. CMOS sensors are larger, less expensive, consume a considerably lower amount of power, and also have a high total bandwidth and speed (*CCD vs CMOS | Teledyne DALSA, 2011*). This comes at a cost, however, as CMOS sensors produce images with higher amounts of noise and lower light-sensitivity. CCD sensors on the other hand are somewhat smaller, slower, and consume about 100x as much power as a CMOS. This comes of course with higher resolution, light sensitivity, and overall image quality. Most projects that require very good image quality have generally utilized CCDs for the reasons listed above. Finally, CMOS are mostly only used for the visible spectrum. This will not be an issue for our design, however if we were to switch to measuring in the infrared it may require switching the sensor out altogether. When designing a spectrometer, there are generally three variables that come into play when choosing the size of a detector: bandwidth, groove density of the grating, and focal length of the focusing lens. The focal length of the focusing lens is generally chosen afterwards and fitted to the detector size, however (*Photonics Spectra CCD vs CMOS: Facts and Fiction, n.d.*).

For our case, we have a bandwidth of around 300 nm, and a groove density of 31.6 grooves/mm. The lab which is sponsoring this project already has a sensor, the atik apx60 CMOS sensor, which is a high resolution, low power instrument used across a wide variety of spectrometry and microscopy applications. As this sensor both has the specifications that we are looking for in a sensor and will minimize the cost of the overall project by using a device that the lab already has in stock, we chose to use this sensor rather than compare other expensive and equally as effective sensors.

3.2.1.5 Optical Fiber

The optical fiber that feeds into the spectrograph will have a significant effect on the resolution of the spectrum. The fiber will serve as the entrance slit for the light from the rooftop solar spectrometry system. The smaller the input slit, the better the resolution of our system. However, a smaller input slit also results in lower light-throughput. Because we are imaging the sun and will already be needing to decrease the input light so as to not have an oversaturated signal, this will not be an issue. There are many kinds of fibers to choose from on the market, varying in size, bandwidth, materials, and number of modes it is capable of transmitting. For our purposes, we are looking to choose a fiber which can transport a signal the distance from the roof to a lab in the same building. The diameter should be as small as possible to maximize resolution and should have a coating which is

resistant to the heat of the sun, as a portion will be on the rooftop connected to the solar spectroscopy system. We also want to reduce noise as much as possible. Fibers can be made to transport many modes of light (multimode fibers) or a single mode (single mode fiber, SMF). Single mode fibers have often been utilized for astronomy purposes, mostly because the large telescopes required a fiber diameter big enough to couple the light into, and the multimode fiber allowed a higher amount of information to be processed. However, many astronomers have been searching for methods to couple the light into the smaller, single mode fiber, for many reasons. Multimode fibers have an issue with something termed, “modal noise,” where the various modes become a part of one another’s signal along the transport along the fiber, resulting in a less than optimal resolution on the other end. This issue, as well as an issue with light escaping from the core into the cladding, increases with the length of the fiber, making it difficult to bring the light very far from the telescope systems. Because single mode fibers only transport one mode and this mode results in very little leakage into the cladding of the fiber, the light can be transported much further with single mode fiber. As mentioned before, astronomers also sought out single mode fibers for their high resolution. Many have begun utilizing special fibers which convert multimode signals into single mode, called, “photonic lanterns.” One drawback to consider however is that single mode fibers are generally more expensive than multimode fibers (*Single Mode vs. Multimode Fiber Optic Cables* | Cleerline SSF Fiber, 2019), (*To CCD or to CMOS, That Is the Question* | B&H Photo Video pro Audio, n.d.). Because our system is capturing the very large, very bright sun, our telescopes are significantly smaller than the average telescope. For this reason, we expect to encounter little to no issues with coupling light into a smaller entrance aperture. As we do not need to transport multiple types of information, and are looking to reduce noise, and need to transport the signal a relatively long distance, we have come to the conclusion that a single mode fiber is the best option for our project. A fiber can be separated into three parts: the core, the cladding, and the coating. The coating will be the part that protects the fiber from damage, either from weather or other causes. Because a portion of the fiber will be out on the roof, we need a coating which protects the fiber against up to 100 degrees Fahrenheit, as well as heavy rain and wind. Next, the fiber must be designed to guide light in the visible spectrum. Many single mode fibers are designed for the infrared, which is done by adjusting the refractive index difference between the fiber core and fiber cladding. Unfortunately, the complicated part of this project comes with the fact that we are looking to evaluate light in the visible end of the spectrum (400-700nm, peak at 550nm). Most single mode fibers are optimized for the infrared, at peak wavelengths of 1300 nm and 1550 nm. There do exist some fibers developed for the visible range, however, which have been tabled and compared below:

Fiber	Thorlabs SM400	Newport: F-SA Optical Fiber, Singlemode	Thorlabs: SM600
Operating wavelength	405-532 nm	488-633 nm	633-780 nm
Cladding Diameter	125 μm	125 μm	125 μm
Coating Diameter	245 \pm 15 μm	245 μm	245 \pm 15 μm
Coating Material	Dual acrylate	Dual Acrylate	Dual Acrylate
Operating temperature (degrees Celsius)	-55 to 85 $^{\circ}\text{C}$	Not Given	-55 to 85 $^{\circ}\text{C}$
Attenuation	≤ 50 dB/km @ 430 nm ≤ 30 dB/km @ 532 nm	50 dB/km @ 488 nm	≤ 15 dB/km
Mode Field Diameter	2.4-3.5 μm	2.8-4.1 μm @ 488 nm	3.6 – 5.3 μm @ 633 nm
Numerical Aperture	0.12-0.14	0.1-0.14	0.1-0.14

Table 3.5: Mounting Optics Selection

3.2.1.6 Mirrors

The most prominent aspects of a Fabry-Perot cavity are the partially reflective mirrors; the reflectance and radius of curvature determines the finesse and free spectral range, while coatings determine the transmissive range. Partially reflective mirrors have a partially transmitting coating on one surface and an antireflection coating on the second. Shape and surface quality are important factors in mirrors (as well as any optical surface). Any flatness in deviation can be described as either peak-to-valley flatness or root mean squared (RMS) flatness. Peak to valley is an absolute value while the RMS refers to a range of flatness. If the input wavefront needs to be preserved, a flatness of $\lambda/10$ or better flatness should be chosen. The surface quality is characterized by a scratch and dig number that describes the maximum number of imperfections a surface can have without severely increasing scattering. Hence, the smaller the scratch-dig number, the lower the scatter. Improved scratch-dig marginally increases the optics cost but is beneficial for demanding systems that require low scatter. For the Fabry-Perot etalon in this project, we do not need to minimize scattering so drastically, so we can look towards a moderate option, such as 40-20. The shape and reflectivity of the mirror, however, is incredibly significant in a Fabry-Perot cavity. Newport, Thorlabs, and Edmund Optics have a collection of broadband dielectric mirrors with a variety of shapes, sizes, and reflectance. Two flat mirrors could have a reflectance greater than 90%, but to reach the expected finesse of 100, the 98-99% range would still be a suitable option. Another option for the FPE design is to use a curved mirror followed by a flat mirror; this would increase the finesse and mode spacing but would require mode matching of the input beam. Below is a stability diagram that demonstrates that both of these configurations will generate a stable optical cavity.

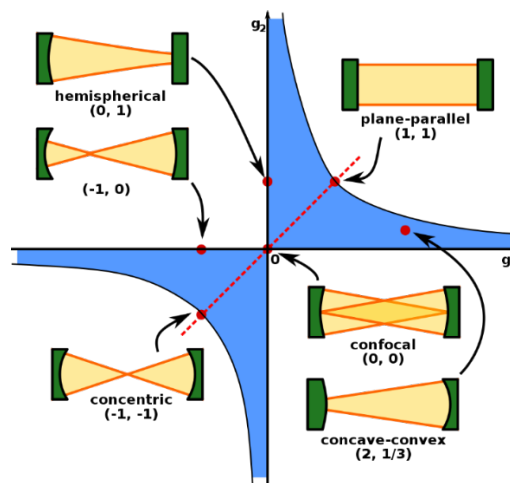


Fig. Stability diagram for a two-mirror cavity with various configurations. The shaded areas show the stable region. Image by FDominec – own work. Licensed under GNU Free Documentation License (<https://creativecommons.org/licenses/by-sa/3.0/legalcode>), via Wikimedia commons.

3.2.1.6.1 Coatings

The various coatings include metallic, dielectric, and ultrafast. Metallic coatings are generic and have a broad spectral range of 450 nm to 12 microns. Metallic coated mirrors provide a constant phase shift and are insensitive to polarization and angle of incidence. However, this coating is more susceptible to damage. Dielectric coated mirrors are composed of several different transparent layers that provide a greater selectivity for reflection wavelengths and reflectivity than regular mirrors. Dielectric mirrors have a range of several 100 nm. Dielectric coatings are also more durable and easier to maintain. The coating causes dispersive effects for ultrashort pulses that results in various phases at wavelengths. For our applications, we will not be using ultrashort pulses, so this should not be an issue. Mirrors can be ordered from any optics distributor with various specifications. Let's take Newport for example, who has a wide range of coating options. The metallic coatings all have an average reflectance of at least 90%. Newport offers Zerodur mirror substrates that have a nearly zero coefficient of thermal expansion, making it suitable for high thermal stability. Below, we have compared the selection of coatings from three different vendors.

Comparison of Mirror Coatings sold by Thorlabs.

Coating Type (Metallic)	Coating code	Wavelength Range	Reflectance
	E01	350-400	$R_{avg} > 99\%$ Pulse
	E02	400-750	$R_{avg} > 99\%$ Pulse and continuous wave
Protected Aluminum	G01	450 nm - 20 microns	$R_{avg} > 90\%$ @ 450-2000 $R_{avg} > 95\%$ @ 2-20000
Protected Silver	P01	450 nm - 20 microns	$R_{avg} > 97\%$ @ 450-2000 $R_{avg} > 95\%$ @ 2-20000

In order to increase the finesse and free spectral range, we are looking for a coating with a reflectance higher than 85% for a flat surface, 98% and a wavelength range of approximately 400 nm – 700 nm. From the tables, it can be seen that gold coatings correspond with the near infrared (NIR) to infrared range and silver corresponds with a visible to IR range. Aluminum and silver coatings would achieve the etalon's spectral range, leaving us with Thorlabs's EO2 or P01 coating, Newport's ER.2, BD.1, and BB.1 coatings, and the protected or enhanced aluminum from Edmund Optics as highlighted in each table. It is important to note that a particularly beneficial characteristic of a flat etalon mirror is an antireflective

back surface, but we were unable to find one at the time that matched the criteria we were looking for.

Radius of Curvature

Moving forward from reflectance, radius of curvature is also important in considering mirrors for a Fabry-Perot cavity. If we are going to improve the etalon, we can use a hemispherical configuration: one concave mirror with a radius of curvature greater than or equal to the length of the cavity and one plane mirror (radius of curvature of 0). This configuration would benefit from a reflectance of 98% or 99%. Thorlabs has a variety of concave mirrors for the visible range with the EO2 coating of 99%, meeting the criteria. Concave mirrors from Newport, however, only have metallic coatings in which the ER.1 would be the best option. It can be seen below that there is a wider variety of options provided by Thorlabs, though it is more costly. We've compiled a list of suitable mirrors from the three vendors so that we can make an informed decision about what we can use to build our design.

Using the information from the tables in this section, it was possible narrow down the selection to only flat mirrors, with reflectance between 98% to 99% that will produce etalon characteristics compatible with the spectrograph. This will be discussed further in the optical design chapter.

Final Mirror Comparison

	Identifier	Reflectance	L (mm)	FSR (GHz)	FWHM (GHz)	Finesse	Price (for 1)
Thorlabs	BB1-E02P	99% @ 400-750 nm	5	30	0.095	315.738	\$107.29
	PF10-03-P01P	97% @ 450 nm – 2 μ	5	30	0.282	106	\$80.94
Edmund Optics	24-029	98%-99% @400 - 750 nm	5	30	0.19	158- 315.7	\$250

Mounts

In order to get the two parallel mirrors precisely aligned, we can use a piezo controller, which eliminates the need for precise hands-on adjustments. Thorlabs sells controllers and mirror mounts with piezo adjusters to fit 0.5-2-inch mirrors. This will minimize drift and enable the Fabry-Perot cavity length to be in the nm- μ m range. This range is significant in increasing the free spectral range of the cavity. After careful consideration and calculations done in our design chapter, we

have achieved a cavity length in milometers, eliminating the need for the piezo controller. Instead, we will use mirror mounts and a translation stage to initially adjust the distance by hand. Common mirror mounts include the fixed mounts and cage plates. A cage plate assembly would be beneficial in ensuring that the two mirrors are parallel in the final product, but they would hinder our capability to finely adjust the cavity length in the initial testing and fabrication. Standard fixed mounts are secure and would be a decent option, however the distance between the mirrors will be increased by the thickness of the mount and we need a cavity length as little as 5 mm. This may also lead to limitations from mounting post and any use of translation stages. Another option was fixed self-centering jaw clamps that would enable the mirrors to protrude, minimizing the distance between the mirrors without interference from other components. However, they can be less stable than the standard fixed mounts and they enable light to pass around the mirror which would just introduce stray light into the system. Both Edmund Optics and Thorlabs sell such jaw clamps, but those on the market from Edmund Optics are thinner, causing a more protruded center. There are also thinner mirror mounts that would be an option for an improved prototype. In the early stages of building the etalon, it is important account for minor, though necessary adjustments, so we chose simple manually manual kinematic mirror mounts.

3.2.1.7 Broadband Sources

For a Fabry-Perot cavity to act as reference calibration for the spectrograph, the incoming light must have a broad wavelength range. Since we are working in the visible spectrum, a white light source can be used as the incoming light. Important properties of broadband sources include color temperature, color rendering index (CRI), luminous efficacy, and coherence. Colors are known to have “warm” and “cool” tones, determined by the temperature of a blackbody radiator. This temperature, specified in Kelvin, results in a color impression if the thermal light that matches most closely to the light of the source. Lower temperatures correspond to an optical power in the infrared range. At higher temperature, the maximum intensity of the spectrum increases and shifts to a shorter wavelength. As the color temperature increases the color tones change as follows: red, orange, yellow, warm white, and cool white. For reference, direct sunlight has a color temperature of 5900K, daylight is 6500K, warm light is 9500K, and cool light is 11500K or higher. Color rendering index is the measure of how well colors can be perceived when objects are illuminated with the light. In the case of the Fabry Perot etalon, we do not need to worry about the CRI. Instead, the spectrum will be more impactful. Luminous efficacy is the generated luminous flux divided by the radiant flux or electrical power. Luminous flux, the emitted optical energy per unit time, considers the sensitivity of the human eye while radiant flux does not. When working with the radiant flux, the luminous efficacy is dependent on the optical spectrum of the light source. Increasing operating temperature increases the luminous efficacy, decreases operating electrical power, and increases luminous efficiency (luminous efficacy/ maximum possible value of the efficacy). For any broadband source, temporal and spatial coherence are low, the latter causing difficulty in focusing light to a tight point. Thorlabs sells compact stabilized

broadband light sources that vary in emission spectra and offer free space and fiber coupled outputs. They also sell a collimation adaptor separately.

Incandescent Lamps

There are various white light sources including incandescent lamps, gas discharge lamps, fluorescent lamps, light emitting diodes (LEDs), and even lasers. Incandescent lamps are common light bulbs that naturally emit light with a smooth and broad optical spectrum. The spectrum has a color temperature of the order of 2500K, a warm light tone. Thermal radiation from an electrically heated filament, typically tungsten or halogen, produces this spectrum predominantly in the infrared range with a varying operation voltage across lamps. A lack of the visible spectral region results in a low luminous efficacy and reduced lifetime.

Gas Discharge and Fluorescent Lamps

Gas discharge lamps generate luminescent light by sending an electric discharge through ionized gas. The resulting spectrum is commonly in the visible or ultraviolet regions. High pressure arc lamps operate continuously at higher current densities and gas temperatures, have enhanced radiance and luminous efficacy. Long arc lamps produce higher average powers, but short arc lamps are beneficial when the light is to be collimated or focused, because they produce a small light-emitting volume. The lifetime varies according to the type and operating conditions: long when high power density is required, long lifetimes are harder to achieve. Fluorescent lamps produce fluorescent light generated by irradiation of a phosphor with light from an electric gas discharger a more structured white light and have a low color rendering index. Gas discharge lamps, however, have several environmental burdens and safety hazards due to hazardous and poisonous substances if mishandled.

Light Emitting Diodes

Light emitting diodes (LEDs) are another option that generate light through electroluminescence, though they do not generate white light. The center wavelength of the emitted spectrum is determined by the bandgap energy of the semiconductor. White LEDs are either made up of red, blue, and green emitted light or a blue LED and phosphor that absorbs some of the blue light and emits fluorescence at longer wavelengths. From the emission spectra below, we can see that the white LED has a broader, more continuous bandwidth than alternative sources.

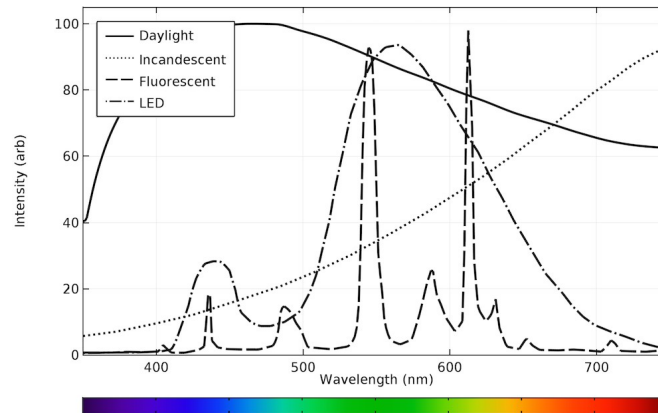


Fig 3.2.1.7.1 Comparison of emission spectra of various broadband sources (Smith, 2023)

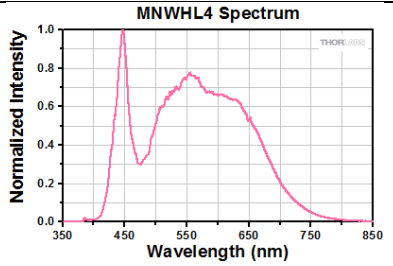
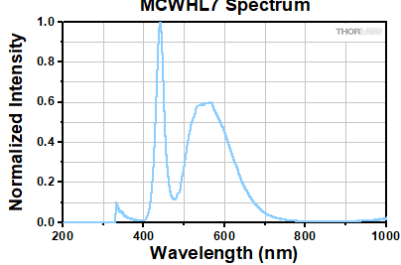
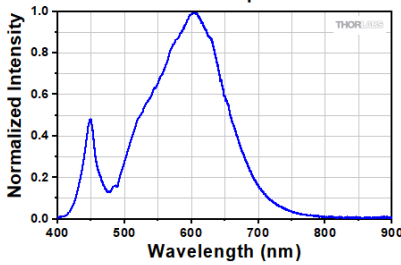
Before choosing the appropriate broadband source, it is also important to compare their efficiency and lifetime to account for the fact that the source will be constantly running. A full comparison of the broadband sources is demonstrated in the next table.

Comparison of General Broadband Sources

	Incandescent Lamps	Gas Discharge Lamps	Fluorescent Lamps	Light Emitting Diodes
Spectrum	Infrared	Smooth in the visible and/or ultraviolet regions	Visible or ultraviolet Varying power spectral density	Visible
Color Temperature	Soft white	Varies with gas	Soft white, bright white, daylight	Warm white, cool white, daylight
Efficiency	Limited luminous efficiency	Moderate-High	Moderate-High	High quantum and power efficiency
Lifetime	1,200 hrs	10,000 hrs	15,000 – 20,000 hrs	25,000 hrs

With this comparison, we determined that over the alternatives, a white LED will produce the ideal spectrum with a high efficiency and long lifetime. Fiber coupled white LED sources are available, though they reach the thousands in price. Thorlabs does offer cheaper options from \$440 to \$800, with the most ideal option being at a color temperature of 4000 K. The output power of the fiber coupled sources is dependent on the output fiber's core diameter, so the output power is limited to 27 mW. To account for cavity loss, we are currently prioritizing a high output power and broad spectrum. Such an output power may be enough, but either way we will need to conduct tests to determine how the source will be impacted by the system. An alternative option would be mounted white LEDs that are high in power and can be paired with a collimating lens. Thorlabs also sells such LEDs with color temperatures from 4000 K to 6500 K that both emit a relatively broad spectrum with options for high output power. The neutral white option in the table below is an appropriate combination of high power with a spectrum that consistently spans the visible spectrum.

Comparison of Mounted White LEDs

	Output Power (mW)	Color Temperature (K)	Spectrum
MNWHL4	740	4900 (Neutral White)	
MWUVL1	235		
MCWHL7	930	6500 (Cold White)	
MWWHLP2	1713	3000 (Warm White)	

In order to use the white LED, we must also get a T-Cube LED Driver. This is a manual driver with a mode for constant current, which is necessary for the LED to act as a continuum source. This source can drive LEDs with currents from 200 mA to 1200 mA, and the output power can be varied.

With MNWHL4 source, a compatible collimating lens can be chosen. Since we want the entirety of the incoming beam to hit the cavity, the collimated beam must be less than the diameter of the mirrors. Considering a 40 mm mirror, the collimating lens should be less than 1.5 inches. An ideal lens choice would be achromatic to prevent chromatic aberration and coated with an antireflection surface for the spectrum of the white LED (400 – 700 nm) to maximize transmission. Aspheric lenses are typically used to collimate incoming light sources and their shape minimizes spherical aberration. Thorlabs happens to sell a 25 mm Aspheric Condenser Lens with an antireflective coating over 350 – 700 nm. This was a beneficial component, though we went with a plano-convex lens with a 35 mm focal length that enabled better collimation with less divergence than the condenser lens.

3.2.2 Hardware System

For the hardware that we used in our project to integrate into our system, we needed to do a lot of research as far as which parts will be best to use for our system. Some of the comparisons that we made were based on the different types of power supply that can be used for the system. From there after deciding on the power supply we needed to figure out the types and features of each one to make the right decision. With the power supply researched we end up looking into the different types of plugs that can be used and their functionality, prices, capability, and durability. Another hardware part we researched was the types of motors that we can use for our weather machine, as well as the motors that we used for the mount of the actual system. The different types of cameras that are integrated in the system for the picture portion that need to be included. The PBC board, and finally the actual weather machine that protects the system from severe weather.

3.2.2.1 Power Supply

For the power supply that we are planning to use in our system we had different options to choose from, our first thought was to go with solar power, we also had the option to do DC power supply or AC power supply. Our interest on solar power supply is mainly because since the system that we are building will be for the roof of the UCF CREOL building it was the kind of obvious way to go. Since solar power supply is generated directly from the sun and our goal is to be tracking the sun continuously. One great thing about solar power is that is renewable and sustainable since the sun is a constant source of energy. The solar power supply does not produce any emission that can lead to pollution of the environment. In the long run the use of solar power supply becomes cheaper to use since no fuel costs are considered. One disadvantage of using solar power is that it can be less

reliable, which was one of the reasons why the sponsor wanted us to use a different method. It is less reliable because it must be relied on weather conditions, and as we all know Florida weather is extreme. If we chose to do the solar power supply, we were going to have to also think of a method to store energy in our system so that the project could always stay on even if it was nighttime or a cloudy day. Solar power is cleaner and a more sustainable option for energy generation.

Now on the other hand AC power supply is generated from power plants that burn fuel like coal or natural gas. AC power relies on non-renewable resources that are finite and can be depleted. AC power is also a big factor for killing the environment since it generates greenhouse gases that contribute to climate change. AC power can be costly due to the need to purchase fuel and maintain power plants. One of the main reasons for which electric power for the consumers goes up 4% every year. AC power is more reliable than solar power since solar power depends on weather conditions while AC power can be available everyday all day as long as there is fuel to be burned. And although solar power is cleaner AC power is more reliable and widely available.

The sponsor wants the power supply to be a plug-in method, so we end up choosing the AC power supply method for our system. An AC power supply is a type of power used to supply alternating current power to the load of the system. Power systems are primarily characterized by their range of voltage, the frequency, if it is either a plug and sockets, grounding (earthing system), and the protection that needs to include against overcurrent damage, electric shock, and fire hazards. AC power plugs and sockets allow electric equipment to be connected to the primary alternating current power supply. The electrical sockets and plugs differ from one another in voltage and current rating, their shape, the size and the connection type.

There are several different types of AC power supply systems available on the market, each with their own advantages and disadvantages. A plug is the movable connector attached to an electrically operated device, and the socket is fixed on equipment or a building structure and connected to an energized electrical circuit. The plug is a male connector, often with protruding pins that match the openings and female contacts in a socket. Some plugs have female contacts that are used only for an earth ground connection. Some plugs have built-in fuses for safety. To reduce the risk of electric shock, plug and socket systems have safety features in addition to the recessed contacts of the energized socket. As mentioned before when working with AC power we want to consider the grounding, the polarization, voltage rating and frequency. Below we want to share more in-depth detail of why these factors are taken into account.

When dealing with the polarization of the plug, where a neutral conductor exists in the supply wiring, the polarization of the plug can improve the safety features of it by preserving the distinction that is in the equipment. In some designs, polarized plugs cannot be mated with a nonpolarized socket. As far as the grounding or

earthing of the plug goes, a third contact for a connection to earth is intended to protect against insulation failure of the connected device. The plug is often designed in a way that the earth ground contact connects before the energized circuit contacts. Finally, the voltage ratings of plugs and power cords, where the voltage and current is always assigned by the manufacturer. The use of a plug with the inappropriate voltage rate can cause a safety hazard. Plugs are categorized in types. When comparing these different types of AC power supply plug, it is important to consider factors such as compatibility with different types of outlets and ease of use. The standard US two-prong plug is easy to use and compatible with most of US's outlets but may not be suitable to use in other countries since for the 14 different types each country has a preference and a more commonly use one. The types include A, B, C, D, E, F, F/G, G, H, I, J, K, L. The characteristics of some of the types that we looked into using are listed below.

The Type A (NEMA 1-15) is an ungrounded plug. Which has two parallel blades and are rated 15 A at 125 volts. They do not provide ground connection but fit a grounded NEMA 5-15 receptacle. Most of them are polarized via a wider neutral blade. The advantage of a plug type A is that include easy availability and compatibility with many North American electrical outlets. A disadvantage of this plug is that it is not compatible with many international outlets, which makes it difficult to use outside of North America.

The type B (NEMA 5-15) plug is grounded it has two flat parallel blades plus a ground pin. This plug is rated 15 A at 125 volts. The ground pin is longer than the line and neutral blades so that when it gets inserted the plug connects to the ground before it connects to the power of the socket. This B-plug is also a North American plug as well as used in the United States, Canada, and Mexico. Advantage of the B-plug include safety and reliability due to the grounding pin, and compatibility with many North American electrical outlets. But just like A-plug it has the disadvantage of not compatibility with most international outlets.

The type D plug with two pole and an earthing pin, use with an AC 50-60 Hz circuit with up to 250 volts rated at 2 A and 5 A. The plug has three round pins arranged in a triangle, with the larger top pin being the earthing pin. This plug is polarized and infused and not interchangeable between current ratings. The type D plug is an Indian plug and is primarily used in South Asia, including India, Sri Nepal, and Bangladesh. Advantages of the D type plug include compatibility with many international outlets and most importantly the ability to handle high voltage. When it comes to the disadvantage for this plug include potentially unsafe wiring and an increased risk of electrical shock.

Type M plug are the same as type D but with a rating of 15 A and 30 A. This plug is also an Indian plug. It has the advantages of compatibility with many international plugs, as well as the ability to handle high voltages and lastly the

safety feature due to the grounding pin. The main disadvantage for the M type plug is its size, which may make it difficult to use with some outlets.

The type G plug is rated 13 A at 250 volts. This plug has three rectangular pins forming an isosceles triangle. This plug includes a fuse rated that protects its flexible cord from overload and fire hazard. This type of plug is British, and it is used in the United Kingdom, Hong Kong, and some other countries. Some advantages of this plug include the safety feature due to the inclusion of a fuse, the compatibility with many international outlets, as well as the ability to be able to handle high voltages. Importantly this plug is larger than many other plug types, which makes it somewhat less portable and potentially difficult to use with some outlets. We originally wanted to use a type G plug since it checked off most of the functionalities that we want to achieve and more, like the inclusion of the fuse, and the handleability oh higher voltage, but not that many places in the US have sockets for this type of plugs. We will instead be using a type B, since this type is grounded, polarized and has a rating that will be able to manage the current and voltage that will be integrated in our system design. Figure 3.2.2.1 summarized the plugs type that we made research on to make a decision as far as which one to use.

Type	Standard	Rating	Earthing (Grounded)	Polarized	Fused	Insulated pins	Price range
A	NEMA 1-15 polarized	15 A 125 volts	No	Yes	No	No	\$5.00- \$30.00
B	NEMA 5-15	15 A 125 volts	Yes	Yes	No	No	\$5.00- \$30.00
D	BS 546	6 A 250 volts	Yes	Yes	Optional	Optional	\$10.00- \$40.00
M	BS 546	15 A 250 volts	Yes	Yes	Optional	Optional	\$10.00- \$40.00
G	BS 1363	13 A 250 volts	Yes	Yes	Yes	Yes	\$2.00- \$15.00

Figure 3.2.2.1 Plugs type (Wikipedia., 2003)

After making all the necessary research to make a decision on the power plug that we want to use for our system we made the decision to use the plug type B. we decided to use this plug type because this one will be able to meet the voltage that

we want to use in our system, it meets the current that we want to have our system to support, it is a reliable durable plug. It is a plug that will resist polarization.

3.2.2.2 Weather Station

As part of the weather protection system, our observatory needs real-time sensors ready to provide meteorological data. At the same time, accurate and reliable weather data is essential to ensuring optimal performance of the observatory and data analysis as we need to keep track of weather conditions every certain time while tracking the sun and analyzing its spectrum. There are two ways to approach this. First, we could design our custom sensor integrated system. This system should be water/dust resistant and include the following sensors: anemometer (wind speed and direction), temperature, humidity, barometric pressure, solar radiation, UV index, and rainfall detection. Second, we could purchase a ready-built weather station kit that already comes with all these sensors integrated and it is ready to use. There are many factors to consider when making this decision. Some advantages and disadvantages of using a ready-built weather station system rather than a custom-system design are:

Advantages	Discussion
Convenience	A ready-built weather station provides a convenient solution as they come pre-assembled and calibrated. This could save us time and effort compared to designing and integrating a custom sensor system
Compatibility	Weather stations are designed to work seamlessly since compatibility between sensors and the data acquisition system is assured. This could eliminate extensive testing and troubleshooting during integration with our observatory
Accuracy and Calibration	Manufacturers ensure calibration processes in order to get accurate measurements. This results in reliable and precise data collection
Established Performance	There are very popular brands that we have found during our research that have been used for different projects and applications. They are often designed to meet industry standards and are tested in various environments
Support and Documentation	This equipment usually comes with comprehensive documentation and user manuals. Also, some manufacturers can provide customer support, firmware updates, and resolve potential issues

Table (3.2.2.2a). Ready-built weather station advantages

Disadvantages	Discussion
Limited customization	This station kit offers a fixed set of sensors and features. When additional sensors are required, customization options may be limited
Cost	Weather stations can be relatively expensive compared to designing and integrating a custom-designed sensor system
Dependency on manufacturer	Depending on their complexity, when using these weather stations, the customer relies on the manufacturer for ongoing support and maintenance. That is why it is important to find a very simple system that won't require this level of dependency
Integration limitations	Integrating a weather station into a specific project or setup may pose challenges due to physical space constraints, wiring, or power limitations. Custom-designed solutions can be more flexible
Compatibility with existing infrastructure	Weather station data format, software and integration compatibility may cause some constraints. One example could be communication protocols

Table (3.2.2.2b). Ready-built weather station disadvantages

Our decision to use a ready-built weather station kit or design a custom-sensor system depends on our next evaluation factors such as customization requirements, budget, accuracy needs and integration considerations. Selecting the appropriate weather station type is very important for the success of our project. If we decide to go for a ready-built weather station, we will need to select a product that includes all the necessary sensors while ensuring accuracy. By employing the recommended weather station kit, our observatory can collect comprehensive weather data for an effective solar spectrometry analysis and the weather protection system reliability.

We conducted research for ready-built weather stations with temperature, humidity, barometric pressure, anemometer, solar radiation, UV, and rainfall detection and came out with the following products as the most popular and reliable on the market:

Brand	Product model	Sensors	Features	Price
Ambient Weather	WS-2000	Anemometer, rainfall, UV, solar radiation, barometric pressure, temperature, humidity, dew point, wind chill	LCD display tablet, Water/dust resistant, Wi-Fi, 5V DC adaptor, Power Consumption 0.5W and 1.25W during Wi-Fi config mode	\$299.99
AcuRite	Atlas 01108M	Anemometer, rainfall, UV, Light intensity, barometric pressure (from the screen), temperature, humidity, Lightning detection	Non-WiFi HD Display, 5V power adapter, battery option for backup, lightning detection 1 to 25 miles, Water/dust resistant	\$218.16
Davis Instruments	SKU 6357	Anemometer, Rain detection, temperature, humidity,	Solar-powered with lithium battery backup, extreme testing, corrosion protected, UV protected	\$350
Oregon Scientific	WMR89A	Anemometer, rainfall, optional UV, humidity, barometric pressure, heat index, dew point, wind chill	Water/dust resistant, LCD screen, long-range transmission 330ft., AC adapter and battery for backup	\$199.99

Table (3.2.2.2c). Most accurate weather station equipment brands

3.2.2.3 Computer – MCU

Our observatory platform depends on a computer system which is capable of operating at across various organizational levels and can perform mission critical tasks to achieve our desired results. This means that the choice of a computer system will have an enormous impact on our finished product. In this section, we will compare different types of computer systems often used in embedded systems, and then discuss a select few commercially available systems.

First, let's take a look at microcontrollers and microprocessors. A microcontroller is an individual integrated circuit (IC) programmed to perform a specific application, which will usually be integrated with additional peripherals. A microprocessor is a central processing unit (CPU) that is on a single IC (Desk, 2021). These definitions tell us that microprocessors are more flexible in the applications they can execute than microcontrollers, which can only perform the singular task they're programmed to perform. Also, notice that both microcontrollers and microprocessors are individual ICs, often used as parts of larger systems. Microcontrollers will put the required peripherals (ADCs, DACs, Timers, etc.) into the IC, while microprocessors will be connected externally to other components (think of how a motherboard houses the CPU on a personal computer, 'PC'). Neither microcontrollers nor microprocessors will be sufficient on their own to compose our computer system, they will need to be integrated into larger systems for our purposes.

So, what kinds of systems do we have available for our project? There are three notable choices that we have considered: System on Chip (SoC), System on Module (SoM), and Single Board Computers (SBC). The System on Chip is an IC that integrates all of the components of a computer system (*What is a System on Chip (SoC)?*). This makes the SoC a standalone computer, making it more efficient in terms of cost and power consumption, but less flexible in terms of components. A System on Module is a circuit which integrates all of the required system functions into a module, with space for additional components (*System-on-Modules (SOMs): How and Why to Use Them*). The SoM can be thought of as a motherboard which is capable of functioning on its own but can include other components not already present. A Single board Computer is a complete computer system on a single circuit board (*What are single-board computers?*). The SBC often includes a SoC but does not offer any expansion slots for peripherals.

These systems encapsulate different design philosophies that determine their use cases. SoC is a single chip that has all of the components of a computer system, but it is typically integrated into larger systems like SBCs that can add additional peripherals while making use of their performance. The SoM provides a modular design that makes it more extensible, whereas SoCs and SBCs are static devices ("System on Module VS Single Board Computer,"). The SoC and SoM both

provide the necessary components of a computer system on a single circuit board, while the SBC integrates various circuit boards to achieve the functionality of a PC(akshaybotre203). Of these systems, we will focus our attention on SBCs and SoMs. SoC's will not be our main focus since they may require more complex board design to integrate them along with the rest of our hardware components. The SBC will have everything we need to build our observatory out of the box, not requiring any additional parts. Meanwhile, the SoM will offer flexibility in terms of components in case we need to extend its capabilities later on. Now we will take a look at the commercially available options for our computer.

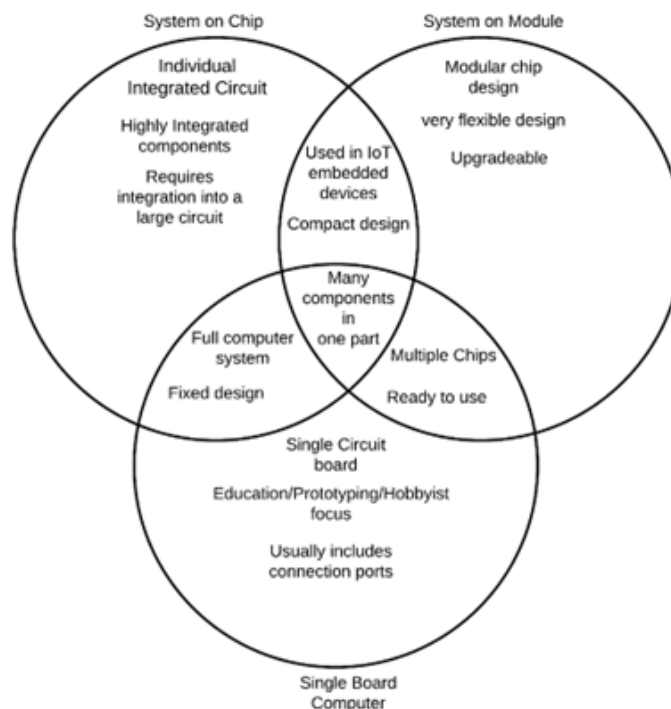


Figure 3.2.2.3.1 Comparison of SoC, SoM and SBC systems

First, we'll look at the Raspberry Pi line of systems. The Raspberry Pi is a series of SBCs developed by the Raspberry Pi foundation, a UK-based charity whose mission is "to enable young people to realise [Sic] their full potential through the power of computing and digital technologies."(*About us*).(). For our comparison, we will be taking a look at their three lines of products: the Raspberry Pi, Raspberry Pi Zero, and Raspberry Pi Pico. Each of these products has undergone several revisions, so to make the comparison fair we will be looking at the latest revision for each product.

First, we'll observe the standard Raspberry Pi. The current version is the Raspberry Pi 4 model B. The Pi 4 is an 85 mm by 56 mm single board computer boasting a powerful Quad core Cortex-A72 processor, and up to 8 GB DDR4

SDRAM. The Pi 4 offers a variety of different connectors: 2 micro-HDMI ports, 2 USB 3.0 and 2 USB 2.0 ports, and a Gigabit Ethernet port. There are also some notable features including H.265 (4kp60 decode), H264 (1080p60 decode, 1080p30 encode), a 40 pin GPIO header, and a Micro-SD card slot to store data and load the operating system(*Raspberry Pi 4 Tech Specs*). I point these features out because all of these features are important to achieving our objectives. The High Efficiency Video Coding shows that the Pi 4 is capable of handling intensive image processing applications, which will assist us in capturing images from the camera and transferring them over USB. The 40 pin GPIO header will allow us to integrate the many sensors required to implement our weather station and sun tracking functionalities.

Now let's take a look at the Raspberry Pi Zero line of products. The most current version is the Raspberry Pi Zero 2 W. The Pi Zero is a 65mm by 30mm board with a 1GHz quad-core 64-bit Arm Cortex-A53 CPU. It offers 512MB on-chip SRAM with a mini-HDMI port, a micro-USB port, and H.264, MPEG-4 decode (1080p30); H.264 encode (1080p30)(*Raspberry Pi Zero 2 W*).(). The Pi Zero also has an unpopulated 40-pin header footprint, so some assembly may be required . The Pi Zero is the smaller, slightly less powerful version of the Pi 4, but what it loses in performance makes up for in a smaller form factor. This makes the Pi Zero ideal for Internet of Things (IoT) applications.

Finally, we'll examine the Raspberry Pi Pico. The newest Pico is the Raspberry Pi Pico W. The Pico is a tiny 21 mm by 51 mm board with a Dual-core Arm Cortex-M0+ processor and 264kB on-chip SRAM. It offers 26 GPIO pins and 2 MB on-board flash memory. The Pico is a small device meant to perform simple tasks. It's best suited to niche IoT applications and starter projects. Unfortunately, this means that it's probably not well suited to our project.

The next line of products we're interested in is the NVIDIA Jetson series of products. These systems came as a recommendation from our project sponsor, Dr. Eikenberry, as the NVIDIA jetson line is commonly used in astronomical computing applications. According to NVIDIA, "Each NVIDIA Jetson is a complete System on Module (SOM) that includes GPU, CPU, memory, power management, high-speed interfaces, and more. They're available in a wide range of performance, power-efficiency, and form factors so they can be used by customers across all industries. Jetson ecosystem partners provide software, hardware design services, and off-the-shelf compatible products from carrier boards to full systems, so you can get to market faster with AI embedded and edge devices."(*NVIDIA Jetson*).(). The clear focus of the jetson line is producing AI-enabled embedded applications at large scale. This motivates the system to have fast processors and multi-core GPU systems. This is ideal for our purposes as we can leverage AI models to detect whether it's expected to rain or not, and with what likelihood that will happen.

NVIDIA has four series of NVIDIA Jetson products: the Jetson Orin, the Jetson Xavier, the Jetson TX2, and the Jetson Nano. Each one is designed to fill a specific niche for embedded applications. The Orin series offers the most powerful systems of the bunch. The Xavier series is a more balanced design intended for usage in fully autonomous machines. The TX2 is a smaller family of embedded modules that are optimized to maximize performance while lowering power consumption. Finally, the Nano line is the smallest of the bunch, designed to be a small computer with the performance and power to run modern AI workloads. Of these four series of products, we will be looking closer at the Orin and Nano lines of computers. The Xavier line is better suited to large-scale industrial products, which are beyond the scope of our project. Meanwhile, the TX2 sits in the middle, between the Nano and Orin lines of products, but not different enough from either one to stand out.

The Jetson Orin line has three series: the Jetson AGX Orin, Jetson Orin NX, and the Jetson Orin Nano. Of these three the AGX has the fastest processors, up to 2.2 GHz on a 12 core ARM Cortex 64-bit CPU, while the Nano has the slowest processors, that being a 6 core ARM Cortex 64-bit CPU at 1.5 GHz. Both should be more than fast enough for the applications we need them for. The AGX offers up to 64 GB DDR5 RAM, the NX has up to 16 GB DDR5, and the Nano has up to 8 GB. Each one offers several USB 3.0 and USB 2.0 ports, high efficiency video coding, and display ports. They all have pins that support UART, SPI, I2C, I2S, and other standards for embedded system sensors. The Nano offers an impressive 7 W– 10 W power consumption, while the AGX is much more power hungry, with anywhere from 15 W – 60 W (*The Future of*

Industrial-Grade Edge AI).

The Jetson Nano is an individual product line, offering big performance in a small form factor. The Jetson Nano has a Quad-core ARM® Cortex®-A57 MPCore processor that runs at 1.43 GHz. It runs on 4 GB DDR4 with 16 GB eMMC flash memory. The Nano also includes USB 2.0 and USB 3.0 connectors, and contains UART, SPI, I2C, I2S, and GPIO connectors. The overall power consumption of the Nano is 5W – 10W. This makes the Nano an interesting choice, because it has strong performance for a small computer at a lower price point.

We have looked at several different product lines offered by the Raspberry Pi foundation and NVIDIA. So, which one should we use for our project? Well, the computer will have three main operations: using the weather station to predict the short-term climate, tracking and imaging the sun, and operating the observatory platform. To achieve these operations, we need a computer that will be able to capture and compress images quickly, possibly operate an AI model, and read and transmit data. With these considerations in mind, the NVIDIA Jetson Nano is the best choice for our project. The Nano has all of our required connections, it delivers the performance to run modern AI, and it comes in a small package. All of these factors combined make it a great choice for an observatory platform where we

want to keep the platform small, we need to capture and transmit data, and we need to be able to predict weather events before they happen. Thus, we will be using the NVIDIA Jetson Nano for our project.

	Jetson Orin Nano series		Raspberry Pi		
	Jetson Orin Nano Developer Kit	Jetson Orin Nano 8GB	Raspberry Pi 4 Model B	Raspberry Pi Zero	Raspberry Pi Pico
CPU	6-core Arm® Cortex®-A78AE v8.2 64-bit CPU 1.5 GHz		Broadcom BCM2711, Quad core Cortex-A72 (ARM v8) 64-bit SoC 1.8 GHz	single-core CPU 1 GHz	Dual-core Arm Cortex-M0+ processor 133 MHz
Memory	8GB 128-bit LPDDR5		8GB LPDDR4-3200 SDRAM	512 MB RAM	264kB on-chip SRAM
USB*	USB Type-A Connector: 4x USB 3.2 Gen2, USB Type-C Connector for UFP	3x USB 3.2 Gen2 (10 Gbps), 3x USB 2.0	2x USB 3.0, 2x USB 2.0	micro USB On-The-Go (OTG)	1x USB 1.1
Display	1x DisplayPort 1.2 (+MST) connector	1x 4K30 multi-mode DP 1.2 (+MST)/eDP 1.4/HDMI 1.4**	2x micro-HDMI	Mini HDMI	
Other I/O	40-Pin Expansion Header(UART, SPI, I2S, I2C, GPIO), 12-pin button header, 4-pin fan header, microSD Slot, DC power jack	3x UART, 2x SPI, 2x I2S, 4x I2C, 1x CAN, DMIC & DSPK, PWM, GPIOs	40-pin header	40-pin header	26 GPIO pins, 3 Analog inputs, 2 UART, 2 SPI, 2 I2C, 16 PWM
Power	7W - 15W	7W - 15W	15 W		
Mechanical	100 mm x 79 mm x 21 mm	69.6mm x 45mm	56.5mm x 85.6mm	65mm x 30mm	51mm x 21mm

	(Height includes feet, carrier board, module)	260-pin SO-DIMM connector			
--	---	---------------------------	--	--	--

3.2.2.4 Motors

3.2.2.4.1 Stepper Motors

Stepper motors are the heart of the solar tracking system since their accuracy and efficiency will mean a successful implementation of our project concept. They are a key component that plays a very important role in ensuring precise and accurate movement of the observatory platform (telescopes and cameras). This research section focuses on discussing various types of stepper motors that we could use in our senior design project for the solar tracking system. From a solar PV panel perspective, solar tracking systems aim to optimize energy capture by aligning solar panels with the sun's position, maximizing the exposure to sunlight. For our project point of view, we do not need PV panels because we are not going to be using solar energy for our device. In this case, the observatory platform will be our focus instead of a solar PV panel. The use of stepper motors for solar tracking systems could provide precise control of the observatory platform, reliable performance and the ability to maintain static holding torque.

For this discussion, we conducted research on stepper motor types for solar tracking applications. The most commonly stepper motor types used in solar tracking systems are hybrid stepper motors, permanent magnet stepper motors, and variable reluctance stepper motors. Each one of them exhibits unique characteristics in terms of torque output, accuracy, speed, cost, availability, size, power consumption, and weight. In a review study by Anuraj et al., authors mention that stepper motors are commonly used in positioning control applications. According to them, five characteristics are very important when selecting a stepper motor: brushless, load independent, open loop positioning capability, good holding torque and excellent response. They recommend hybrid stepper motors and describe what a typical controller for this type of stepper motor should include: logic sequence generator, power drivers and current limiting circuits (Anuraj & Gandhi, 2014).

In another research literature, Malav et al., authors recommend the 17PM4054 stepper motor model which, according to them, provides very precise, extremely cost-effective motion control. It is a 2-phase motor, and it moves at 1.8-degree increments at 200 steps/revolution. It is brushless and maintenance free. It does not require complicated expensive feedback devices. They also provide the electrical and physical specification of the stepper motor as it follows (Malav & Vadhera, 2015):

Step angle: 1.8 deg, Steps per revolution: 200, Angular accuracy: +/-3%, Phases: 2, Operating temperature: -20 to 40 degrees C, Radial: 6.8kg at shaft center, Axial push: 2.7 kg, Axial Pull: 6.8kg.

The following is a comparison table for the most popular stepper motor for solar tracking applications from our research:

Comparison Field	Hybrid Stepper Motor	Permanent Magnet Stepper Motor	Variable Reluctance Stepper Motor
Description	Magnetized rotor with teeth and a stator with windings	Energizing the stator windings aligns the rotor with the magnetic field	Exciting the stator windings aligns the rotor to minimize magnetic reluctance
Torque Output (N.m)	0.05 – 20	0.1 -1	0.05 -0.5
Accuracy (degrees)	0.05 – 1.8	0.2 - 2	0.5 – 2
Speed (RPM)	100 – 6000	100 - 3000	500 – 3000
Cost (USD)	\$50 - \$200	\$20 - \$100	\$30 - \$150
Weight (Kg)	0.5 – 2	0.2 - 1	0.3 - 1
Size (Length x Diameter)	42 x 42 mm – 86 x 110 mm	20 x 20 mm – 42 x 42 mm	20 x 20 mm – 57 x 57 mm
Environmental Impact	Low	Low	Low

Table (3.2.2.4.1a). Most popular stepper motor types for solar tracker applications

From all the research and the comparison table we can conclude that Hybrid Stepper Motor will be our desired option when designing the hardware. Then, considering that the platform where telescopes and camera will be placed weights approximately 5-pounds, the sun moves across the sky at an average of 0.25 degrees per minute (the sun moves one sun-diameter every two minutes) and, the radius stepper motor shaft used for this type of systems is approximately 0.25 inches, we proceed to calculate the required Torque from each hybrid stepper motor including a 20% safety margin for a better accuracy when tracking the sun:

$$\text{Torque} = (\text{total weight platform}) * (\text{stepper motor shaft}) * \pi * 0.1130 \text{ N.m/lb.inch} + 20\%$$

$$\text{Torque} = (5\text{-pounds}) * 0.25 \text{ inches} * \pi * 0.1130 \text{ N.m / lb. inch} + 20\%$$

$$\text{Torque} = 1.0924 \text{ N.m} * 1.2 = 1.3109 \text{ N.m}$$

From these calculations, we conclude that the stepper motors will need to have a holding torque of at least 1.3109 N.m.

Based on research and the most popular hybrid stepper motors used for these types of solar tracking systems, we selected hybrid stepper water resistant motors considering their high quality, accuracy and IP65 rating required for outdoors. Also, a closed-loop stepper motor is preferable since we can be able to monitor if the motor misses a step during movement which allows us to correct it. See table below for options comparison:

Stepper Motor	Step Angle	Holding Torque	IP Rating	Dimensions (mm)	Voltage Range (V)	Temperature Range (°F)
NEMA 23 Stepper Motor 3Nm IP65	1.8°	3 N.m	IP65	76 x 42 x 29	12-24	-4 to 158
NEMA 34 Stepper Motor 5Nm IP65	1.8°	5 N.m	IP65	110 x 62 x 42	12-24	-4 to 158
NEMA 42 Stepper Motor 10Nm IP65	1.8°	10 N.m	IP65	132 x 76 x 55	12-24	-4 to 158
NEMA 51 Stepper Motor 15Nm IP65	0.72°-1.8°	15 N.m	IP65	145 x 90 x 60	24-48	-4 to 158
NEMA 43 Stepper Motor 12Nm IP65	0.9°-1.8°	12 N.m	IP65	115 x 65 x 40	12-24	-4 to 158

Table (3.2.2.4.1b). NEMA hybrid stepper motors with IP65 rating

Since the solar tracker system needs to be accurate enough to have the telescopes and camera pointing always in the right direction, we have selected the hybrid stepper motor with the best step angle degree that can keep up with the sun's path movement velocity of 0.25 degrees every minute and have enough torque to guarantee the platform movement based on previous calculations.

3.2.2.4.2 Weather Protection motor

For the weather protection station that we built for us to use in our system we integrated a motor that responsible for closing and opening the station in case of

severe weather, like rain or strong wind. When looking into which type of electric motor to use, I came across distinct types with contrasting functions and capabilities. There are the AC Brushless Motors, the DC Brushed Motors, the DC Brushless Motors, the Direct Drive Motors, the Linear Motors, the Servo Motors, and the Stepper motors. Before deciding which one we were going to use for our system, I made sure to compare all 7 of them as far as cost, capability, durability, efficiency and functionality.

The AC Brushless Motor is one of the most popular motors, as far as motion control goes. The way this motor operates is relying on permanent electromagnets. This motor consists of an outside stator that produces a rotating magnetic field, and an inside rotor that produces a second rotating magnetic field. It uses induction of a rotating magnetic field generated in the stator so it can turn the stator and rotor at a synchronous rate. The brushless wound-rotor doubly fed synchronous motor system has an independently excited rotor winding that does not rely on the principles of slip-induction of current. It is synchronous and can function exactly at the supply frequency or sub to super multiple of the supply frequency. This motor has a life expectancy of 10 to 20 years. They range from \$75.00 to \$600.00 dollars. This type of motor is adaptable to meet the needs of a variety of functions, since they are efficient and have low noise. They can be used and be found in pumps, water heaters, garden equipment, ovens, and off-the-road motorized equipment.

The DC Brushed Motor the brush orientation on the stator is what determines the current flow. The brush's orientation relative to the rotor bar segments is decisive in some of the models. In any DC brushed motor design, the commutator is important. It is an internally commutated electric motor, that runs from a direct current power that uses an electric brush for contact. These motors can be varied in speed by changing the operating voltage or the strength of the magnetic field. The speed and torque characteristics of a brushed motor can be altered to provide steady speed or speed inversely proportional to the mechanical load. These types of motors are often used for electrical propulsion, cranes, paper machines and steel rolling mills. Due to the brushes wearing down and having to be replaced, this type of motor is being replaced by brushless DC motors in many applications. These motors range from \$35.00 to \$500.00 dollars. The life expectancy for this type of motor is 2,000 to 5,000 hours (about 7 months). Figure 3.2.2.4.2.1 shows the way the DC brushed motor functions and the rotation where you are able to see the brushes rotation directions using the pole. Figure 3.2.2.4.2.2. shows the motor breakdown.

The following graphics illustrate a simple, two-pole, **brushed**, DC motor.

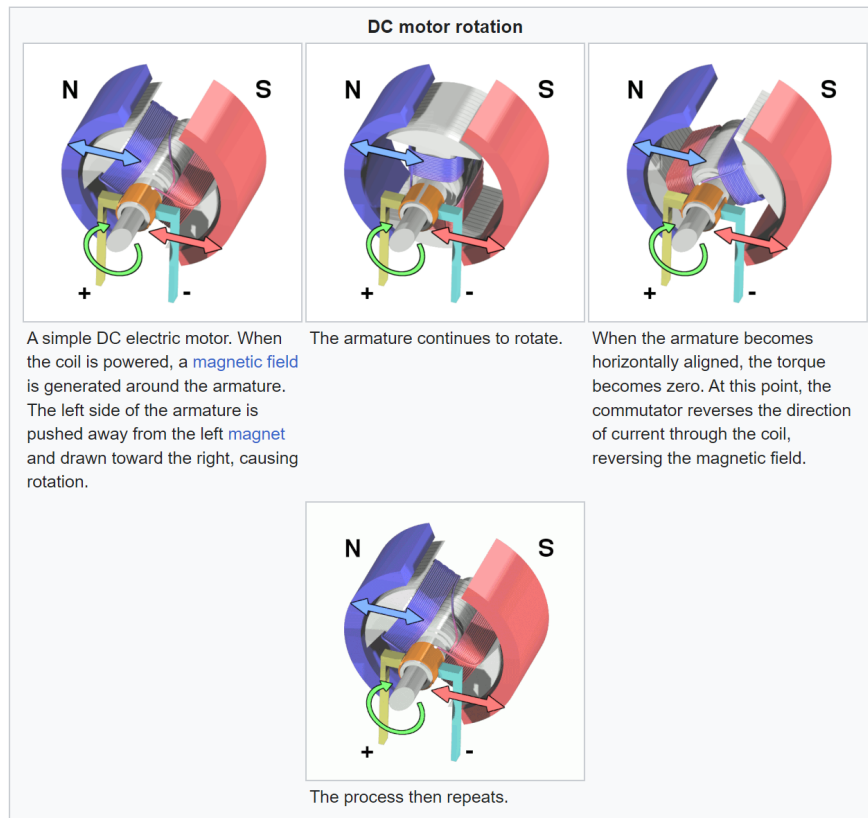


Figure 3.2.2.4.2.1 DC Brushed Motor Rotation (Wikipedia., 2023)

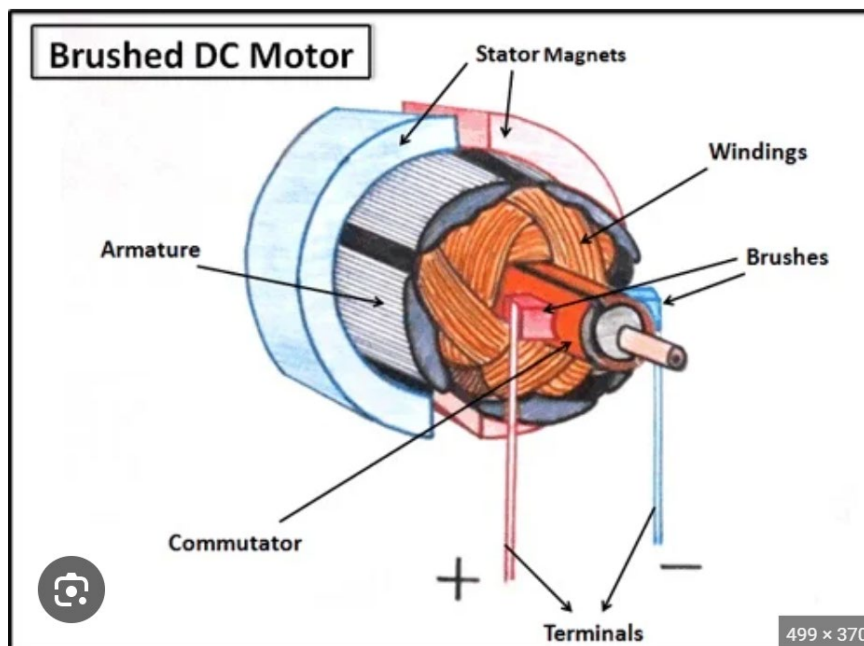


Figure 3.2.2.4.2.2 DC Brushed Motor Breakdown (Wikipedia., 2023)

The DC Brushless Motor was originally developed to achieve higher performance in smaller space than the DC brushed motor, and they are also smaller than comparable AC models. The advantages of a brushless motor over brushed motors are high power-to-weight ratio, high speed, nearly instantaneous control of speed and torque, high efficiency, and low maintenance. For this type of motor an embedded controller is used for the operation facilitation in case the slip ring or commutator are missing. The controller adjusts the phase and amplitude of the DC current pulses to control the speed and torque of the motor. These motors are also known as electronically commutated motors. This motor uses a direct current electric power supply. Brushless motors can be used in such places as computer peripherals like disk drives, and printers, hand-held power tools, and vehicles ranging from model aircraft to automobiles. In brushless DC motors, an electronic servo motor replaces the mechanical commutator contacts. An electronic sensor detects the angle of the rotor and controls semiconductor switches which switch current through the windings, either reversing the direction of the current or, in some motors turning it off, at the correct angle so the electromagnets create torque in one direction. The elimination of the sliding contact allows brushless motors to have less friction and longer life. Their working life is only limited by the lifetime of their bearings. These motors can range from as low as \$85 dollars to \$800 dollars depending on the series, watts, volts, and torque desired. Below is an illustration of the DC Brushless Motor where the difference can be seen between the brushless and the brushed. Figure 3.2.2.4.2.3 illustrates this.

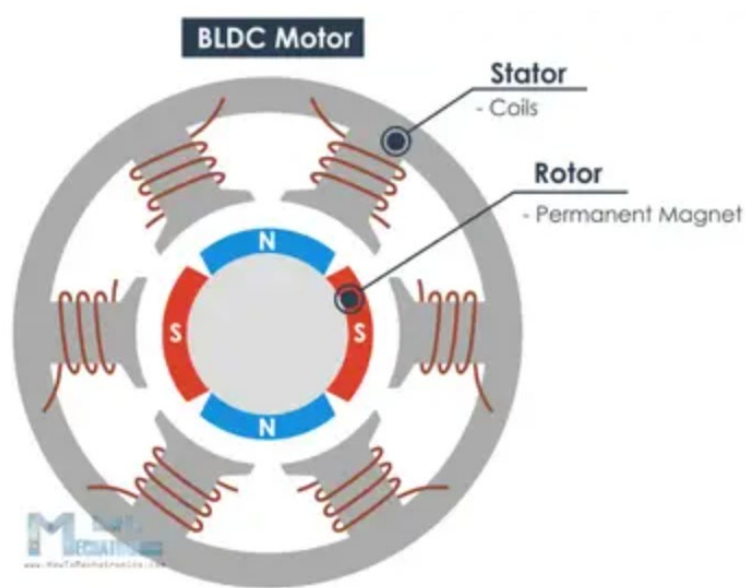


Figure 3.2.2.4.2.3 Brushless DC Motor (Wikipedia., 2023)

The Direct Drive motor is a high-efficiency and low-wear technology implementation. This motor is known for being able to accelerate quickly. It can be used to replace conventional servo motors and their accompanying transmissions. This type of motor is characterized by smooth torque transmission, and nearly-zero backlash. The benefits of this type of motor are the increased efficiency and its being a straightforward design with fewer moving parts. This is due to reduced power losses from the drivetrain components. It also includes the benefit of being able to deliver high torque over a wide range of speeds, fast response, precise positioning, and low inertia. Direct Drive motors can be used in phonographs, telescope mounts, ski lifts fans, computer hard drives, washing machines, and CNC machines. The life expectancy for these motors is 10 to 15 years. They range from \$200.00 to the \$700.00 dollars. Figure 3.2.2.4.2.4 below shows the inside of a Direct Drive Motor illustrating the coils, the stator as well as the rotor of the motor.



Figure 3.2.2.4.2.4 Direct Drive Motor (Wikipedia., 2023)

The Linear Motor has an unrolled stator and an unrolled rotor, that produces linear force along the device's length. This motor is typically faster and more accurate than rotatory motors. For this motor, a typical mode of operation is as of Lorentz-type actuator, in which the applied force is linearly proportional to the current and the magnetic field. This motor is commonly found in high accuracy engineering applications. Linear motor is usually of the AC linear induction motor design with an active three-phase winding on one side of the air-gap and a passive conductor plate on the other side. Some applications for these motors are high performance industrial automation equipment, like ball screw, timing belt. This motor provides a combination of high precision, high velocity, high force, and long travel. The life expectancy for this type of motor can go from 5 to 20 years. They range from \$25.00 to \$500.00 dollars.

The Servo Motor is any motor coupled with a feedback sensor to facilitate positioning. Rotary and linear actuators are used in this motor. These motors are known for their advanced positioning ability while being able to provide stable torque from a low- to the high-speed range. The off part of these motors is that they require additional control devices such as sequencers and servo amplifiers, which at the end of the day will add extra cost to the design if this one was chosen. The servo motors range from \$208.00 to thousands of dollars depending on the series purchase.

The Stepper Motor uses an internal rotor that is electronically manipulated by external magnets. The motor's rotor can be made with permanent magnets or a soft metal. As windings are energized, the rotor teeth align with the magnetic field. Which allows them to move from point to point in fixed increments. It is a brushless DC electric motor that divides a full rotation into a number of equal steps. This motor is known for its property of converting a train of input pulses into a precisely defined increment in the shaft's rotation position. They have many applications, for lasers and optics they are frequently used in precision positioning equipment such as linear actuators, linear stages, rotational stages, goniometers, and mirror mounts. This motor typically lasts 10,000 hours (about 1 year 1 and a half months). They range from \$12.00 to \$100.00 dollars. Figure 3.2.2.4.2.5 shows a table with a summary of the 7 motors that we research to make a decision as to which one to use for our system.

Motor	Price Range	Durability
DC Brushed	\$35.00-\$500.00	7 months
AC Brushless	\$75.00-\$600.00	10-20 years
DC Brushless	\$85.00-\$800.00	Bearings lifetime
Direct Drive	\$200.00-\$700.00	10-15 years

Linear	\$25.00-\$500.00	5-20 years
Servo	\$208.00-\$1k	5-10 years
Stepper	\$12.00-\$100.00	10,000 hours

Figure 3.2.2.4.2.5 Motors summary

After doing all the necessary research to pick the right motor for the attachment of the weather machine that we used in our system, we concluded that the best choice for this was the linear actuator motor, which we use a linear actuator. We chose this one mainly because of the efficiency and durability of the motor, it was also a fairly economical motor so that we was able to stay within the budget provided. There was a servo DC motor that I investigated and compared as far as the torque, efficiency, weight, power rating and price range. Below is a table showing the comparison between the servo motor and the chosen linear actuator. At the end of my research, I chose the DC house 6 inch stroke linear actuator, that has a 12 volts rating, because of the cost, which was way cheaper than our second choice, the fact that it can resist temperature from -65 degrees F to 400 F. lastly because of the power rating and the voltage rating.

Comparisons	Trinamic Motion Control GmbH	ECO-Worthy Linear Actuator
Torque rating (oz-in/mNm)	8.85/62.58	1000 N
Temperature tolerance	-10 C- 123 C	-65 F – 400 F
Efficiency (%)	85	80
Voltage rating (VDC)	24	12
Price range	\$90.00	\$41.00
Weight (lbs)	0.662	1.771



4.0 Standards and Design Constraints

In this chapter we will be discussing the different standards that we looked into related to our project and the development of our system. We will also discuss the constraints that we can face in the process of building our system as far as manufacturing constraints, time constraints, and more. A brief comparison of constraints between existing calibration technologies discussed is shown below.

Constraint Comparison Between Existing Calibration Technology

Technology	S-MASS	Frequency Comb	Hollow Cathode Lamp Calibration
Economical	Little to none, have a budget of approximately \$20,000	Expensive*, but the lasers used are commercially available	Restrictions on the use of Thorium causes impurities
Health and Safety	Safety hazards are very low (class 3B laser)	Generally utilizes a class 3R laser. Slightly more hazardous for construction and operation than S-MASS	May contain toxic and/or flammable metals
Manufacturability	Cost-effective, but lower stability caused by environment	Access to customized components, enabling atomic stabilization.	Commercially available, can be paired with etalons to improve stability
Sustainability	Limited by continuum source lifetime and weather effects on platform.		Limited by lifetime of hollow cathode lamps

4.1 Optical Standards

There are a variety of relevant optical standards in the development of our project, including laser safety, broadband lamp safety, lens coating standards, optics and fiber optic handling, and fiber coatings.

Laser Safety

In this section we will discuss eye safety as well as general safety requirements set forth by ANSI standards for activities which utilize lasers. Because we are also discussing eye protection in general, requirements which stretch beyond laser protection are briefly discussed. We will be discussing two ANSI standards: ANSI Z87.1, and ANSI Z136.1. An important standard to follow with this project is the ANSI Z87.1 standard, which dictates the protective eyewear necessary while working with blunt impact, radiation, splashes and droplets, dust, and small particles. The process of putting this device together will present possible hazards, including laser exposure, soldering, and heavy objects. These all require eye safety standards. Z87.1 standards require that eye protection equipment be marked with the type of protection that they provide. These include impact, splash and/or dust, and optical radiation protection. These umbrella categories then branch down into various subcategories, such as wavelength range of radiation protection. To be impact rated, the protective glasses must have a minimum of 2.0 mm thickness, with no upper limit thickness. Lasers used during the construction of this project will consist primarily of HeNe lasers utilized for alignment. These require eye protection, which are standardized for wavelengths ranging from 400 to 700 nm. This brings us to the topic of laser classifications. Lasers can be divided into class-based system, ranging from 1-4, and can be subdivided into M,R, and B classes. ANSI Z136.1 stipulates the recommended safety practices for each class. This includes protective eyewear and nominal hazard zones (NHZ). NHZ's describe the radius around an operating laser within which all persons must wear the proper eye protection, and outside which it is safe to remove laser-protection gear. The classifications stipulated by this ANSI standard are 1, 1M, 2, 2M, 3R, 3B, and 4. Class 1 lasers do not require any safety measures, as they present minimal risk to the user, and Class 4 lasers require strict regulations and safety practices. Classes are determined by wavelength, exposure time, and average power. Below we describe each class, a basic description, and whether eyewear is required. The type of eyewear is not specified however, as this can vary within classes. The specific recommendations and requirements for different types of lasers and lab hazards varies slightly from ANSI to other standardizations. For instance. Another standardization does not define laser classes in the same way as the below table. Other standardizations rather define lasers in classes of 1,2, 3a, 3b, and 4, where 3a is basically 3B in the ANSI standard, and 3B is 3R in the ANSI standard.

Class	Description	Safety Requirements
1	Less than 0.39 mW for visible light.	None
1M	Potentially hazardous if viewed through collecting optics	Eyewear recommended if viewed through collecting optics
2	Less than 1 mW of power. 400-700 nm, 1mW or less, safe to view within the blink reflex of 0.25 seconds	Eyewear recommended Do not intentionally stare into beam or resist blink reflex. NHZ distance: roughly 23 feet
2M	The same requirements as class 2 requirements, but may be hazardous, even to the blink reflex, when viewed through collecting optics	Eyewear recommended. Do not stare into beam or resist blink reflex.
3R	Potentially hazardous under certain viewing conditions, but unlikely. For visible light, emits between 1 and 4.99 mW No fire or diffusion/reflection hazards	Avoid intentional exposure to beam. NHZ distance: 52 feet Eyewear recommended.
3B	For visible light, Between 5 and 499.9 mW.	Eyewear required. NHZ distance: 520 feet Unsafe for direct exposure or long specular viewing. Avoid direct skin contact.
4	For visible light, emits above 500 mW of power. Extreme hazard to eye and skin contact, will burn through materials.	Eyewear required. NHZ distance: 733 feet for a 1 watt beam, 2320 feet for a 10 watt beam.

Table 4.1.1: Laser Classifications and Safety Standards

Safety of Lamps and Lamp Systems

Since we will be using a broadband source for the Fabry-Perot etalon, we should consider guidance and safety standards according to IEC 6247:2006 and IEC TR 62778:2014. (*IEC 62471:2006 | IEC Webstore*, 2006) The former standard pertains to photobiological safety of lamps and lamp systems, specifying exposure limits, reference measurement techniques, and classification. The latter is a technical report that addressed the risk groups for white light sources and introduced alternative risk assessments.

The exposure limits are based on irradiance and radiance. Irradiance is used to determine criteria regarding light that is focused on the retina while radiance is typically used to determine exposure limits in regard to skin exposure or the surface of the eye.

IEC 6247 applies to electrically powered incoherent broadband sources in the range of 200 nm to 3000 nm and classifies them into four risk groups: exempt (RG0), low risk (RG1), moderate risk (RG2), and high risk (RG3). The aversion response gives sources in the visible range leeway that decreases the hazard in RG1 sources. All exempt sources and visible RG1 sources are safe to use. Nonvisible low risk sources should be treated as moderate risk sources. Moderate risk sources are not likely to cause retinal damage under short exposure, so it is advice to not stare at the source. High-risk sources are unsafe and should not be looked at. If being used, appropriate measures should be taken to avoid exposure. A source emitting a wavelength range of 400 – 700 nm, like the white LED we will use for the etalon, introduces retinal blue or thermal hazards. This could correspond to either the moderate or high-risk classification.

Lens Coatings Standards

In this section we will discuss restrictions set forth by the US. Code of Federal Regulations (CFR) and the Department of Transportation (DOT) regarding optics with thin films made from radioactive materials. Thin film lens coatings containing radioactive material have been existent and in use for nearly 70 years, with thorium and uranium. These materials are often preferred on lenses over other, non-radioactive materials as they are incredibly effective as antireflective coatings (thorium) and highly reflective coatings (uranium). The CFR and DOT place very strict regulations regarding the use, transportation, and possession of such radioactive materials. Thorium and Uranium pose risks to general health. If inhaled, these substances increase the risk of lung and pancreatic cancer, and exposure may cause an increased risk of bone cancer. Radioactive materials, which contain either uranium or thorium, are called source materials. Thorium Tetra Fluoride (ThF_4) is commonly used as a very effective antireflective coating from the infrared to the UV region of the spectrum, while uranium oxide UO_2 is less common but sometimes used as a highly reflective coating for the wavelengths in the UV region of the spectrum. While restrictions are generally very heavy for such materials, the 10 CFR 40.13 sets forth examples of materials containing source material which are exempt from most restrictions. One of these defines source material used in thin optical coatings. This code states that, “any chemical mixture, compound, solution, or alloy in which the source material is by weight less than 0.5% of the mixture, compound, solution or alloy” (10 CFR 40.13) is exempt from the other restrictions set forth in the 40 CFR source materials regulations. In these amounts, the source material poses little to no risk to those working around or with the optics in question. However, this is the maximum percentage for the new fabrication of optics with thin films containing source materials. If we obtain optics that have already been manufactured, the maximum allowable source material percentage by weight is 10%. This percentage is higher if the lenses were manufactured before August 27, 2013. If the lenses were manufactured before this date, they may have less than 30% source material by

weight to be exempt from regulations. This is as long as the exempt lenses are not shaped, grinded, or polished. This is to prevent any damage that the source material could have on personnel handling the optic. August 2013 is a benchmark for the minimum allowable source material as in 2013 the CFR reevaluated the regulations regarding source material and became stricter with the use of these radioactive materials in optics.

10 CFR 40.52 place regulations on the initial transfer of source material for the fabrication of thin film coatings. These state that a license must be retrieved before transporting any source material. The applicant must include information regarding the chemical and physical form and maximum quantity of source material in each product, a description of manufacturing methods that will ensure that the coatings are unlikely to be removed under handling and use conditions, quality control procedures followed during the fabrication of thin-films, proposed labelling methods, and the means of providing radiation safety precautions and instructions relating to handling, use, and storage of products to be used (10 CFR 40.52).

The DOT requires radioactive labelling of any materials containing source material. Transporting these materials requires a Hazardous Materials Safety Permit.

Optics Surface Quality

The Fabry-Perot etalon could be considered a sensitive system because we want to maximize the output power. The system could be more affected by scattering causing imperfections in the lenses and mirrors. However, since we will be in the visible range, the system will have a higher tolerance for imperfections compared to the ultraviolet range. This is because higher wavelengths experience less scattering. It is also important to note that the lower the tolerance of imperfections on an optic, the more expensive the optic becomes.

According to MIL-PRF-1383 and ISO 10110-7: 2017, surface quality is characterized by a Scratch-Dig number or grade. The standard for visually inspecting optic surface quality using Scratch-Dig is MIL-PRF-13830. This indicates that optics can be visually inspected in a dark room with the optic illuminated by a 40W incandescent lamp or 15W cool white, fluorescent lamp. (*Understanding Surface Quality Specifications* | Edmund Optics, 2023)

Scratch-Dig relates to the apparent brightness of a scratch or apparent diameter of a dig in an optic. Scratch-Dig also represents the maximum grade for imperfections on the surface. The scratch number can be 10, 20, 40, 60, or 80 and the dig number can be 5, 10, 20, 40, or 50. The lowest brightness of a scratch correlates to 10, while the highest correlates to 80. The dig number is given by $1/100$ mm, so a 0.2 mm diameter dig would have a dig number of 20. Digs can be bubbles. The typical scratch-dig number for many applications is 40-20, while applications with more precision may require 20-10. Such imperfections can limit

the capability of an optical element by introducing unwanted scattering. Imperfections can occur in any stage of optic manufacturing, so it is important to consistently check the surface quality visually and dimensionally.

The maximum number of imperfections an optic can have is also determined by the size of the optic, specifically the ratio of the scratch or dig to the overall area of the optic's surface. For circular optics, the combined length of the scratches are limited to one quarter of the optic's diameter. The ratio of individual scratch length to the surface diameter is multiplied by the sum of the number of scratches present. This calculation determines if the surface is within the maximum scratch specification. For optic surfaces with the maximum acceptable scratches, the calculation must be less than half the maximum scratch specification, while surfaces without existing scratches must be less than the maximum specification. As for digs, the sum of the dig numbers must not exceed two times the dig specification. For example, two 10 mm digs must be separated by a minimum of 1 mm. It is standard that digs within 2.5 microns can be ignored.

ISO 10110-7 expands on MIL-PRF-1383's subjective evaluation methods by adding dimensional analysis using microscopy. This process is expensive and more time consuming, but its quantitative nature improves precision. Imperfections are not distinguished by digs or scratches, but rather a combined number of imperfections. The maximum defect size is limited by the grade number, which is characterized by the square root of the area of the maximum acceptable imperfections.

Optic Handling

We must take optic handling and cleaning seriously when developing our product. Proper optic handling is important in keeping optical components clean, damage free, and working at top conditions. Optics should be unpacked in a controlled, clean environment. Oil from skin can damage an optic's surface quality, so it is recommended to wear powder-free gloves, hold optics at their edges, and use appropriate tools for smaller optics. Before use, optics should be inspected by holding it near a bright visible light source and viewing it at different angles and only cleaned when necessary. It is beneficial to clean the edges of the optic first to prevent spreading debris onto a freshly cleaned surface. There are a multitude of guidelines when cleaning an optic, with the first being to use a canned air duster to prevent digging the dust into the surface. If the optic is still dirty after dusting, a lens tissue and solvent. Options for a solvent include isopropyl alcohol or a mix of 60% acetone and 40% methanol. To combat streaks from a slow evaporation time, it is important to wipe the optic slowly. Since we may be working with plastic optical housing, we must never clean them with acetone and only use the air-duster, reagent grade alcohol, or de-ionized water and mild dish soap.

When using solvent and tissue, there are also various cleaning techniques to account for the state of the optic. For light cleaning of unmounted optics, it would be beneficial to use the “drop and drag” technique: lay an unfolded lens tissue over the optic, drop on the solvent, and slowly drag the tissue. Tools, such as tweezers can be useful for holding smaller optics in place while cleaning. Tweezers can also be used in the “brush” technique, where the lens tissue is folded to the size of the optic (while taking care to avoid touching the part of the tissue that is to clean the optic), gripped by the tweezers, and coated in solvent. This makeshift brush is applied with light pressure to slowly wipe the optic’s surface. Another common approach, particularly beneficial for cleaning stubborn stains, is the “Wipe” technique where the lens tissue is folded and carefully hand wiped across the surface. A method that is beneficial for softer coatings is the “Immersion” technique, which is simply immersing the optic in acetone and drying it by carefully blowing the solvent from one direction. When storing optics, they should be individually wrapped in lens tissue, and placed in their designated container to be stored in a controlled environment.

Fiber Optic Handling

Similar to optic handling, fiber optic handling has a set of guidelines to prevent damage and maximize the fiber’s capabilities. When discussing fiber optics, there are four categories of damage: fatigue, compressive, abrasive, and particulate. Fatigue damage occurs in a humid environment, causing imperfections to extend over time. When placed under long term stress, the strength of the fiber would degrade. Compressive damage is classified as a pinch or clamp in the fiber that damages the coating and/or the glass. Abrasive damage occurs when the fiber is scraped or scratched. Lastly, particulate penetration is when a hard particle penetrates the coating of the fiber.

To minimize fatigue damage, it is important to follow recommended stress guidelines for the specific optical fiber being used. Fiber optics have a proof stress that the fiber must not meet over a period of time. Typically, a fiber should not be under stress higher than half of the proof stress for a time on the order of one second. An important guideline to keep in mind for our case is long-term stress, which should remain less than one fifth the proof stress. A way to minimize stress is to limit the exposed fiber’s bend radius. For example, for a 100 kpsi proof-tested fiber, the bend radius should be no tighter than 13 to 30 mm.

When handling optical fiber, it is important to take precautions to prevent compressive, abrasive, and particulate damage. We must keep in mind to never place anything on an optical fiber, including but not limited to tools and components. If any tool is used to handle or mount a fiber, the gripping ends must be a smooth and nonabrasive soft material. We must also keep the fibers off uncontrolled and/or dirty surfaces, where they can be stepped on or broken.

Gloves may be used to prevent damage, but it may make it difficult to feel any existing damage along the fiber. Guidelines for preventing abrasive damage also include ensuring that no sharp edges of the workspaces touch the fiber and to carefully account for fingernails and jewelry. Immediate and proper disposal of broken fibers, cleaves, and stripped coating is also key in preventing damage of remaining fiber.

Working with optical fiber consists of stripping, cleaving, and splicing the fiber. When stripping the coating from the fiber, it is recommended to strip the least amount of coating as possible to limit the exposed glass and minimize potential for damage. Once stripped, the fiber should immediately be cleaned with isopropyl alcohol and then cleaved. When cleaning, it is important to take care in handling the fiber to avoid contact with the exposed glass. If splicing is needed, the splice must be completely covered by either a splice protector or a recoating. Splices should then be proof tested to ensure that the strength of the fiber remains intact.

Optical Grating Handling

Optical gratings have very delicate coatings which can be easily damaged if handled incorrectly. Oils from skin will dramatically affect the optical quality of the gratings, so gloves should be worn at all times when handling optical gratings. Gratings should also be used and stored in dry locations where little to no moisture is present. When using with high intensity light such as with laser beams, ensure that the direction of diffraction is known, to prevent accidental diffraction of light into eyes or laser-sensitive equipment. If broken, do not attempt to handle the grating without the proper PPE. Broken gratings can be sharp and cause injury if handled improperly (*07.Blaze Wavelength*, 2018).

4.2 USB Standards

One of the relevant standards for our project is the Universal Serial Bus (USB) standard. The USB standard is an industry standard for specifying the physical interfaces and protocols for connecting and transferring data and power via USB connectors. The standard is maintained by the USB Implementers Forum, USB-IF, a non-profit corporation founded by the group of companies that developed the Universal Serial Bus specification. It was initially developed to standardize the numerous connectors that personal computers had in the 1980s and 1990s. At the time, each computer peripheral had a different kind of interface, such as a serial or parallel port, which made it hard for consumers to use certain products on their PCs. Thus, a consortium of corporations got together to develop a simple connector that would allow faster data rates for peripherals and other devices, and the USB standard was born.

The USB standard has been through four major revisions, each of which brought new functionality to the existing design. The first standard to be released was USB

1.0, which made its debut in 1996. It offered data transfer of 1.5 Mbps and 12 Mbps. These different speeds were offered so that it could support different devices such as printers and disk drives, which ran better with faster data transfer, and things like keyboards and mice, where data transfer rates were less critical. However, it wasn't until the 1998 release of USB 1.1 that the USB standard became widely adopted. The USB 2.0 specification was announced in April 2000 and released in 2001. USB 2.0 increased the data transfer speed up to 480 Mbps, twenty times faster than its predecessor. USB 3.0 was released in November 2008, adding a SuperSpeed operation mode that allowed for data transfer speeds up to 5 Gbps. The 3.0 version of the USB standard would also receive two additional iterations, called USB 3.1 and USB 3.2. USB 3.1's second generation included a new form of the SuperSpeed mode called SuperSpeed+ that doubled the speed of transfer when compared to the SuperSpeed mode. Then, the USB 3.2 iteration increased the data transfer rate again up to 20 Gbps and changed the naming of the previous iterations. Finally, the latest revision is USB4 which will add two new modes that allow for data transfer rates of 20 Gbps and 40 Gbps. In late 2022, there was a new iteration on the USB specification released that was called USB4 2.0 which is where we are at today.

There exist a number of different USB connectors that have become ubiquitous across a wide variety of different peripherals. The latest USB connector is the USB type C, or just USB-C connector. It is a rectangular plug with rounded corners that allows it to be inserted without the classic issue of not knowing which way the connector is meant to be plugged in. This latest connector has started to become widely adopted among smartphones and tablets, where a small and easy to use plug is preferable. The USB type A is by far the most widely used of the USB connectors. This connector is a rectangular shape with a rectangle of the connecting pins inside. This is the most popular USB connection since it has been adopted by many computer peripherals such as keyboards, mice, hard drives, flash drives, printers, game controllers and many other common peripherals. USB type B is probably the least popular of the USB connectors. This connector is square shaped with a notch on the top. This connector was typically used in external storage devices such as optical drives or hard drives.

There are a few notable limitations or disadvantages to the USB standard. Most notably, the USB standard specifies that USB cables can only have a length of up to 5 meters. This severely limits the range that USB cables can be used over without requiring additional hubs or cable extensions. Communications over USB are also limited between the host and the peripheral because it is a single connection. Also, despite all of the advancements that the USB standard has experienced, USB connections are still significantly slower than Gigabit Ethernet connections.

The main use of a USB connection in our project will be as a means to transfer data. This is because we have to be able to capture data from various sensors and from a camera, and we need to be able to transmit that data over a cable connection to a target system. The sun imaging camera that we use will have to be connected to our computer via USB. This will allow us to capture images of the sun with relative ease. Then, depending on the weather station we choose, we may be able to connect the weather station via USB to the computer. This will be critical to our ability to read real time weather data that we can then use to predict incoming weather events. If we choose a weather station that is not USB enabled, we may have to use more complicated methods for the transmission of data, such as UART, I2C, or SPI. These are all viable methods for transmission, but they're more complicated than USB and would require setting up the specific configurations for our system. This is why the use of USB is so important because it standardizes communications between the host device and the peripherals that we may choose to use for our project.

Furthermore, we will need to write our own programs using USB connections in order to transfer data from our computer to a designated receiver. Once we have captured the images of the sun from our sun imager, the next hurdle is to then transmit those images to the CREOL photonics lab. We should also consider transmitting the sensor data from our weather station so that we can store all of the relevant data we've captured. This will be done by writing a script that can use USB to transmit the data we have captured. We will also need to write another program or script for the receiving computer at the lab, so that it will properly receive our data.

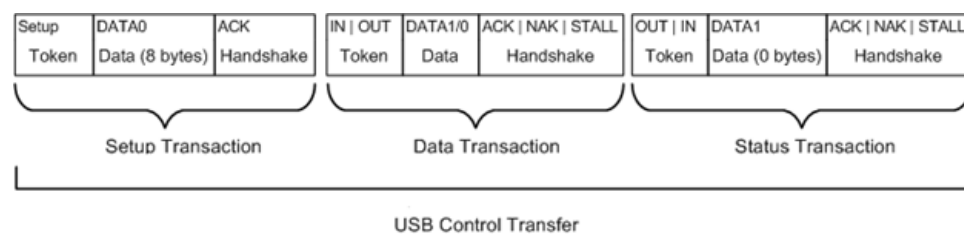


Figure 4.2.1 USB Packet Data Header

So how do we intend to implement a USB connected program on our computer? We have several options available for our purposes. If we used a Windows Operating System on our device, we may be able to use WinUSB, a USB device driver provided by Microsoft. This driver allows you to communicate with USB devices by using a ready to use interface. WinUSB provides a library of functions and API that simplifies USB communications on Windows platforms. Another option would be to use the libusb library. Libusb is a C library that provides generic access to USB devices. The libusb library provides several advantages over WinUSB. It is a cross-platform library, which means that it is portable between

devices. It operates at the user level, so no special privileges are required from the operating system in order to fully use USB communications. Finally, the library is version-agnostic, so it supports all versions of the USB standard. All of these factors make libusb a very attractive option for implementing USB communications across devices. Our most likely implementation is using a library like PyUSB. PyUSB is “an API rich, backend neutral Python USB module easy to use”. PyUSB is very similar to libusb, but implemented in Python instead of C. In fact, the PyUSB library started as a wrapper library of libusb, making it useable in python. This makes PyUSB the most logical choice for our project, since Python is a simple, easy to use language and we can quickly make use of the PyUSB library.

4.3 Manufacturability Constraint

As stated in an article that we used for research for our constraints, “Criteria and design knowledge include the preferences and constraints for evaluating designs concepts”. So, in other words by evaluating the constraints that our project can come across we can address the situation ahead of time and be able to adjust if necessary. It also stated that “The more constraints a problem has, the less solutions space is available. Therefore, constraints must be expressed explicitly with a systematic and consistent representation scheme” [1]. By doing this the constraints at hand can be studied and manipulated by the engineers and end up with several advantages.

4.3.1 Deadline

As a group we all realized that one of our biggest constraints is the time, in other words the deadlines that we need to meet to have our system ready. With the sponsor requirements that we need to meet as well as the deadlines for the class that are put in place, two semesters to work in the prototype that we need to present is cutting it tied. We choose to talk about the manufacture constraint because this takes into account the time spend on the project, the physical requirement of the project, some of the specification that need to be met for the sponsor, and the accuracy the system needs to function on. After Covid 19 hit us worldwide having to get merchandise or any type of product on a timely manner has become a challenge. A great example is when I took Junior design last semester, the class end up just doing the computer simulation of the project due to not being able to get the necessary parts need it to actually built the project that we need it to build. Which for this case this year is not different that before. Things has gotten better but there still struggle to get the parts need it in a timely manner. We our planning to combat this constraint by making sure so figure out in early stage of our research the necessary parts need it for our system so that we can order them early and be able to get them in on time for senior design two so that we can start building with enough time to finish our project. If for some reason we come across the situation that our part did not arrive on time, we want to have a

back up order on the second choose of our part. Another factor that can help this constraint is that the sponsor offered to let us use some of the parts we might need from the CREOL engineer department if they have them on stock.

Considering the precision needed in Fabry-Perot etalon alignment, the time it will take to achieve such precision could take weeks. Collimating white light must be precise to account for the varying wavelength's optical paths and the mirrors must be parallel with a limited cavity length range. Taking into account round trip cavity loss, it will also be a challenge to couple the output into a single mode fiber. These challenges will take time to overcome in the fabrication process, and we plan to start as soon as possible to take the time required to achieve our specifications.

4.3.2 Dimensions

As far as the manufacture of our project goes another constraint that we are facing is the dimensions that we need to meet by the request of the sponsor. Our sponsor wants the final result to be the size of his laptop as a 3-dimensional size. Which is approximately a 15x15x15 inches. The constraint with this is that base on these dimensions we feel that the amount of component that need to be inside it will require a bigger space to fit it in. Since the system needs to include all the electrical parts, as well as the optical parts. We need to fit in the two telescopes, the camera, microcontroller and so on. We are trying to use the telescope that are size of a thumb, this can give us flexibility on the inside space of the system but can lead to the resolution view through it to not be as high as need it, since the image taken by the camera needs to be to a resolution of 10^5 .

4.3.3 Accuracy

Our system is to have a weather machine that protects our system from severed weather. The constraint in the manufacturing that we are facing in this part of the project is making it accurate to the sensitivity and the extreme weather changes that Florida faces. As we all know Florida is notorious for its unexpected weather. It can be nice and clear at 9:00 am and 30 minutes to an hour can pass and it becomes an ugly breezy, stormy day in the blink of an eye. We are trying to incorporate a code in our system that can detect a pattern for the weather change thought out a longer period instead of a sudden change in the weather, so that the weather system won't be opening and closing consistently, but to be closing with in a range of humidity change of certain degrees.

4.3.4 Fabry-Perot Etalon Precision

Broadband Fabry-Perot cavities have previously been implemented in astronomical spectrograph calibration. They have been used to aid in the precision of laser frequency combs, but also as a stand-alone calibrator at a lower cost with relatively high precision. The necessary precision for astronomical spectrographs is to be 1 m/s or less. The Fabry-Perot etalon would not provide an absolute

frequency reference, so to achieve such precision, the etalon would need to be stabilized. The cavity width is sensitive to the environment and susceptible to drift that would decrease the precision. Stabilizing the system would require a temperature-controlled environment in a vacuum space.

One approach is to consistently recalibrate the etalon and compare its spectrum to a Hollow Cathode Lamp's known frequency. However, this method requires the temperature to be actively controlled. The research labs in CREOL do have thermally stabilized systems, but that is not a goal we can realistically achieve due to its expensive and long-term development.

The Etalon can only be manufactured to a limited stability. Professional astronomical spectrographs can distinguish a 600 KHz drift. Unfortunately, such a high precision is simply not obtainable for our project, as it will be in free space. Taking this into account, we should be able to demonstrate a 600 MHz shift instead. In order to achieve a more precise product, the FPE would need to be temperature controlled and/or vacuum spaced. This would significantly drive up the cost as well as the time it would take to design and implement the system. The output from the etalon would also have significantly less power than the input, increasing the difficulty in collecting the output into the spectrometer. The manufacturing for this portion was cost-effective because we designed the most realistic designs suitable without building the etalon for a vacuum. If time and resources permit, the most advanced form of stabilization we would have been able achieve would be a temperature-controlled environment maintained within 0.6 degrees.

4.4 Maintenance and Reliability Constraint

4.4.1 Solar Tracker System

The maintenance and reliability constraint for the solar tracking system of the observatory involves some key considerations so we can ensure that the system operates efficiently and consistently over its lifespan. We need to design a system that minimizes maintenance requirements and maximizes reliability leading to optimal long-term functionality. It is important to consider that the observatory will be outdoors, and it will be exposed to extreme weather conditions that are characteristic of Florida. We can address this constraint by prioritizing easy maintenance, durable components selection, designing a strong weather protection system, a good self-calibration and diagnostics system, keeping monitoring and reporting documentation, testing the product in extreme weather conditions before delivering it, and providing a good training to the people that will be operating it on the customer's side.

The system should be designed with ease of maintenance allowing for easy access to components when servicing to minimize downtime. We should use corrosion-resistant materials and protective coatings to safeguard against harsh environmental conditions. The observatory systems should have self-calibration

and diagnostic capabilities to identify issues and solve them quickly, also to detect potential problems in the short and long term.

Furthermore, the inclusion of both monitoring capabilities and reporting documentation allows the customer to track the system performance, detect deviations, and take timely corrective actions. A service plan for replaceable components is also necessary when it does not require specialized tools and complex disassembly which can reduce considerably maintenance time and costs.

Considering the system expected life is very important, discussing component wear and degradation over time. Our design should minimize wear and tear through careful selection of components, appropriate maintenance strategies and preventive measures. During the development of our project, we should give special attention to the testing and validation phase exposing the observatory to various weather conditions and operating several scenarios to identify potential reliability issues early on.

By adhering to the maintenance and reliability constraint, our observatory solar tracking system will show enhanced longevity and require minimal maintenance. These will guarantee a very efficient solar tracking system throughout its operational life.

4.5 Sustainability Constraint

For our product there are several factors to consider when it comes to the sustainability of our system. First of all, our product should be able to have a long-life expectancy. It is desirable for our system to be able to last a couple of years, to give enough time to the astrophotonic research department to get all the desired information using our product. For this to be possible our system will need to be well built and meet the required specification of being resistant to severe weather since our system will be placed on a building roof, which makes it a constraint in our part for the sustainability factor.

A constraint that we faced during the creation of our design was the determination of the right type of material to use for the main base and platform of our system. We need it to be able to choose a type of material that is sustainable. We need it to be able to choose material for the outside part of the system that would be able to be weather resistant. The chosen material needed to be able to not be heavy.

So, we investigated using Plexi glass as the main coverage surrounding of our system but came up with the conclusion that Florida is super-hot. The system is desired to be used on the roof and the components in our platform would overheat and damage. We suggested integrating a fan inside the system to maintain the components at a desired temperature but ended up having to think about how that air was going to ventilate. We thought about using wood, but the same problem arises as the heat in Florida would make the system become moldy due to the humidity. Another type that we thought about was metal but ended up moving away

from that approach due to how heavy the system could have become. All this factor become a sustainable constraint for us since the system needs to last a while and with Florida temperatures this would made our system not last enough time been functional.

The user should have minimal interaction with the optical system, and simply gather the data it collects. The lifetime of etalon in the system is dependent on the lifetime of the etalon's source, so a white LED continuum source has the potential for longer operation than alternate sources. The precision needed for the etalon decreases the sustainability, because if a small bump hits the system and moves any piece out of alignment, it will stop working. Unfortunately, this may also be time-consuming to re-align. To combat this, we will prioritize durable mounts and a covering for the system to protect the system from outside effects as much as we can. The product could be improved with better features and specs in new models through implementation of temperature control and combining calibration methods to improve etalon stabilization and higher sustainability.

4.6 Social Constraint

Everyone knows that society has different beliefs. As far as this goes the different social values to take into account when building our product becomes a constraint for us since it is hard to create a product that someone will not be against off. In our case there would be some with the believes that we should not be looking into the out of space resources since they feel that this can be a form of exploitation. There are also does that have the believe that there isn't anything in out of space that we can find any good resources for humankind and won't be against it but wouldn't invest their time or money in the product of this type. This product is meant to be used in an overall system that can get data that can result on a lifechanging phenomenon in which society can feel strongly against it while others will feel this can be a second alternative for humankind resources.

4.7 Risk

Although the optical system is meant to be a hands-off product, there is still a possibility of bumping the system and misaligning or damaging components. As stated before, re-alignment of the system would be time-consuming. However, there is a risk of damaging the optical fiber used in the system and properly replacing them could be a set-back for the user. We can combat this by exploring the use of various coatings that may protect the fiber.

Safety Requirements for Product Operation

- No tools or materials in optical system.
- Do not look directly at the white LED source in the optical system.
- Follow fiber and optic handling guidelines if optical system repair is needed.
- Follow relevant building codes when installing the rooftop system and fiber optic cables.
- For repairing rooftop system, follow safety practices.
- Ensure that all electrical components and connections comply with relevant electrical safety standards.
- Do not attempt to modify or tamper with electrical components to maintain safe operation.
- Acknowledge that the plexiglass box is constructed with flame-retardant materials to reduce fire hazards during product operation.
- Avoid overloading the system to prevent overheating of electrical components, particularly the power supply PCB and external power supply converter.
- Be aware of the product's ventilation system to facilitate the dissipation of heat generated by electronic components during operation.
- Exercise caution around moving parts, such as the door linear actuator motor, and refrain from interfering with its operation to prevent accidental contact.
- Recognize that the product is designed to shield sensitive electronic components, reducing the risk of electromagnetic interference (EMI) and radio-frequency interference (RFI) during regular use.
- Avoid placing other electronic devices in close proximity to prevent interference.
- Follow provided instructions for proper door operation and be mindful of potential obstructions to prevent damage to the door linear actuator motor.
- Familiarize yourself with emergency shutdown procedures in case of any issues with the door operation.
- Be aware of system response to extreme weather conditions and allow for automatic shutdown when necessary.
- Recognize that the camera solar imager is securely mounted and avoid attempting to adjust or tamper with its position during operation.
- Use the Jetson Nano's user interface as instructed for monitoring and controlling the system during regular operation.
- Follow the recommended maintenance schedule to inspect components for wear, damage, or malfunction during regular operation.
- Ensure that all users are adequately trained in safe product operation, installation, and maintenance practices to enhance overall safety awareness and compliance.

5.0 Comparing ChatGPT and Similar Platforms

In this chapter, we will be comparing the functionality and efficiency of different Large Language Model platforms such as ChatGPT to identify their advantages and disadvantages. We also explore other AI platforms beyond LLMs.

5.1 Definition and Introduction

What is ChatGPT? Well, according to ChatGPT, “ChatGPT is an advanced language model developed by OpenAI. It is based on the GPT (Generative Pre-trained Transformer) architecture, specifically GPT-3.5. GPT-3.5 is trained on a large amount of diverse text data from the internet and can generate human-like responses to prompts or questions.” It is an artificial intelligence that can generate text, sometimes called a large language model, developed to respond to written input. This form of artificial intelligence comes from a field of study called natural language processing, the study of how computers and human languages interact. ChatGPT was trained on massive text data sets, including books, websites, internet forums, and just about any form of written text available to a computer. This has given the AI a vast body of information that can be considered, so it shows ‘knowledge’ over a large domain of topics. It’s ‘knowledge’ and responses are made by reading a word and assigning probabilities to words that are likely to come after that word, then selecting a word to continue its message and iterating. As ChatGPT itself says “It’s important to note that the responses generated by ChatGPT are based on patterns learned from the training data and are not the result of true understanding or consciousness.”

However, ChatGPT is not unique in its implementation of a large language model. In fact, ChatGPT is based on the GPT-3.5 AI model, but there is a more recent model called GPT-4 available. GPT-4 is purported to be able to solve more difficult problems with greater accuracy, have more advanced reasoning capabilities, and be overall safer. There are many new LLM’s coming out that can generate text like ChatGPT can, for example, Microsoft Bing has included an AI model called Prometheus that integrates OpenAI’s GPT model. This allows Bing to be the first ever AI powered search engine, allowing Bing to optimize search results and provide a better user experience. There are also other models, such as Anthropic’s Claude-Instant and Claude+ models. The Claude models are AI assistants intended to help users’ complete tasks. Claude-Instant is a faster model, which can handle casual conversation, summarize text, and understand documents. Meanwhile, Claude+ is a more powerful model that can do more tasks including complex reasoning, creative thought, and coding.

It's more than just LLM's, as the same GPT-3 models used to develop ChatGPT have also been used to create an AI model called DALL-E. DALL-E and DALL-E 2 are deep learning models produced by OpenAI that generate images from text-based inputs. The AI reads through the input and runs it through the GPT-3 model to produce an image similar to the description given. In fact, there are many new AI models such as GitHub Copilot, Midjourney, Stable Diffusion, Boomy, and more. These programs can write, draw, create new music, code, and do a wide range of tasks. These applications are all set to be revolutionized by the current AI boom. The impact these programs will have on their respective fields is unprecedented. With that being said, let's take a deeper look at ChatGPT and large language models.

There are several models beyond ChatGPT, such as the previously mentioned Claude, but also others such as Google's Bard AI. To compare these models, we intend to ask each model increasingly complex questions that will test their ability to perform logical tasks, perform creative tasks, and write or debug code. This will allow us to determine which model is best suited to which task.

5.2 Q&A comparison from different platforms

For this test, we selected a very simple problem and a complex one. Questions were asked to various popular free AI platforms.

Simple math problem for the first test: Please, provide the result of 100 divided by 7.

Complex problem: Find the inverse function of $f(x)$: $f(x) = \ln x + 1$, $x > 0$.

AI Chatbot/Platform	Simple Problem Answer	Complex Problem Answer
ChatGPT	14.2857	So, the inverse function of $f(x)$ is given by: $f^{-1}(x) = e^{x-1}$, $x > 0$
Chatsonic	14.28 (rounded to two decimal places)	No response
Microsoft Bing AI	14.2857142857. Would you like me to round it to a certain number of decimal places?	The inverse function of $f(x) = \ln x + 1$, $x > 0$ is given by $f^{-1}(x) = e^{x-1}$
Bard AI	14.2857143 (+Python code)	We can see that $f(f^{-1}(x)) = x$, which means that $f^{-1}(x)$ is indeed the inverse function of $f(x)$

It could be observed that responses were very close for both the simple and the complex question. When trying the complex question with Chatsonic platform, the chatbot did not give any response. Bard AI and Microsoft Bing AI took longer time

to answer than ChatGPT. It is important to highlight that these AI tools do not always give correct answers. For example, in a question asked to ChatGPT “How many letters does the word ‘nineteen’ have?” it answered correctly but after we answered to the AI that the answered was incorrect and gave it a incorrect answer “twelve”, the chatbot changed its response to the incorrect answer. This proves that AI uses context to answer questions and it can mislead anyone in any wrong direction.

5.3 Software (model types) comparison

We previously mentioned that ChatGPT is a kind of Large Language Model, a type of artificial neural network with many parameters that are trained on unlabeled text, which emerged around 2018. However, these are not the only kind of language model used in natural language processing. There are a few other notable types of models such as the n-gram model and the exponential, or maximum entropy model. In the field of natural language processing, language modeling is the use of statistics and probability principles to assign a probability to the occurrence of a sequence of words. These models are trained on large bodies of text in order to produce models that are accurate to how human language works. Language modeling is applied to many common tasks such as speech recognition, machine translations, sentiment analysis, and more. In order to better understand ChatGPT, we will be taking a look at different kinds of language models and their applications.

Large language models are the most recent innovation in the field of natural language processing. The most basic design is the use of a neural network trained on large quantities of text using a form of supervised learning. A neural network is a network of nodes organized into various layers, one initial layer that takes inputs, one or more hidden layers, and an output layer. Each node in the neural network is connected to another node and carries a corresponding weight value associated with it. Then if the output of a node is above a specified threshold, the node is activated, sending data to the next node in the network. The kind of neural network used in large language models in particular is a kind of neural network called a recurrent neural network. Recurrent neural networks allow for feedback from previous inputs to influence the current input and output. This kind of approach is very effective at modeling complex behaviors such as human language but requires large data sets to be trained properly. It also allows for language models that can consider context when analyzing human language. This makes large language models the most advanced kinds of language models we have developed so far.

The N-gram model is a previous kind of language model used to predict text. This model is different from LLMs because it does not make use of neural networks, instead it assigns probabilities to the likelihood of a word appearing based on the

previous N words in the sentence. I think this example from Speech and Language Processing by Daniel Jurafsky & James H. Martin sums it up best: “The bigram model, for example, approximates the probability of a word given all the previous words by using only the conditional probability of the preceding word. In other words, instead of computing the probability we approximate it with the probability.” There are also some variations on the N-gram model such as the cache language model. The cache language model keeps a cache of words that occur elsewhere in a given text and assigns higher probabilities to them. This ensures that text about specific topics, such as a presentation about an obscure condition, can still be predicted accurately despite using words that are relatively rare. The N-gram model has some key limitations, such as the fact that the number of parameters increases exponentially as the order of the n-grams increases. There is also no way to generalize from the training sets to the test set for an n-gram model.

Another type of language model is known as the maximum entropy model. Maximum entropy models are based on the principle of maximum entropy, which states that “when estimating the probability distribution, you should select that distribution which leaves you the largest remaining uncertainty (i.e., the maximum entropy) consistent with your constraints”. This means that we need to assume as little as possible or introduce no additional assumptions into our probability distribution. These models are more classical forms of machine learning models, using heavy statistics to predict linguistic classes. This means that in application, the models were often used in sentiment analysis problems, or to predict different preferences based on given information.

The last model we’ll look at is called the positional language model. In the paper “Positional Language Models for Information Retrieval”, researchers Yuanhua Lv and ChengXiang Zhai proposed the positional language model, where “The key idea is to define a language model for each position of a document, and score a document based on the scores of its PLMs.” The positional language model is based on two main heuristics that are often used in language modeling: that certain words or combinations of words occur close to each other, and that certain passages contain more relevant information than others. This allows the model to summarize a given document by identifying the most relevant information and analyzing the passages in which it is contained.

Each of these models was developed with a different question in mind. The latest large language models are an evolution beyond the previous n-gram models, whose main role was to try and predict human speech. This means that those models are capable of predicting the next entry into a given sequence. The maximum entropy model was a general statistical principle that was applied to natural language processing in order to classify different contexts, which meant that it could be used in sentiment analysis to guess what the author was feeling.

Finally, the positional language model was intended to extract relevant information from text. Thus, creating a model suitable for summarizing a document or body of work. It's important to understand how each model approached different tasks because it can give us a greater appreciation for how advanced current LLM based applications, such as ChatGPT, are.

6.0 Optical Design

6.1 Spectrograph Design

This system was designed in three steps: 1) locating possible components, which is done first, as the available components available to us will determine the possible types of spectrometers that we can make, 2) mathematical calculations, which will involve the determination of the type of system/components chosen in the above section, by working through the resulting resolving power, size, and price of the system, and finally, 3) zemax, where the chosen design and components are modeled and optimized. Step one is already completed in the section titled, "Comparison and Selection of optical components." In that section, the parts to be utilized in our final design were shown, but the process for choosing these components was not explained. This will be seen as we move to step two, the calculations. This spectrometer was initially designed as a 4f system. However, we want to keep this system compact and less expensive. Due to this, we then reduced this system to a 3f system. This was accomplished by placing the focusing lens as close to the dispersing optics as possible. This changed the angle of the incident light onto the detector, but not the location on the detector that the light is focused. If we were to take the light from the focusing optic into a fiber to be sent into a separate system, the 3f system would not be possible, but because the light from the focusing lens is incident directly onto the detector, this does not affect the quality of the resulting spectrum. The system was designed in two waves: first, the system was designed and optimized in a non-cross dispersed design. This allowed us to ensure that the initial and most basic aspects of the spectrometer design were done correctly. This initial version was the demoed version on August 3rd, at the end of the Senior Design 1 course. Upon completion of this design, the prism element was added. The system was then re-optimized for resolution and magnification. Adding the prism changed the direction of dispersion, which required us to adjust the sensor position and lens distances to account for the prism's size and dispersion.

Initial Calculations:

The design was first calculated for a simple transmission grating, with a groove density of 18,000 grooves/mm, and a size of 50x25 mm. This is based off of a simple grating of the highest possible groove density, and largest possible size. This is done to see how high of a resolving power can be achieved utilizing a non-echelle or cross-dispersed system. We wanted to know if it is possible to achieve the desired results this way, as a simple spectrograph with a single grating will be far less expensive than a cross-dispersion echelle spectrograph. The fiber as well as the sensor are already chosen for this design, as we are quite limited when it

comes to selecting a single mode fiber which is designed for the wavelength that we want, meaning that the rest of the system will be designed around these factors. The fiber, SM400, is designed for wavelengths of 400-532, but can be used outside of this range. This was chosen due to the fact that 532 nm is the primary wavelength we want to make sure is measured. The camera selected is the atik apx60, as it is the best sensor for this design. To understand the resolving power of the system, we use the following equation:

$$R = \frac{mW\lambda}{\sigma\phi_{slit}D}$$

Where m is the dispersion order, W is the width of the grating, λ is the wavelength of the light, σ is the pitch of the grating, ϕ_{slit} is the resolving power of the entrance slit, and D is the diameter of the telescope lens. In order to utilize the numbers that we have, from the specs sheet of the single mode fiber, grating, and sensor, we must redefine this equation in terms of numerical aperture and diameter of the fiber rather than the power of the opening slit and diameter of the telescope lens. We accomplish this using the following equations:

$$\phi_{slit} * EFL_{tel} = x_{slit}$$

$$\frac{F}{\#} = \frac{EFL}{D}$$

$$\frac{F}{\#} = \frac{1}{2NA}$$

We can now define the resolving power with the following equation:

$$R = \frac{mW\lambda}{\sigma(2NA * D)}$$

Where NA is the numerical aperture of the entrance slit, which is the numerical aperture of the single mode fiber, and D is the diameter of the entrance slit. When solved for the first order of diffraction, with a width of 50, a wavelength of 532 nm, a pitch of 0.00055 mm (1/groove density), an NA of 0.13, and a diameter of 3 μ m, the resulting resolving power is 61,384. Now, our minimum resolving power that is accepted for this system is R=50,000, so one might see these calculations and decide that this will work. However, this is a theoretical number that does not account for real-life aberrations which will decrease the resolving power. We want to design a system which provides theoretically much higher resolving power numbers, to provide more wiggle room for the actual design of the system. This wiggle room must account for lenses which are a couple mm off of the exact desired focal length calculated and aberrations due to lenses. For this reason, we choose to design a system which provides much higher resolution as well as bandwidth. This will be a cross-dispersed echelle spectrograph. Below is a figure

[illegible]

The goals of this system require a spectrometer which produces high resolving power over a broad bandwidth. As has been discussed in the optical components comparison and selection section of this paper, most spectrographs generally choose between prioritizing bandwidth and prioritizing resolution. However, there is a design which solves this problem, called the cross-dispersion spectrometer. A cross-dispersion spectrometer utilizes two dispersion elements: these can be two gratings, a grating and a prism, or even two prisms. The most common design utilizes a grating for dispersion, followed by a prism for cross dispersion. Some designs place a prism before the grating, however this solution increases aberrations, and reduces the resolving power. This design will utilize an echelle grating. This grating yields a very high resolution, with a very large blaze angle, and is designed for a specific diffraction order output. However, the bandwidth of the highly resolved diffraction order is very small. When light is dispersed utilizing an echelle grating, many diffraction orders will spatially overlap with one another (Zang, 2022). Each overlapping diffraction order has a different wavelength, and free spectral range (FSR). The cross-dispersion element (a prism in our case) takes the light from the echelle grating and disperses the overlapping diffraction orders. This results in light which is dispersed in a different direction than it was dispersed from the grating (vertically rather than horizontally), with wavelength

varying by diffraction order rather than repeating (BHROS Dispersion, n.d). Below is a figure showing the spectrum obtained from a crossed-dispersed spectrometer. This maintains the high resolving power, while providing a much larger bandwidth than would normally be possible with echelle-grating. This is also often designed utilizing a reflective grating as well as mirrors. Echelle gratings are often divided into the categories named R2, R3, etc. where the number after R refers to the tangent of the blaze angle of the grating. We will be choosing to use an R2 grating, meaning that the blaze angle is 63.4 degrees. Higher R values are less common, and result in a higher resolving power but lower efficiency. The R2 gratings chosen to compare with calculations are identical in size and blaze angle at 50x25 mm and 63 degrees, varying only by groove density, with the first being 31.6 grooves/mm and the second being 79 grooves/mm. The determining factor here is the size of our detector, which is 36x24 mm. Higher groove density will provide a higher resolving power, but may not allow the full spectrum to fit onto the detector. The below figure depicts a spectrometer using a transmission grating as the initial dispersing optic, and a prism as the cross-dispersing optic. It is clear from this figure how the order of diffraction is the new factor which tells us the location of specific wavelengths of light, rather than physical distance from the center of any one diffraction order.

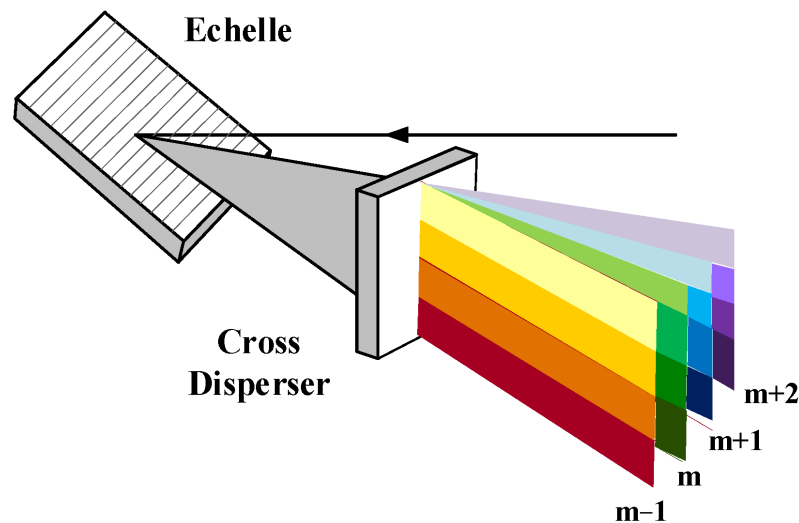


Figure 6.1.2: Cross Dispersed Echelle Layout (Zang, 2022)

The resolving power of an echelle crossed dispersed system found using a different formula than a simple spectrometer, with the following equation defining the total resolving power of the system:

$$R = \frac{2d \tan \theta}{2NAx_{slit}}$$

Where d is the spot size on the grating, θ is the blaze angle, NA is the numerical aperture of the entrance slit, and W is the width of the entrance slit. Because the grating is now tilted, d must be calculated using the following equation:

$$d = W \cos \theta$$

Where W is the width of the grating, which is 50 mm, and θ is the blaze angle, 63.4 degrees. Using these values, we get that:

$$d \approx 22.7 \text{ mm}$$

We solve for resolution now using the d value solved above, the blaze angle of 63.4 degrees, a numerical aperture of 0.13 as listed in the spec sheet of the SM400 fiber, and the width of the slit being the mode field diameter of the fiber (MFD), which is roughly 3 μm . Using these values, we get that the resolving power is roughly 128,000. This number will not be the actual resolving power of the system due to aberrations and imperfect equipment, but this is a good theoretical number to begin with, as it ensures that despite a decrease in this number, we will still reach the resolution requirements of the system. Now that we know that the cross-dispersed echelle system will work, we must use calculations to determine the lenses that will be used in this system. This system requires either two lenses or two mirrors, one to collimate the incoming light onto the grating, and the other to focus the light coming out of the prism onto the detector. The calculations are the same for mirrors or lenses. An important factor for this part of the design is the magnification of the system. The constraint given to us by our sponsor is that the resolution of the sensor should be around 3 pixels/spot on the detector. Our sensor has pixel dimensions of 3.5 μm x 3.5 μm . If we want 3 3.5 μm to span a spot on the detector, that means that the image of the entrance slit must be 10.5 μm on the detector, where the entrance slit is roughly 3 μm . This tells us that we want the system to provide a magnification of 10.5/3, which is a 3.5 times magnification. To achieve this magnification, we utilize the following equation:

$$M = \frac{f'}{f}$$

Where f' will be the focal length of our focusing lens (f_2), and f will be the focal length of our collimating lens (f_1). We still need one more equation to solve for these two values, however. We want our first lens to have the same numerical aperture as the entrance fiber. We know that the numerical aperture of the fiber is 0.13, and the equation for the $F/\#$ is listed previously, as the ratio between the focal length of the lens with the diameter. The diameter of the lens must be the same as the spotsize on the grating. We have already calculated this value to be roughly 22.7 mm. Therefore, setting the $F/\#$ equal to 0.13 with the diameter set to 22.7, we get a focal length for the collimator to be roughly 87.3 mm. We then use this

number with the above magnification equation to find that the camera lens will have a focal length of roughly 305 mm.

Now, we know the lenses, fiber, detector, and have two grating options. We now delve in to the grating equation and the Littrow configuration, where we calculate the diffraction orders which correspond to each wavelength and the free spectral range at both extremes of the spectrum. The grating equation is the most important aspect of this design, followed by the free spectral range in reference to the peak wavelength and the diffraction order. These equations are as follows:

$$m\lambda = \sigma(\sin\alpha + \sin\beta)$$

And,

$$\Delta\lambda_{FSR} = \frac{\lambda}{m}$$

Where α denotes the incident angle of the light onto the grating, β denotes the exit angle, σ is the pitch of the grating, and m is the diffraction order. We will begin this design by calculating for Littrow, and then tilting the grating in zemax to enter into quasi-littrow configuration. These terms are defined in the parts comparison and selection, where we discuss echelle gratings. Because Littrow configuration gives us the same angle exiting as entering, this equation now becomes:

$$m\lambda = 2\sigma\sin\delta$$

Where δ is the angle of both incident and reflected/transmitted light. We will now refer to the light after dispersing from the grating as reflected light, as both echelle gratings being compared are reflective gratings. This angle will be 63 degrees, for the blaze angle. Now, we solve for the diffraction orders which correspond to the two extremes of our spectrum. We need these values to both calculate the FSR of the spectrum, and to design in zemax. We will be using the diffraction order at each end of the spectrum to test the spectrograph in zemax to ensure that all wavelengths are incident on the detector. Our goal for this design is to have a bandwidth of 370-940 nm. When we plug these values in individually to the equation, once for the pitch from the 31.6 grooves/mm grating and again for the 79 grooves/mm grating.

For the 31.6 grooves/mm,

$$\begin{aligned} m_{370nm} &= 152 \\ \Delta\lambda_{FSR370nm} &= 2.44 \text{ nm} \\ m_{940nm} &= 60 \\ \Delta\lambda_{FSR940nm} &= 16 \text{ nm} \end{aligned}$$

For the 79 grooves/mm grating,

$$\begin{aligned}m_{370} &= 60 \\ \Delta\lambda_{FSR370\text{ nm}} &= 6.2\text{ nm} \\ m_{940} &= 24 \\ \Delta\lambda_{FSR940\text{ nm}} &= 39.2\text{ nm}\end{aligned}$$

We can see that while the 31.6 groove/mm grating takes about 90 diffraction orders to span the bandwidth we need, the 79 grooves/mm grating takes only 36. However, the FSR of the 79 groove density grating is more than double that of the 31.6 grooves/mm grating. This larger FSR will result in a spotsize that is too larger for the sensor. We therefore design the system with the 31.6 groove/mm grating. We now know the exact design calculations for our lenses, grating, sensor, and fiber. The last component that has not yet been discussed is the prism. The prism will be an equilateral prism made out of F2 glass. This was chosen because equilateral prisms provide the lowest beam path deviation while providing a high resolution to the system. The F2 glass is optimal for visible and near infrared light, which is the precise wavelength range that we are evaluating.

The final thing we need to address is the dispersion of the light after passing through the dispersive optics. As the light disperses, the beam spot size will increase until the dispersed light reaches the camera lens, requiring a larger and larger lens to be the camera lens. If we design this to be a 4f system, with the camera lens having a focal length of 300 mm, the diameter of the lens must be very large. As we have seen while comparing lenses for use in the system, lenses drastically increase in price as the diameter is increased. We want to keep the price low, but avoid vignetting. We will attempt to decrease vignetting to the best of our ability by shifting this design from a 4f system into a 3f system. Here, instead of the camera lens being placed a focal length away from the dispersing optics, it will be placed as close as possible, but the detector will still be located a focal length away from the camera lens.

Zemax Modeling

To begin, the system is entered in as paraxial mode with only the lenses and grating, and with the ideal focal lengths of the collimating and focusing lenses. The prism has not been added. The object is given a radius of 1.5 μm because the fiber has a diameter of 3 μm . The below figure is shows the basic design for a spectrometer in the Littrow configuration:

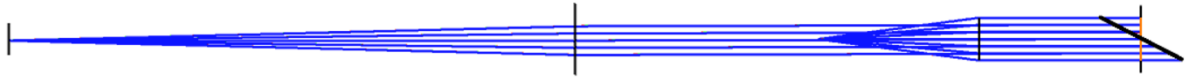


Figure 6.1.3: Zemax Paraxial Littrow Configuration

Using this initial zemax setup, we found the actual spot size of the image on the detector and the resolving power, which was measured from the zemax spot-diagrams for wavelengths of 371nm, 532 n, and 940 nm:

Wavelength	Spotsizes	Resolving Power
371 nm	10 μm	119,053
532 nm	10 μm	123,158
940 nm	11 μm	124,112

Table 6.1.1: Wavelength vs Spotsizes in Littrow Configuration

These vary slightly from the initial calculations, but these variations are small enough to not be of concern. The next step is to tilt the grating on a different axis, so that the dispersed light is redirected away from the incoming light, bringing the system into Littrow Configuration. This is accomplished by making coordinate breaks in the zemax file, and inserting angles to rotate the system about the x,y, or z axis. Note that the blaze angle is met by tipping the grating about the x axis, and the grating is then tilted about the y and z axes to redirect the beam. The grating was tilted on two different axis, as simply rotating on one axis redirected the beam upward, which was an undesired result. We aim for this system to remain in the x-z plain, where y is the axis which points perpendicular to the table. The result is the following paraxial beam path, with the beginning of the system being the blue point further to the right, and the end being the red point further to the right. This design is the 4f system. Now that we have designed the ideal system with the perfect focal length and a 4f relay, we will remove an f, insert a prism, and observe the resulting image on the sensor. This will be followed by inserting non-paraxial lenses, and optimizing for aberrations. A result of angling the system into Quasi-Littrow configuration is that the resulting spot on the detector as well as the grating is along the diagonal. This will be re-evaluated once the actual components have been entered into the system. The below system depicts a simple two lens spectrometer with an echelle grating, before the prism is added. This is done to find how much the grating needs to be tilted by so that the light is re-directed away from the oncoming light beam.

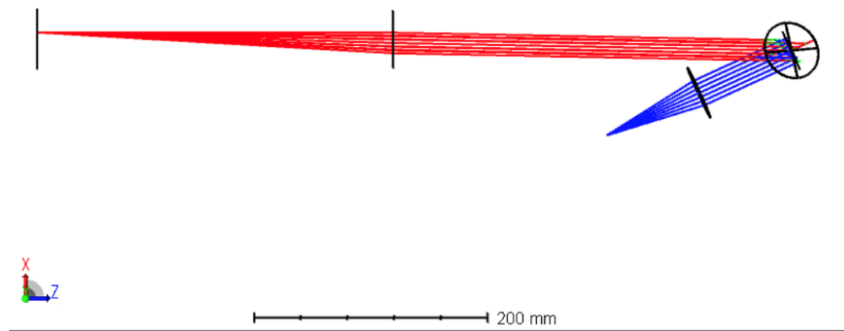


Figure 6.1.4: Zemax tilted grating for Quasi Littrow Configuration

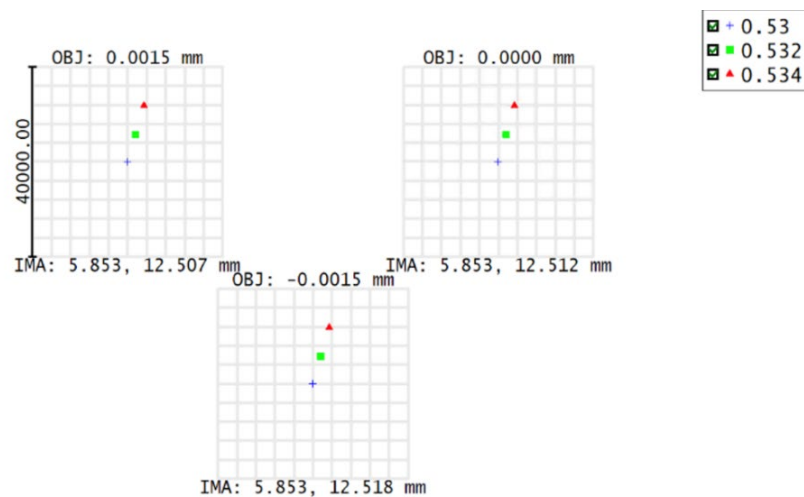


Figure 6.1.5: Crooked Spot on detector

We can see from the spot diagram that a single diffraction order results in a spot which is at an angle. We want to know that the diffraction orders which correspond with the extremes of the spectrum (371 and 940 nm) are not too spread out from one another. If they are, then we know that the system will not fit on the detector. After measuring the coordinates resulting from the diffraction order which corresponds with 371 nm, we switch the wavelengths to be 940, and the diffraction order to $m=60$. We want to see how much of a physical shift across the detector is seen from one end of the spectrum to the other. Unfortunately we cannot see all diffraction orders at once (due to limitations of the Zemax software), so they must be analyzed one at a time and compared. The results are seen in the table below:

Wavelength	Diffraction Order	y-axis coordinate	x-axis coordinate
371 nm	150	-12.928 mm	16.541 mm
940 nm	60	5.380	41.404

Table 6.1.2: Wavelength and Diffraction Order Vs. Coordinates on Detector

This tells us that the width of the spectrum on the detector is about 18.8 mm, and the height is about 25 mm. This fits on our detector, despite being somewhat crooked.

The next step is to add the actual prism. When we shift into the cross-dispersed design, we put the lenses back into paraxial mode so that we can add the prism without the real-life optics of the lenses getting in the way at first. A prism was manually simulated in Zemax by inserting two faces, separated by F2 material, and at a 60-degree angle with one another. To place each lens in the beam path, coordinate breaks had to be added to the system to apply coordinate shifts and rotations. Each component was individually tilted with respect to the system, and then the whole system was tilted so that the following lens was placed in line. In the end, 9 coordinate breaks were applied to the system.

As stated earlier in this paper, a full, custom lens system was designed for the collimating and focusing lens components of this spectrometer. However, the cost and time constraints of this project did not allow for custom lens system to be applied to this project. For this reason, pre-designed and optimized Cannon lenses were utilized instead. These provided the desired light throughput and specs for the system, while greatly reducing cost. Below is the paraxial Zemax spectrometer.

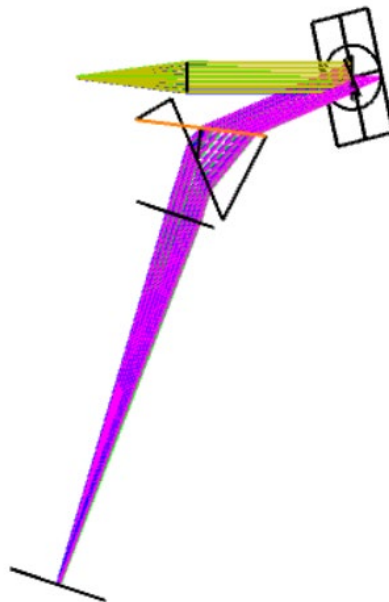


Figure 6.1.6: Zemax Paraxial Cross-Dispersed Echelle Design

The next step is to design the mounting plate and mounts for each component in the system. We did this by exporting the Zemax ray trace of the system with Cannon lenses as a solid ray into Solidworks. We were then able to design the

mounts and mounting plate around the beam path to ensure proper alignment. The Zemax ray trace of the spectrometer with Cannon lenses can be tricky. These lenses are optimized and are designed to provide minimum aberrations. We do not know the exact lens system that is contained within the cannon lenses, but can control the F number and focal length. To simulate these cannon lenses, we represented the spectrometer as a paraxial system. The cannon lenses still contribute some aberrations, so this is not a completely accurate representation. However, we were just interested in recreating the beam path with as much accuracy as possible, and the paraxial representation was able to serve this purpose. Knowing the exact tip and tilt necessary for the grating, and the exact placement necessary for each optic so that they are placed in the ray path imported from Zemax, the below system was designed:

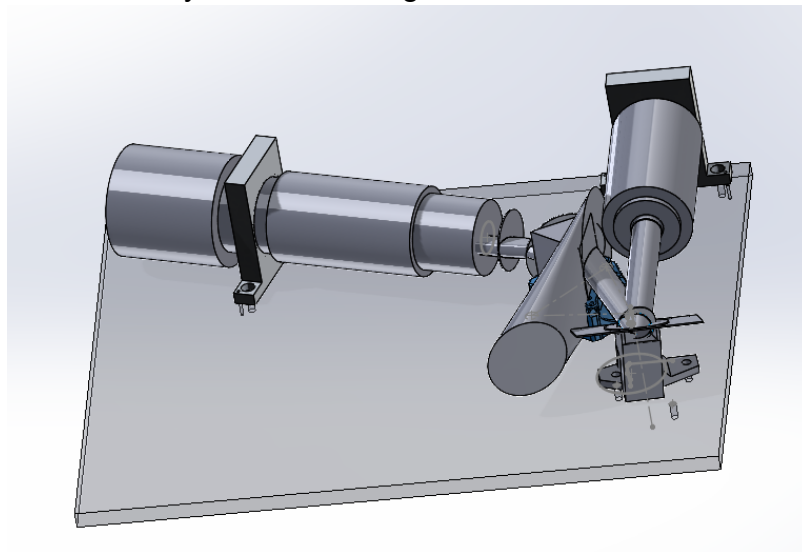


Figure 6.1.7: Solidworks design of spectrometer system mounts

Using this solidworks file, the location for drill holes in the baseplate was found. The size and threads for the mounts for the cannon lenses were designed so that a cannon lens can click into place on one side and on the other side the sensor can screw in to one cannon mount, and the other cannon mount was designed so that a fiber holder can screw into the other side. These items were machined from aluminum. The aluminum plate was machined at the UCF machine shop, and the Cannon mounts were custom ordered. The mounts holding the prism and grating were 3-D printed. These were modeled to provide the height, tilt, and angle that the design required.

The lens system was then taken out of the paraxial and optimized into a system of many lenses, increasing the number of surfaces and therefore improving the quality of the spectrometer system. This optimized system consists of what will be a custom lens system. This system is not applied to this iteration of the project but

is given to the research group funding this project to be applied at a later stage of this research. Below is the zemax ray trace of an optimized design:

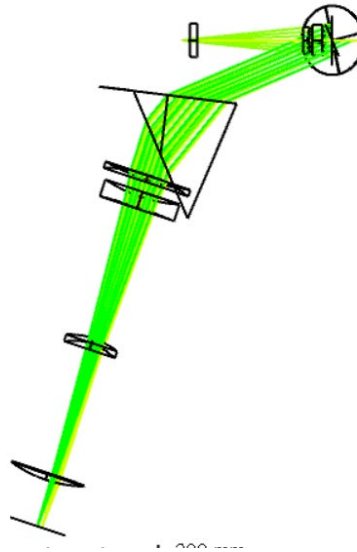


Figure 6.1.8: Optimized Spectrometer with custom lenses

6.2 Fabry-Perot Etalon Design

The Fabry Perot Etalon design is an optical cavity, or resonator, characterized by free spectral range, linewidth, and finesse. Free spectral range (FSR), also called the axial mode spacing, is the spacing between resonator modes. The linewidth or the full width at half maximum (FWHM), is the bandwidth of the resonances generated. The finesse is a factor that describes the loss in the cavity, determined by the ratio of FSR to FWHM shown below. In the context of spectrograph calibration, there are specific criteria the etalon needs to meet. MATLAB was used to determine this criterion as well as check the final etalon measurements.

Etalon Criteria

The first stage of the design was to determine the necessary criteria of the etalon for spectrograph calibration. The etalon's free spectral range should be 3-5 times the resolving element of the spectrograph, this will be referred to as the multiplier. Knowing the spectrograph's resolving power, we were able to calculate the corresponding free spectral range of the etalon using the following:

$$R = \frac{\lambda}{\Delta\lambda_{res}} = \frac{v}{\Delta v_{res}}$$

$$\Delta v_{res} = \frac{v}{R}$$

$$FSR = \Delta v_{etalon} \approx m \cdot \Delta v_{res}$$

Where m is the multiplier, $\Delta\lambda_{res}$ is the resolution element in wavelength, $\Delta\nu_{res}$ is the resolution element in frequency, and $\Delta\nu_{etalon}$ is the FSR in frequency. We will be discussing the etalon in the frequency domain for this design. We consider a central wavelength of approximately 500 nm, where ν becomes 6×10^{14} . With a resolving power of 10^5 , the resolution element is equal to 6 GHz. Since we have a range of options for the FSR, we calculate it with both 3 and 5 as the multiplier, with results of 18 GHz and 30 GHz, respectively.

From here we calculated the required linewidth specification. To prevent line blending, we needed a linewidth that is significantly narrower than the etalon's FSR and the spectrograph's resolution element. So, we aimed for a maximum FWHM of $\Delta\nu_{res}/2$, with a goal of less than $\Delta\nu_{res}/10$. This leads to the criteria of a linewidth less than 0.6 GHz to 3 GHz.

The last determining characteristic for the etalon is the finesse. With the calculated criteria, it would be possible to reach a finesse of at least 25-50. Increasing the finesse increasing the loss that occurs in the cavity, so to maximize the output power, we aim for a lower finesse.

Ideal Etalon Calculations

Now that we have the criteria we need to achieve, there are three factors that need to be determined: cavity's refractive index, mirror reflectance, and cavity length. Options for the cavity medium include glass, air, and vacuum space. Since we want a broadband source, the glass medium would introduce varying refractive indices for the various wavelengths. The vacuum spaced etalon would be ideal, but as mentioned in the manufacturing constraints, it is unrealistic for us to implement. That leaves us with an air spaced cavity, where the refractive index, n , is 1.

Using the equation for Finesse below, we solved for mirror reflectance, R . This gave a reflectance range of 86% to 95%. We were then able to calculate the cavity length, L of approximately 5 to 8 mm using the equations for free spectral range and full width half maximum below, where θ is the angle of incidence of the source onto the first mirror.

$$F = \frac{2\pi}{1 - R^2}$$

$$FSR = \frac{c}{2nL\cos(\theta)}$$

$$FWHM = \frac{c(1 - R^2)}{2(2\pi L)}$$

Actual Etalon Calculations

Within the selected reflectance range and wavelength range of 400 – 700 nm, there is a limited selection of mirrors. The chosen mirror was determined by these factors. We calculated that the chosen component would be compatible using the equations above (FSR, FWHM, F) in MATLAB. With a 99% reflectance, we achieved an FSR that matches the criteria and a FWHM that is less than the goal, but has a higher finesse than expected. Using two of these mirrors 5 to 8 mm apart would be compatible with the spectrograph.

Comparison of Ideal and Actual Calculations

	FSR (GHz)	FWHM (GHz)	Finesse	Reflectance	Cavity Length (mm)	Wavelength Range (nm)
Goals	18 - 30	< 0.6 - 3	>25-50	86%-95%	5 - 8 mm	400 - 700
Actual	18.75 - 30	0.12 - 0.19	160-315	98%-99%	5 - 8 mm	400 – 750

A schematic of the selected components and distances is shown in Figure 6.2.1 below. However, the use of the 300 mm focusing lens is unrealistic to capture the output light of the etalon. An alternative method is to include an aperture stop to control the diameter of the input beam of the last focusing lens. This would have minimized the focal length needed to couple the output into the single mode fiber.

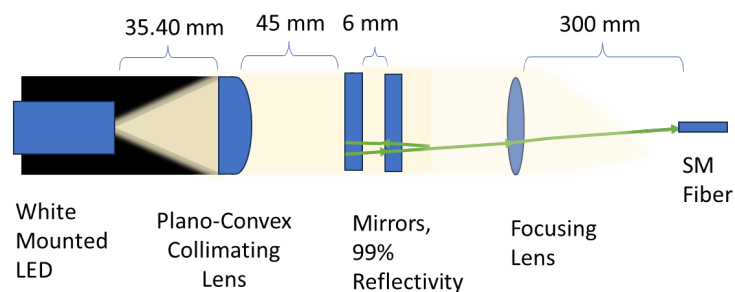


Figure 6.2.1 Schematic of Fabry-Perot Etalon

Etalon Stability Designs

From the beginning of this project, we'd expected that the stability of the etalon would prove to be a major challenge due to the cavity's sensitivity to its environment. Given the time frame and resources, we investigated three different

reasonable solutions: a thermostable mounting plate design, fiberglass mounts, and an enclosure over the optical system.

The first option is a design with the purpose of minimizing the linear thermal expansion and improving the stability of the cavity length. As shown in Figure 6.2.2, the distance between each mirror to its own respective plate mount should be half of the length between the bottom plate mounts, or at least as close as possible. When the metal expands, the mounting placements act as constraints for the sheets. When the bottom sheet expands, the pressure exerted on the constraints will cause the top sheets to contract, counteracting the length of change in length.

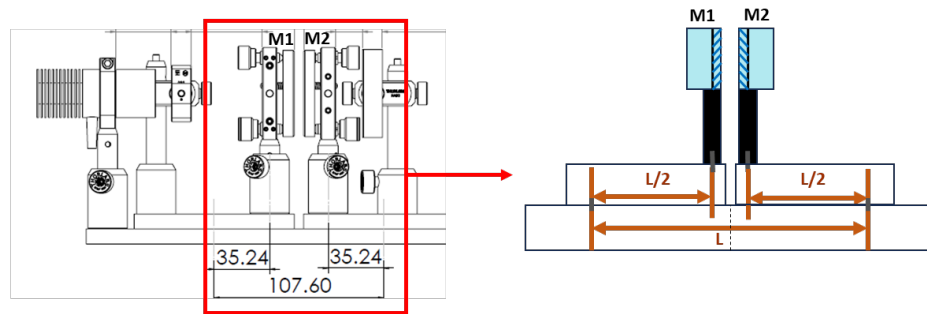


Figure 6.2.2 Thermostable mounting plate design with actual distances

Taking mounts into account, the actual distances are also shown in Figure 6.2.2. Ideally, the mirrors would be in line with the mounting post and as close to the edge of the top plates as possible. However, according to the mounting components, the closest we could design for was $L/3$ rather than $L/2$.

Commercial Fabry-Perot etalons are made with ultra-low expansion quartz. Another material with extremely low thermal expansion is ZERODUR, a glass-ceramic material, previously mentioned as a property of the chosen mirrors. Either of these two options would make an ideal choice for a mounting material, but they would be excessive and expensive. Another option was Invar 36. It is a nickel steel alloy with a low coefficient of thermal expansion. The material that we ended up going with was aluminum, with a coefficient of thermal expansion of $23 \times 10^{-6} \text{ ppm}/^\circ\text{C}$. Utilizing this design, the change in cavity length decreases from 0.0124 mm to 0.0043 mm when the plates are made of aluminum.

Another design we researched was the use of G10 fiberglass to make hollow triangular mounts for the bottom plate of the Etalon. G10 fiberglass is a strong material with a coefficient of thermal expansion of $2 \times 10^{-5} \text{ ppm}/^\circ\text{C}$ and a high resistance to vibration. This would be beneficial in minimizing movement of the mirrors that would interfere with their alignment. A visualization of this design is shown in Figure 6.2.3.

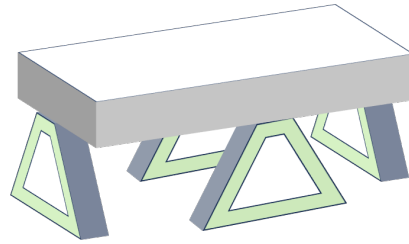


Figure 6.2.3 Thermostable mounting plate design with actual distances

A third option to increase the etalon's stability was an enclosure for the system, whether it just be the etalon or both optical systems, including the spectrometer. The enclosure would start as a plexiglass box with a layer black foam on the interior. The black foam is meant to absorb sound waves as well as stray light. This box would then be covered with a layer of aluminum mylar for insulation. Each of these designs would have been beneficial to implement, especially combined.

7.0 Hardware Design

In this chapter we are going to be focusing on our hardware design in which we are going to be touching base on the schematic of our design, the datasheets and links to our motors, power supply, weather system, sensors, MCU, the platform and type of material that the whole system is going to be built in.

Our system is composed of a collection of different components that work with one another to accomplish what we desire. This system needs to be able to track the sun, and register continuous data, as well as taking images of the sun for future analysis from the Astro photonic department. These images are to be transmitted to the sponsor's office. For which a connection for our system to the lab will need to be implemented.

Based on all the things that we need the system to do, we end it up using 1 motor in our system. There is a DC linear actuator motor designated to the weather protection machine. Since our system needs to be weather resistant our system have a front door that open and close when severe weather is detected.

As mentioned before, it needs to be weather resistant, which a weather station is part of our hardware design. This station is connected to our software so that it communicates with each other so that it knows when to open and close the system. So that it can be protected from heavy winds, humidity, and rain. We have a camera and telescope on the inside platform which are the ones responsible for taking the images and need it for analyzation from the sponsor.

The system have several sensors integrated. There is a light sensor that tells the system where the brightest part of the day is so that it can move it in that direction, this is how we track the sun. The other sensor is to sense the temperature changes so that it is the one to tell the system when to open and close due to weather conditions.

7.1 Initial Design and Related Diagrams

In this section, a general design of the hardware is shown to discuss the different components that are part of the overall electrical block diagram for solar tracking system:

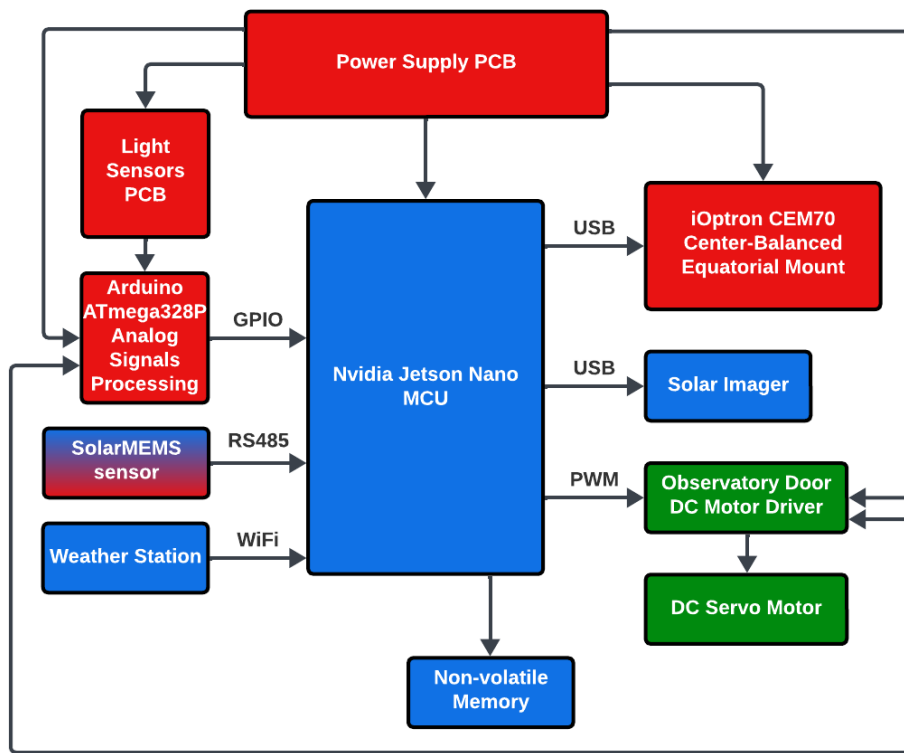


Figure 7.1.1: Solar Tracker system and Data processing overall Hardware Block Diagram

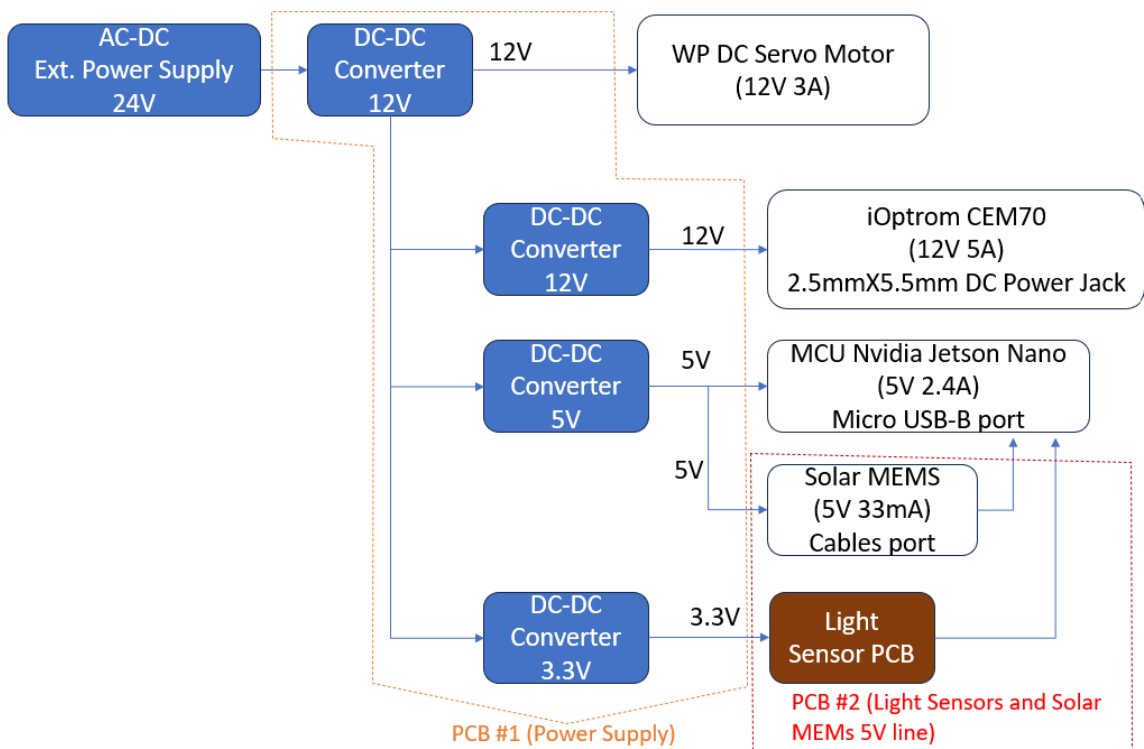


Figure 7.1.2: PCBs Block Diagram: Power Distribution and Connections

From above, Figure 7.1.1 shows the overall hardware block diagram. These diagrams explain how the connection are made and the flow of the solar tracker system operation. On the Figure 7.1.2, it is shown the power distribution among the main components and how the two PCBs will interact between each other. The first PCB, Power Supply, have four voltage lines: two 12V 8A that will be providing power to the iOptrom CEM70 and the door linear actuator DC motor, one 5V 5A that will supply power to the Nvidia Jetson Nano Dev MCU, and one 3.3V 5A for the Light Sensors PCB. The second PCB is the Light Sensors PCB which is set next to the SolarMEMS device. Its function is to track the sun every second by using LDR photoresistors that send analog signals to the Jetson Nano to be processed as Low/High voltage.

7.2 External Power Supply 120VAC/24VDC converter

For the external power supply in our Senior Design project, we have opted for the ANYTITI LED Driver, a robust and reliable power supply unit designed for LED applications. This converter efficiently transforms 120VAC input to a stable 24VDC output, providing a safe and consistent power source for our power supply PCB. Its waterproof design with an IP67 rating ensures durability and protection against environmental elements, making it suitable for various indoor and outdoor applications. The ANYTITI LED Driver, commonly used as an LED driver power supply, boasts ISO certification, attesting to its quality and adherence to international standards. This power supply incorporates multiple safety features, including short-circuit, open-circuit, over-temperature, over-load, and over-current protections, enhancing the overall reliability of our system. The use of aluminum in its construction facilitates effective heat dissipation, contributing to the longevity and stability of the power supply unit. With a power output of 150W and a current rating of 6.25A, coupled with a convenient 3-prong plug with a 4.5 feet cable, the ANYTITI LED Driver proves to be a suitable and efficient choice for our project's power requirements. The reason we selected 150W capacity although we are aiming a <100W system is to overcome power dissipation through converters and assure a reliable power supply on the main input of the system.



Figure 7.2.1: 120VAC/24VDC External Power Supply

7.3 DC/DC Converters

In our hardware design, we have implemented a sophisticated power regulation system featuring four voltage regulator converters to meet the specific power requirements of different components in our Senior Design project. One XL4015E1 regulator is dedicated to supplying a stable 3.3V, 5A output to the Light Sensors PCB, ensuring precise and reliable power delivery for optimal sensor performance. Simultaneously, another XL4015E1 regulator is configured to deliver a robust 5V, 5A output, powering the Nvidia Jetson Nano MCU, a critical component in our system. Additionally, for the iOptrom CEM70 and the door linear actuator DC motor, we have integrated two XL4016E1 regulators. These regulators are tailored to provide a steady 12V, 5A output to the iOptrom CEM79 and a separate 12V, 3A output to the door linear actuator DC motor. After encountering challenges in earlier iterations with the LM2678T-ADJ regulator when supplying power to the Nvidia Jetson Nano MCU, our design underwent several revisions (v1, v2, v2.1, v2.2). Ultimately, we found that the XL4015E1 and XL4016E1 regulators offered a more reliable solution, especially in high-current scenarios.

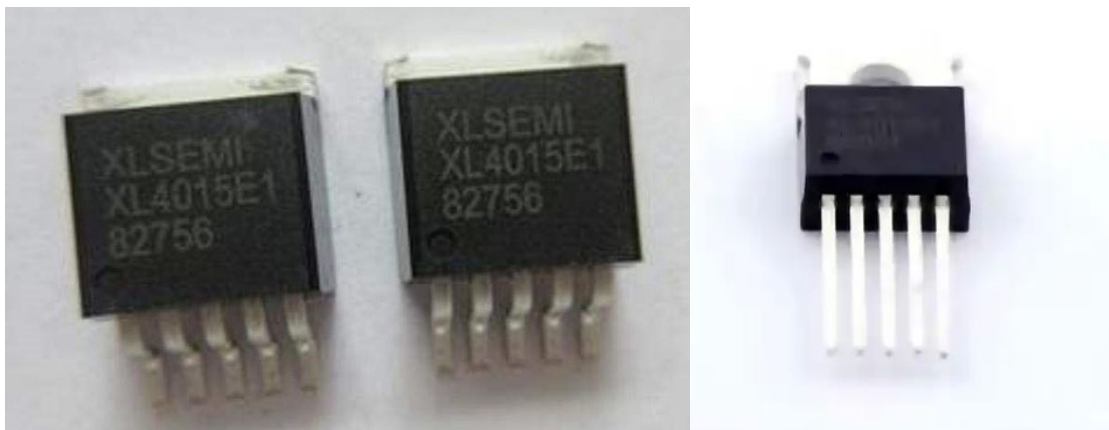


Figure 7.3.1: DC/DC Voltage Regulators: XL4015E1 (left) & XL4016E1 (right)

7.4 Power Supply PCB Designs

Due to the required level of electrical design, we used Altium Designer Professional software to create both the Power Supply and the Light Sensors PCB designs. This software allowed us to get access to real-time libraries for all the components we needed and made the whole design process much easier and smoother. For our main power supply system, we designed a PCB with the capability to provide several required voltage outputs to the solar tracker system and MCU components. It will provide 12V 5A to the iOptrom CEM70 equatorial mount through a DC power jack connector; 12V 3A to the linear actuator DC motor responsible for opening/closing the door of the roof system box and protecting the main components; 5V 2.4A to the Nvidia Jetson Nano MCU through micro-USB;

3.3V 2A to the Light Sensor PCB. We went through several Power Supply PCB design versions:

Power Supply PCB v1: We used this version for reference purposes as a first try on PCB designing.

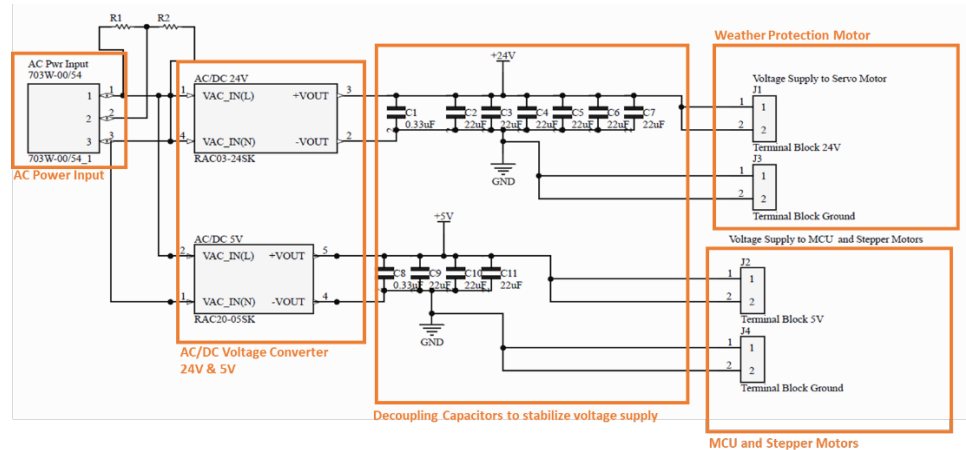
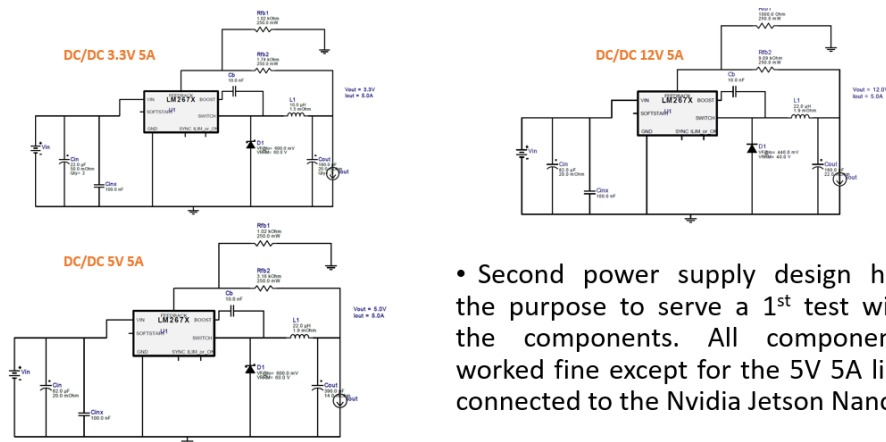


Figure 7.4.1: Power Supply PCB design v1 schematic

Power Supply PCB v2: Tested on breadboard with the main components and had several issues keeping the voltage level on the 5V line.



- Second power supply design had the purpose to serve a 1st test with the components. All components worked fine except for the 5V 5A line connected to the Nvidia Jetson Nano.

Figure 7.4.2: Power Supply PCB design v2 schematic

Power Supply PCB v2.2: We used the same voltage regulators as v2 (LM2678T-ADJ) and modified the design a little based on research. This Power Supply PCB was built, soldered and tested. Unfortunately, this design was working good in several tests until, on one of the tests, the power system started to have a dropped in voltage every time we connected the load to the Jetson Nano.

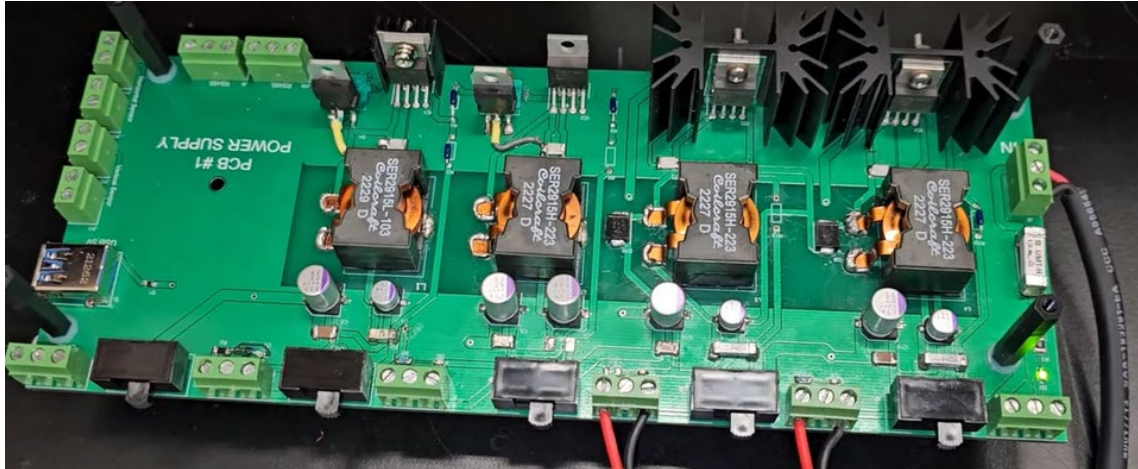


Figure 7.4.3: Power Supply PCB design v2.2

Power Supply PCB v3: We designed a new version of the Power Supply PCB with new voltage regulators. This system was built, soldered, and tested. This Power supply PCB worked very good showing no evidence of voltage drop on any line. We decided this was the way to go since we perfected design components and, after testing, evidenced great performance and reliability.

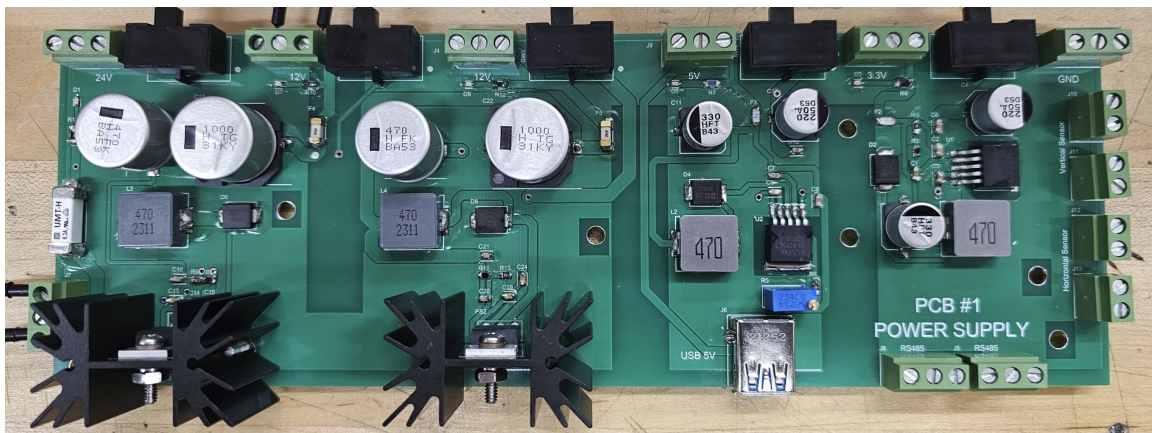


Figure 7.4.4: Power Supply PCB design v3

The Power Supply PCB, which we will be referring to as PCB#1, makes use of four voltage regulators IC: two XL4015E1 and two XL4016E1 which are high efficiency components and allow us to adjust the voltage ranges as we need to take care of voltage requirement. The below Fig. 7.4.1 shows the overall schematic for our Power Supply PCB made using Altium Designer Professional software. Consider that the green boxes are the designators for each one of the voltage line suppliers (which means that, inside of each box, it is different voltage line schematic). This PCB is supplied by an external 120VAC/24VDC power supply with IP67 certification needed for our project requirement to be weather/water

resistant. On this design, we also added decoupling capacitors to stabilize voltage supply, fuses to protect the PCB#1 from the 24VDC external voltage input and to also protect the components we are providing power to, green-LEDs and switches to acknowledge and control whether a voltage line is ON and working well. We went through different versions as we were improving the design based on the output results. We end up at version 3 Power Supply PCB capable of providing the required voltage and current without any issues or drops in voltage lines. See below the overall schematic for the Power Supply PCB design v3.

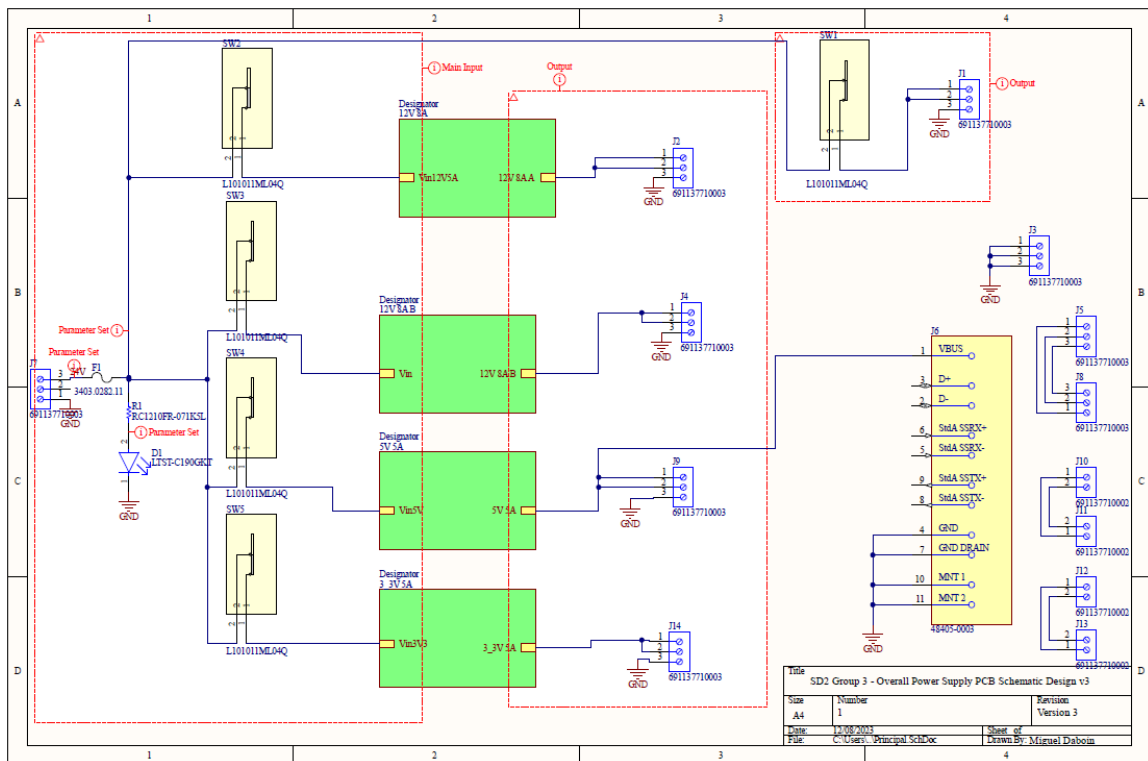


Figure 7.4.5: Power Supply PCB overall design v3 schematic

The green boxes above are used as designators for each one of the voltage lines that provide power to the main components. See below schematics for each one of the voltage lines.

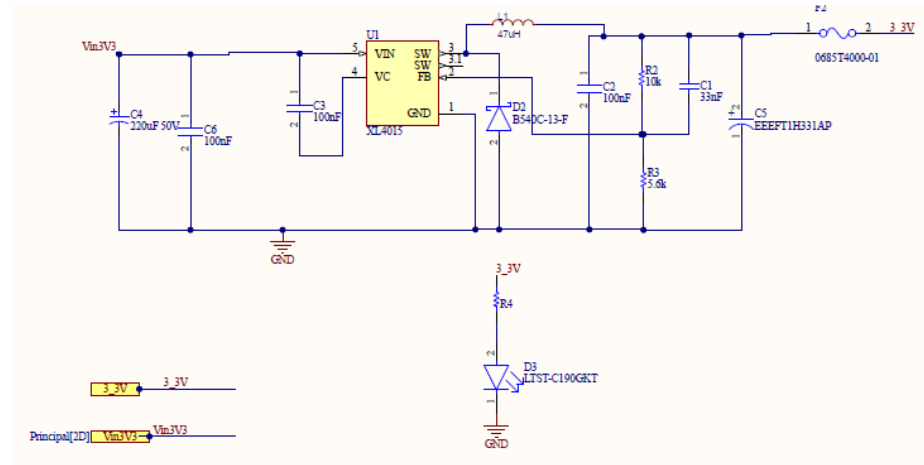


Figure 7.4.6: 3.3VDC line v3 schematic

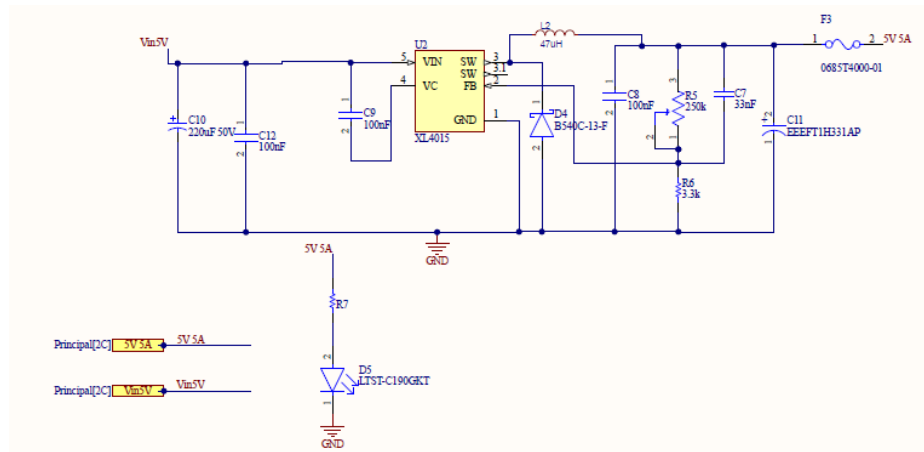


Figure 7.4.7: 5VDC 5A line v3 schematic

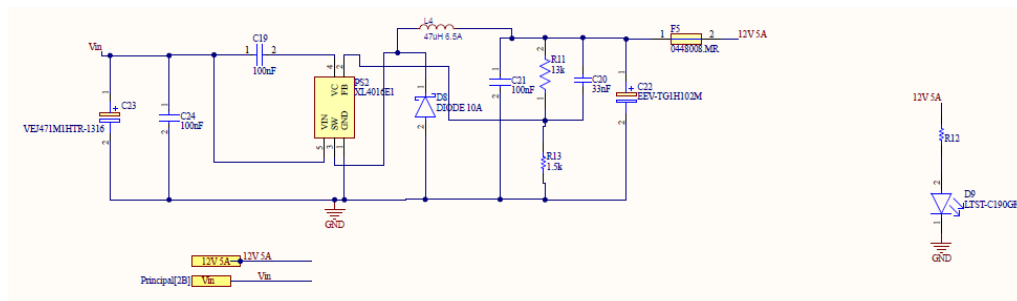


Figure 7.4.8: 12VDC 8A line v3 schematic

After going through PCB design for version 3 of Power Supply, the figure below is our final result.

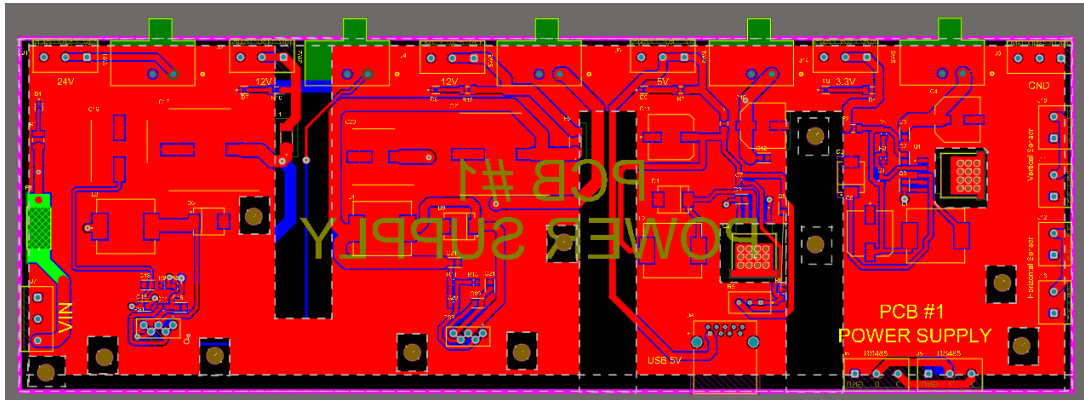


Figure 7.4.9: Power Supply PCB v3 2D View

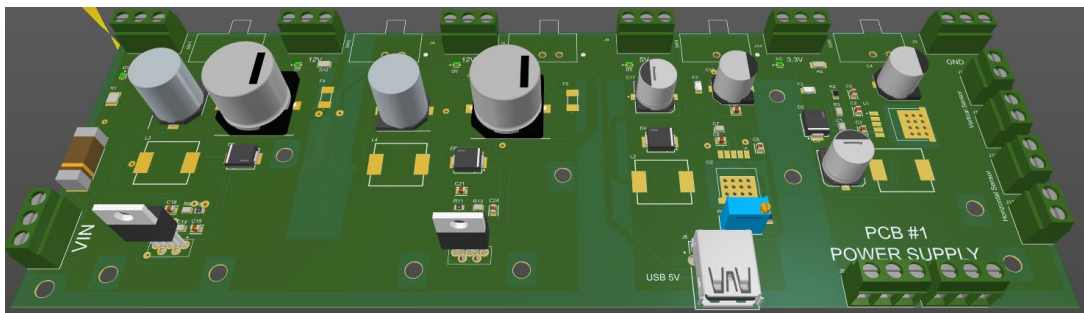
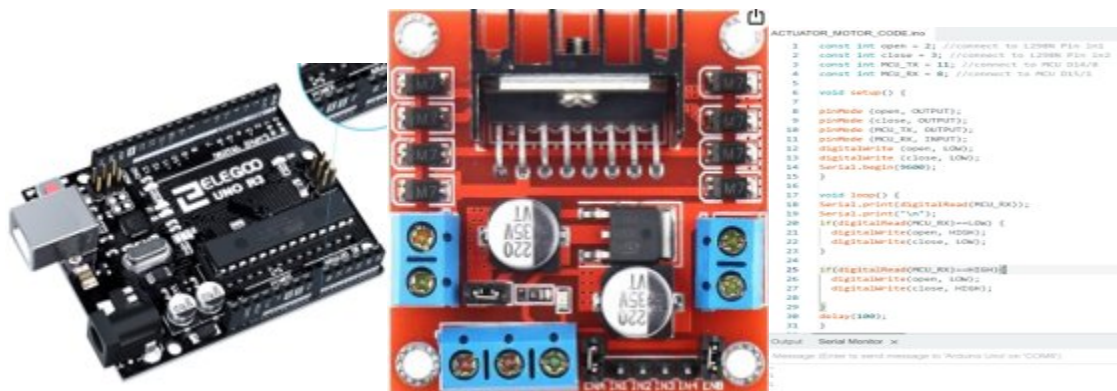


Figure 7.4.10: Power Supply PCB v3 3D View

It is important to consider that some PCB parts did not have the 3D library available and that is why some components seem missing on the 3D view.

7.5 DC Motor / Driver

The DC linear motor for the weather protection of the system, was the motor selected. The motor driver used to control the selected motor to open and close the system was the L298N, which was then connected to the Arduino board by using a simple code that commands the motor to eject/retract when the MCU tells the Arduino to due to weather conditions. Below are the images of the Arduino board used, the motor controller used as well the written code, (order left to right).



7.5.1 Weather Protection System Motor

The system is weather protected, so it was important for us to integrate a way to protect the system. The way we are doing this is by having a DC linear motor that is responsible for closing the front of the door of our observatory. We have the motor in the inside of the box attached to a hinge that opens and closes the door box whenever the software tells it to close due to severe weather. The motor chosen for this portion of the system was the DC motor ECO-Worthy Linear actuator Rated load of 1000N Max travel speed 14mm/s Rated Voltage of 12VDC Rated Current of 3Amps, Operation Temperature of -65F to +400F, Protection Class IP6.

This was the motor chosen because of some of the specifications, which we feel meets what we are looking for in a motor. First, it was in stock with one-day delivery, which is a big plus now a days with all the availability constraints. Another main reason was the fact that the voltage rating for this motor is 12 VDC, which is more than sufficient for what we need it. With a 6 inch stroke to open the door all the way to the 90 degrees need it. With a minimum holding torque of load of 1000 N, it means that it will be able to sustain our door made of plexi glass, to open and close. The actuator motor weighs 1.772 lbs, which is a decent amount that we can work with.

The function of this motor is to enable the system to open and close the front door of our box when the information transmitted to it by the sensors tells it the sun is down for the day, or the day is up for the day. We want the system closed during the nighttime so that it does not get exposed to humidity or to mist during the night. The motor is also integrated to the system connected to the MCU so that it can read the information when it needs to close due to weather conditions via the arduino board.

7.6 iOptrom CEM70 Mount

One of the most critical parts of the solar tracker system is the mount and the dual-axis movement. For our previous design, we had decided to create a dual-axis platform with two stepper motors in charge of the movement of each axis and to point all the solar spectrometry roof components out to the sun. As a request from our Sponsor, this component design was replaced with the iOptrom CEM70 equatorial mount that provides a more accurate and precise movement of the platform. The iOptrom CEM70 is equipped with precision stepper motor with 0.07 angle degrees accuracy for precise and accurate tracking. The mount is connected to the Nvidia Jetson Nano which controls its movement based on the data received from the Light Sensor PCB and the SolarMEMS device.



Figure 7.6.1: iOptrom CEM70 Equatorial Mount

7.7 Weather Station

After a comprehensive review of every weather-station we pre-selected in our research, we decided to go with the Ambient Weather WS-2000 Home Weather Station. This solution comes with most of the weather sensors we need to feed the weather protection system so we can protect the telescopes, camera, and solar tracker mechanism and components from rain, storms and any other extreme weather conditions. Weather sensors are important for collecting accurate data for our systems and for reporting data in real-time together with the camera and telescopes data processing and solar disk studies with respect to weather conditions. These measurements are necessary to accurately accomplish our goals on the weather protection system. Sensors like UV and solar radiation let us identify if we have a cloudy sky. On the other hand, humidity sensor together with relative pressure, temperature and wind speed sensors will let us forecast a storm before it happens. That way we can set the MCU to process this real-time data and decide whether to close or open the weather protection dome that will protect our telescopes, camera and main components. The WS-2000 Weather Station allows to establish API support to retrieve each one of the sensor's data in real-time and historical if needed. This feeds the MCU with the weather data for the weather protection system software which makes the logical decision. Weather station is placed at a certain distance from the Solar observatory and in a high building, so we avoid any interference to data measurements.

Weather sensors integrated in this station are used to get accurate measures of:

Parameter	Description
Dew Point	The temperature at which the air becomes saturated with water vapor, leading to the formation of dew or condensation
Heat Index	Also known as apparent temperature, it assesses how hot the human body perceives the combination of air temperature and relative humidity
Outdoor Humidity	Refers to the amount of water vapor present in the air outside, expressed as a percentage of the maximum moisture capacity at a given temperature and atmospheric pressure
Outdoor Temperature	The measurement of air temperature in the external environment, critical for weather forecasting and understanding climatic conditions
Rainfall	The amount of precipitation in the form of rain that falls from the atmosphere and reaches the Earth's surface
Relative Pressure	Also known as atmospheric or barometric pressure, it measures the force exerted by air molecules in the Earth's atmosphere on a surface
Solar Radiation	The electromagnetic radiation emitted by the Sun across a wide spectrum of wavelengths
UV Level	Measures the intensity of ultraviolet (UV) radiation in its vicinity
Wind Direction	The direction from which the wind is blowing, measured in degrees
Wind Speed	The rate at which air molecules move horizontally past a fixed point in the atmosphere, measured in units of velocity, such as meters per second

Table 7.7.1: Weather Station WS-2000 measurement types from sensors

For the power input, the outdoor system works with 2x AA batteries. On the other hand, the system comes with a Tablet LCD that is placed in one of the CREOL building lab where all the solar spectrometry processing equipment is and, it has a power input of 5V DC and a consumption of 0.5 Watts.

7.8 Light Sensors PCB Design (Layer-1 solar detection)

LDR stands for Light Dependent Resistor. Each LDR sensor acts as a light-sensitive resistor, changing its resistance based on the intensity of light falling on it. By placing two LDRs on each axis, the system can accurately determine the position of the sun in both horizontal and vertical planes. These resistance changes can be measured and processed by the MCU, enabling the system to send data to the MCU and, after processed, make decisions on what direction the platform will move.

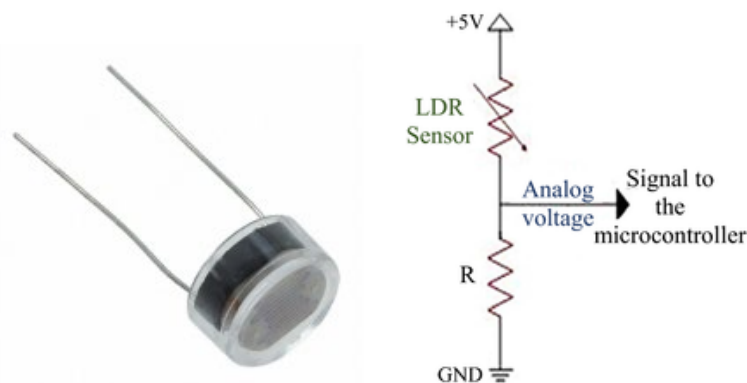


Figure 7.8.1: Photoresistor

Considering the need of having a first device to be able to align all the components on a first-stage position before using the SolarMEMS device, we designed the Light Sensor PCB (PCB#2). For solar tracking system design, we decided to implement a 2-layer sun detection system. The first layer consists of four photoresistor sensors that oversee orienting the platform to the right position after the system resetting from the day before. The solar tracker system is oriented at first to the area of sunrise (East). The function of the first layer is to use four LDR (two for azimuth axis and two for elevation) to send the data to the Nvidia Jetson Nano and very slowly to move the platform to the right position. Once the platform is well oriented, the second layer (sun sensor) will be activated, and the first layer will be deactivated automatically.

This PCB is an analog light tracker which sends voltage high/low signals to the MCU. It was designed as a window comparator circuit. In order to sensing the light, we used simple photoresistors which are completely passive components and have no polarity. The Light Sensors PCB has two-axis (vertical and horizontal) with two photoresistors each and the way it works is that if one of them receives more light than the other (same-axis), it will suddenly change the voltage and, by using

a comparator, we can easily decide in which direction we need to move the platform, so all the sensors balance the light voltage values again. See below the Light Sensor PCB design schematics.

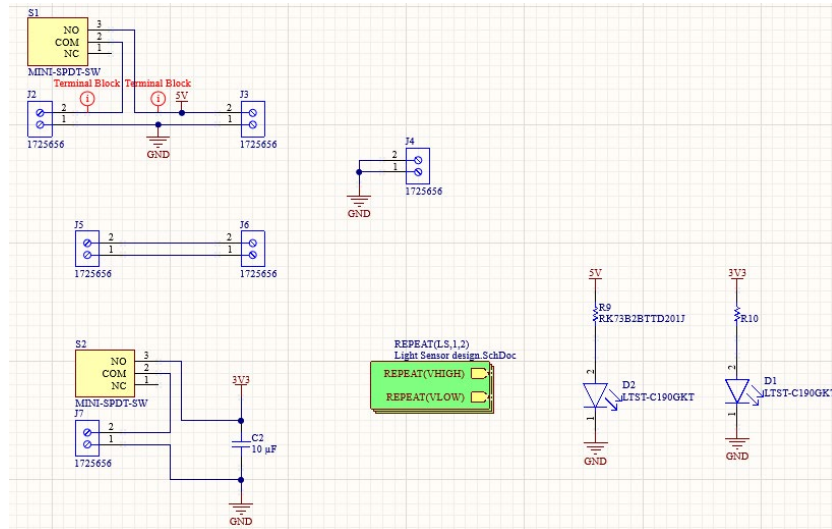


Figure 7.8.2: Light Sensors PCB overall design schematic

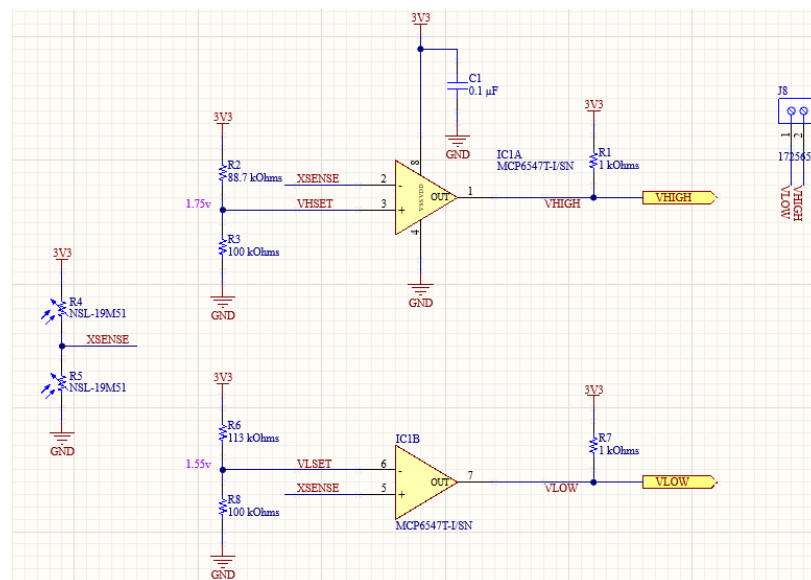


Figure 7.8.3: Light Sensors PCB: Window comparators

The above figures show the overall schematic for our Light Sensor PCB#2 made using Altium Designer Professional software. For a quick explanation on how the Light Sensor PCB works, we can say that each axis is a circuit employing a comparator, a sensor voltage, and two fixed voltages (window comparator definition). The fixed voltages establish the upper and lower boundaries for the acceptable signal voltage range. Should the signal wander beyond these boundaries, the comparator output undergoes a change, effectively serving as an

alarm for the system and sent to the MCU. This lets us to independently assess each comparator to determine whether the sensor signal has deviated excessively in the higher or lower direction.

One of the issues we had with this PCB#2 was that the photoresistors were not able to detect the correct alignment because all the photoresistors were receiving the same light intensity from the sun. From here, we designed an object on SolidWorks software that allows us to make axis photoresistors independent from each other and to differentiate on which direction the iOptrom CEM70 must move. This object is 3D printed and placed on the back of the PCB#2 (where photoresistors are located). See below Fig. 7.8.4 with a 3D printed view of the object placed on the back of the Light Sensors PCB.

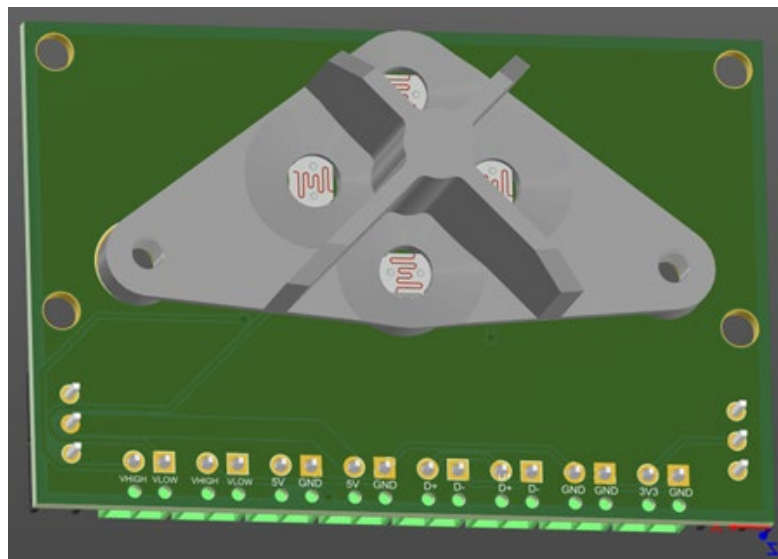


Figure 7.8.4: 3D printed object on top of photoresistors (Light Sensor PCB 3D view)

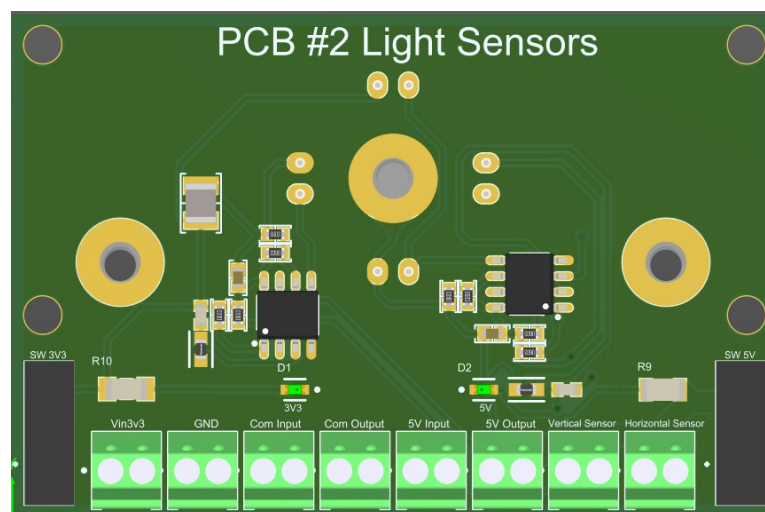


Figure 7.8.5: Light Sensor PCB#2 3D view (front)

7.9 SolarMEMS Sensor (Layer-2)

We used a dedicated solar sensor in combination with our own light sensing PCB to maintain a proper alignment with the Sun's precession. The sun sensor we used was the Solar MEMS Sensor ISS-DX. This sensor communicates to our Jetson Nano by using the RS485 communication protocol, telling us the current light intensity, which we expect to give use peaks when properly aligned with the sun. We used our own specially designed light sensor PCB to determine which direction our system should move. The data from the sensor we designed tells us the specific direction to drive the mount, and the Solar MEMS sensor tells us when we are properly aligned acting as a second-layer solar detection with more accurate measurements and very precise. This way we assure that components inside the box are pointing out to the sun, specifically the sun disk.

Sensor Model	Type	Field of View	Accuracy	Communication Interface	Use Cases
ISSDX	Digital	10° to 120°	0.005° to 0.06°	MODBUS RTU over RS-485	Aeronautics and Renewable Energy Industries

Table 7.9.1: Solar MEMS Sun sensor

This sun sensor measures the angle of the sun ray in both orthogonal axes and the solar radiation. This guarantees a high-accurate solar tracker system with very low power consumption. The sensor has also a level of protection of IP65 which assures the high durability of the system.

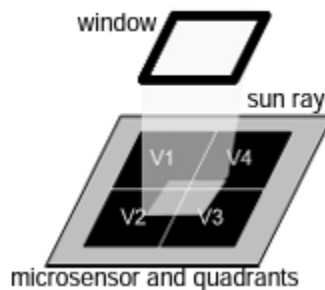


Figure 7.9.2: Photosensors and quadrant distribution

From the above picture, we can observe that the sensor uses the azimuth and elevation axis to measure the angle of a sun ray and solar radiation level on the four quadrants of the detector. Also, a block diagram is provided below for the connection with the MCU. It is important to mention that this sensor uses a RS-485 communication protocol which is widely used in serial communication for transferring data between multiple devices over relatively long distances. RS-485

it is known for its noise immunity which makes it very suitable for various industrial and commercial applications.

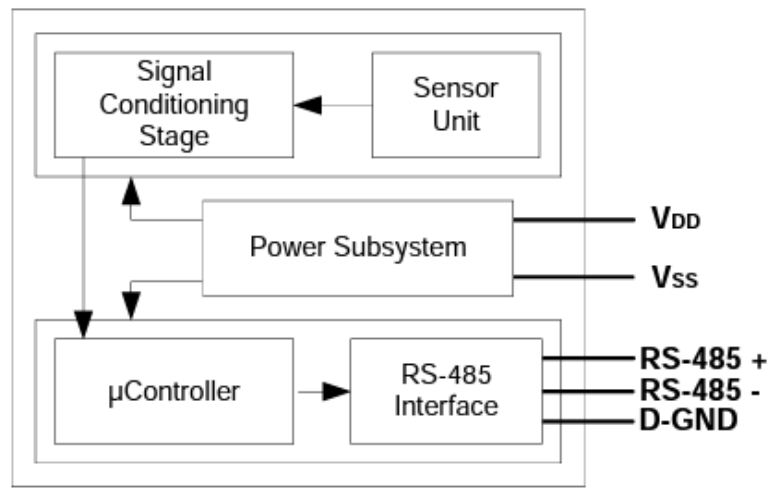


Figure 7.9.3: Block Diagram RS-485 Protocol

The electrical characteristics of the sensor are provided in the following table:

Symbol	Parameter	Min	Typical	Max	Unit
V DD	Supply Voltage	5	5	12	V
I DD	Feed Current	-	33	-	mA
RS-485					
V IH	Voltage Input High	2			V
V IL	Voltage Input Low			0.8	V
V OH	Voltage Output High	3.5			V
V OL	Voltage Output Low			0.4	V

Table 7.9.4: Electrical Characteristics

For our design, we decided to place the sun sensor on the front/middle of the box right behind the door and next to our Light Sensors PCB. The way they are attached to the solar tracking system box, we are able to calibrate them as necessary.



Figure 7.9.5: SolarMEMS Sensor

7.10 Camera

For the camera that will be attached to the one of the telescopes, we selected the Neximage 5 Solar System Imager (5MP). It is a product manufactured by Celestron, a company known for producing high-quality telescopes and imaging equipment. It has a 5 Megapixel color sensor and possess a technology that reduces image noise levels by low-noise CMOS imaging. Its OEM software will allow us to filter out video frames most affected by poor atmospheric conditions which results in clearest frames with high-quality image. Part of the more important features are:

Feature	Description
Sensor Resolution	5-megapixel color CMOS sensor
USB Connectivity	Connects to a computer via USB 2.0 cable
Software	Comes with image capture and processing software
Solar Imaging	Specialized for capturing detailed images of the Sun and solar phenomena such as sunspots, solar flares, and prominences
Planetary Imaging	Suitable for photographing planets like Jupiter, Saturn, Mars, and Venus, capturing planetary features and cloud bands
Telescope Compatibility	Compatible with most telescopes, attachable to the telescope's eyepiece or through a telescope-specific adapter

Table 7.10.1: Neximage 5 Solar System Imager features

The camera is powered by USB through our MCU. The MCU is also in charge of processing the media data for its storage.

7.11 Weather Protection Box

For our weather protection system design, we decided to go with a rectangular clear box that was made of Plexi glass, since it was one of the material types that we founded to be durable, not too heavy so that we can stay withing the weight specifications that we need to meet and water resistant. Picture below is depicting a solid works model of our designed box. The final dimensions of our observatory 24" X 16" X 12". Inside this box we have our light PCB, our MCU, the mini telescope, the imager, the motor driver, our Arduino board and our power supply PCB that provides power to the MCU, to the IOptron, the solar mems, and the light sensor PCB.

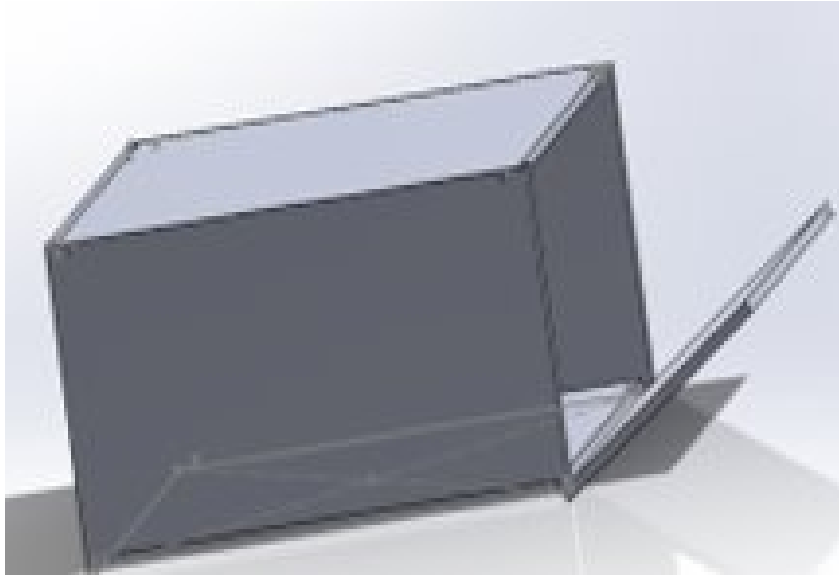


Figure 7.11.1 Solid works picture design of the box

7.12 Main Components Platform

The solar tracker platform, where telescopes, the camera, and the solar detection panel were initially planned to be placed, had an approximate circular shape with a diameter of 5 inches (please refer to the above picture for reference). However, during the development and integration of the systems, we have since modified our approach. The platform's design has evolved to accommodate all components within a protective box, eliminating the need for an external circular shape. This adjustment allows for greater flexibility in optimizing the platform's dimensions, ensuring ample space for mounting components while considering load-bearing capacity and rigidity. Given the outdoor application of the platform, measures have been taken to guarantee protection against direct sunlight, temperature fluctuations, and potential moisture or dust. From a safety perspective, the mounting mechanism has been meticulously designed to prevent any accidental detachment of the main components during operation, minimizing risks associated with potential mechanical failure. The fabrication material for the platform was carefully selected, and after evaluating various options, we opted for plexiglass due to its transparency, lightweight nature, and suitability for our specific application. Plexiglass provides the necessary structural integrity while allowing visibility of the enclosed components. This approach addresses both structural and visibility requirements, aligning with the specific needs of our solar tracker platform.

8.0 Software Design

8.1 Software Design Principles and Patterns

The design of our project's software is dictated by the necessities of our project's sponsor Dr. Eikenberry. We need our observatory platform to perform several tasks ranging from predicting incoming weather to driving motors that will open and close the platform. This means that we need to provide structure for our software before we start to implement any of it, so that we don't end up with "spaghetti" code. If we don't have a set structure to follow, the software will be harder to debug, more prone to common errors, and harder to maintain. This is why we must begin by exploring common software design principles that will guide our design process.

There are many common design principles for software engineering. We will start by first talking about the SOLID design principles. SOLID is a combination of five design principles meant to produce readable and maintainable code.

The S stands for the Single Responsibility Principle. The Single Responsibility Principle states that in object-oriented software, a class should only have one reason to change. This is equivalent to saying that a class should have a single responsibility, or only one job that it does. This simplifies your code since each class will serve one purpose and make its contribution clearer.

The O refers to the Open/Closed Principle. This means that parts of your software such as objects, methods, and classes should be open for extension but closed for modification. Once you have written a function, it should not be modified or changed unless you are fixing bugs. This ensures that the code that is already written will not be overwritten and will behave as expected. The open part means that things like classes or objects can be extended to include new functionalities. This allows our code to be more flexible as the existing classes can meet new requirements that arise as the codebase grows.

The L is the Liscov Substitution Principle. This principle is a little more complicated, and so it's best explained with an example. Suppose we write a program for the local zoo that has different classes for each animal on display. This program has a Mammal class, and specific animal classes such as monkeys, zebras, and lions will be inherited from the Mammal class. The Liscov Substitution Principle says that wherever we can use a Mammal object, we should also be able to use one of its subclasses, such as a zebra, without causing any issues. That is, objects of a parent class should be substitutable with an object of its child class without changing the logic of the program. So, if we wanted to call a function that returned an animal's phylogenetic kingdom, it should return 'Animalia' regardless of whether the function is called on the Mammal parent class, or one of its subclasses. This guarantees that an object of a child class will exhibit behavior consistent with that of its parent class.

For I, we have the Interface Segregation Principle. This is a simple principle that states that for different clients, specific interfaces are better than one general

purpose interface. Another way of saying this is that one type of connection should belong to one interface. This ensures that each connection is independent, which would make them easier to debug.

The last part of the SOLID principles is D, the Dependency Inversion Principle. This principle states that higher level modules should not depend on lower-level modules directly. Instead, they should both depend on abstractions. For example, if we have an Oven class that can turn an oven on and off, it will depend on a Timer class that could count for however long the timer was set and notify the Oven class to turn it on or off. With the Dependency Inversion Principle, instead of letting our Oven class depend on the Timer class, we implement the timer as a Timer interface. This would allow for different implementations of the Timer interface to be used interchangeably, without modifying the Oven class. This reduces the dependence between classes and makes code more modular.

These five principles make up the SOLID principles for object-oriented software design, but they're not the only principles worth taking into account for our project. There are other principles such as the DRY principle. DRY stands for "Don't Repeat Yourself". This means that your code should not be repeated. The functionality of your code should be broken down into smaller pieces so that it can be reused in different situations. Another popular principle is KISS, "Keep It Simple Stupid!". This means that you shouldn't introduce unnecessary complexity to your code. You should keep your functions small and simple. There's also YAGNI, "You Ain't Gonna Need It". This principle states that you should only implement things as you need them.

All of these principles give us a way to structure our code so that we can ensure it is stable, readable, and fully functional. Not all of these principles will be applicable to our project, but they will still provide a solid foundation for our design.

In addition to the common design principles of object-oriented software, we should also look at the common design patterns that will be used to solve common problems throughout our software's development. First, a design pattern is just a general design for a reusable solution that can be used when solving all kinds of issues that occur when designing software. They can be thought of as templates for how a given class or module should operate, why it should be that way, and what the consequences of that solution will be. So, we will be looking at a few specific design patterns, speculating on where they may be helpful to our project, and explaining why we would want to approach our design that way.

The first design pattern we should be acquainted with is the singleton pattern. A singleton is a class of which there can only be one instance at any given time. There will only ever be one object of that class. This pattern ensures that a singleton provides easy access to its one existing instance and controls its own instantiation. The singleton is a very simple design pattern that may be useful in operating the control of our program. We would only ever want there to be one main function, or entry point into the program, so the singleton would work. Now, there may be some issues when using a singleton, as the other parts of our

programs will depend on the main control, instead of operating independently of each other. This could cause issues if their interdependence creates unexpected bugs in our software.

The observer pattern is a design pattern in which an object called the subject maintains a list of dependents called observers. The subject then notifies the observers when a change in state occurs. This then allows the observers to update their own internal states. This defines a one-to-many relationship between objects in our program. We can make use of the observer pattern in our control program. This would enable us to maintain centralized control over the flow of the program while allowing the processes to run independently of each other. This would be ideal for decoupling processes from each other, so individual issues can be resolved at the source. The disadvantage to this approach would be if the processes needed to communicate something to the control flow, they wouldn't be able to since as observers, they can't communicate with the subject.

The strategy pattern is a pattern that enables the program to select an algorithm at runtime. This means that instead of implementing a single algorithm, many algorithms can be implemented, and an instruction can be given to let the program know which algorithm to run at runtime. In practice, the strategy pattern may not be a viable option for our program, but the ability to select an algorithm at runtime may be useful for testing our rainfall prediction program. This will allow us to implement multiple weather predicting algorithms of differing complexity and test their efficacy. In doing so, we can choose the ideal algorithm for our project.

Just as there are common design patterns in software development, there are also some common design anti-patterns. Anti-patterns are like the opposite of design patterns, they are common traps that software developers fall into. These anti-patterns will negatively affect your design and typically lead to bugs in your code. By observing a few anti-patterns, we can commit to writing better code.

The first common anti-pattern is the golden hammer anti-pattern. The golden hammer is when a developer is familiar with a specific technology or concept and applies it to solve every possible problem. This often leads to developers stagnating in their skills or abilities, and they will often apply a specific solution where it doesn't belong. This antipattern is not a huge concern to our application, but still worth mentioning due to its prevalence.

Another common anti-pattern is the blob antipattern. The blob is a pattern where the developer treats the design of an object-oriented piece of software as if it was a procedural program. This leads to the creation of a class or module which carries most of the responsibilities of the program. The class becomes bloated and eventually becomes too difficult to maintain. The blob anti-pattern also breaks the single responsibility principle. The reverse of the blob is another anti-pattern called a poltergeist. The poltergeist is an anti-pattern where many classes have little functionality but are still part of the system. The poltergeist causes the program to be bogged down by unnecessary classes that waste resources. They are inefficient and are often caused by a lack of structure or planning. We intend to

avoid both of these antipatterns by deploying a clear design for the responsibilities of each class and module in our programs. There should not be any cross-contamination of the responsibilities each class will hold.

The last anti-pattern and arguably the worst is the spaghetti code. This is code that was written without planning, designing or any forethought. This leads to software that has no structure. The lack of structure makes the code hard to read, hard to maintain, and often causes bugs in the software. This comes down to the fact that unplanned issues may occur due to unforeseen interactions in the code. Spaghetti code can be mitigated by frequent refactoring of the code, but if it's not done it will inevitably lead to your software needing a full rewrite. We will avoid spaghetti code by thoroughly planning the design of our software before we even write the first line of code. The software we develop needs to be clear and maintainable, and we can do that if we provide a clear structure to the system.

Now that we have covered the basic software design principles, we should decide on which ones will guide our development. The classic SOLID design principles are a good starting point for our purposes, but they're not all directly applicable to our project. So, we will take the relevant principles, the Single Responsibility Principle, the Open/Closed Principle, and the Interface Segregation Principle. These will all be useful in our software's development process. Additionally, we can use the DRY principles to simplify our code. These principles will all help guide our software's development.

8.2 System's Software

Our NVIDIA Jetson Nano computer will need an operating system to run on. Designing our own operating system would be beyond the scope of our project. Instead, we will be using the NVIDIA Jetpack SDK (Software Development Kit). JetPack will provide all of the tools necessary for building applications and includes an operating system for Jetson products. The JetPack SDK includes a Linux kernel, with an Ubuntu desktop environment as recommended by Dr. Eikenberry. In addition to the Linux OS, JetPack provides several libraries and APIs for enabling hardware-accelerated artificial intelligence applications. This kit will make our Jetson Nano capable of running the software we need right out of the box.

Linux is an open-source operating system. Like Windows, it is a program responsible for managing a system's hardware and distributing those resources to other programs. Unlike Windows, Linux offers different distributions, which customize the operating system to meet the user's needs. Ubuntu is a fully-fledged operating system, which was originally based on another distribution called Debian. It is a free and open-source piece of software that has become one of the most popular versions of Linux. The setup for the Ubuntu environment will be managed by the JetPack SDK, allowing us to focus on the more important aspects of our software development.

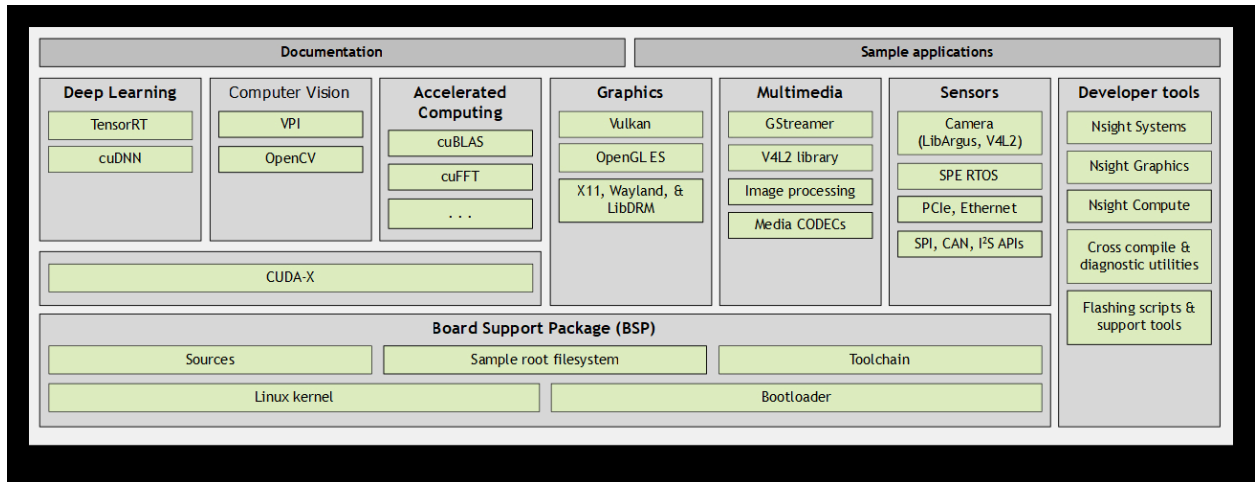


Figure 8.2.1: The contents of the JetPack SDK (Image from NVIDIA)

Our application needs to be able to interface with lower-level components such as motor drivers or sensors. We can do this because the JetPack SDK includes the Jetson Sensor Processing Engine toolchain that supports external peripherals. This lets us have I2C, SPI, UART, GPIO, and PWM signals connected to our Nano. The JetPack SDK also includes support for computer vision applications. This will help us to operate the camera and in capturing images of the Sun.

For our project, we need to be able to establish an SSH connection with our Jetson Nano. SSH, or Secure Socket Shell, is a networking protocol that allows users to securely access a computer over a network. That is, you can remotely access a computer and execute any program on it without requiring you to have physical access to the system. Since our computer will be an isolated system, allowing us to SSH into it will give us the ability to connect to the computer while it is in the field. Then we can debug issues or handle errors as they come up, or transfer files into and out of the machine. In order to use SSH connections, we will need to install an appropriate SSH Client such as PuTTY or MobaXterm and an SSH server such as OpenSSH. The server will be loaded and running on the Jetson Nano computer, while the client will connect to it from an external PC. When we set up the SSH server, we will want to modify the standard settings to ensure we're following the SSH security best practices to guarantee the security of our system. This means that we will need to do things such as changing the default SSH port, generating and using keypairs instead of passwords, and disabling root access.

One of the key considerations when developing our software's design is what language or technologies we will have to use. To facilitate the development of our software, we need to choose a programming language suitable for our project's requirements. Python is a flexible and popular language, which provides ample support for artificial intelligence, robotics, and many other applications. This makes Python an excellent choice for our software. We can leverage the many preexisting libraries to accelerate our progress. Also, Python is a pretty easy to read language that makes it beginner-friendly and well-suited to developing rapid prototypes. The biggest disadvantage of using python to develop our software is that python is not

a particularly fast language, our program will not have good performance. On another platform this might represent a significant challenge, but the Jetson Nano is a very robust platform and offers fast performance. This makes it less of an issue if our program is slow or resource-heavy, but we still need to consider this when we are implementing our software.

Another programming language that we can consider using is C++. C++ is a powerful and efficient language that is used in basically all fields of software engineering and development. Like Python, it is common in computer vision, robotics, artificial intelligence, etc. C++ offers low-level control of a system and higher performance than a language like python. This makes C++ a solid choice for our project's software. It is also worth noting that C++ offers a mature ecosystem of libraries and frameworks that we can leverage to assist in the development of our software. The disadvantage of C++ is that it has a higher learning curve, it is more complex and requires more attention to detail to ensure that our programs are fully functional. When we compare these two languages, we see that Python is better suited to our application, because it will be easier to develop within the given time constraints and provides much of the necessary functionalities in its vast ecosystem of libraries. However, we should not discount the usefulness of C++ if we need to improve the performance of our software.

8.3 Motor Software

For our platform to satisfy our requirements, we need to ensure that the motors are fully functional and capable of controlling our platform. The motors will require a connection to our Jetson Nano computer. The Jetson Nano has a 4-pin header intended for controlling a fan and a 40-pin output. So, we need to find a way to use those pins to output a PWM signal. This will enable us to drive the motors and be critical to ensuring that the motors can be used to open and close the observatory and can aim the platform towards the sun.

As far as the design for the software implementation goes, the software required to drive the motor will depend on whether we use a motor driver or not. If we don't use a motor driver, we will need to connect the motor directly to the Jetson Nano, but this has some potential issues. First, the motor connections may get loose or fray, which would prevent the function of the motors. It would also use important connections that may be required for different purposes. So instead, we will probably use a motor driver.

The motor driver will connect to the Nano via the GPIO pins, and it will generate the PWM signal to drive the motors. The motor software will need to write out to the Jetson Nano's GPIO pins. Writing to a GPIO pin requires calling a function to set it up. Then, the software will be able to write to the pins to move the motors. The motion of the motors is determined by the length of the signal sent, so the longer the PWM signal, the more the motor moves. We will need to determine the smallest possible signal to the motors, to maintain the finest motor control possible. Then, ideally, we will write a module we can use to drive the motor in specific directions. We will use that module to write the program that will manage the

motion of the platform and the program that will manage the opening and closing of the observatory. The observatory program will be simpler, as it only needs to be able to open and close. The observatory motor will only require motion along one axis, which will simplify the process. The platform motor will be more complex since it needs to be able to move the platform three dimensionally. You see, since the sun moves from east to west, the platform will need to rotate around the Z-axis, and since the sun rises and falls through the year, the platform will need to rotate about the X-axis as well.

Unlike the other components, which have already had some functionality made available via libraries, the motors do not have the same level of support for the Jetson Nano. There are some codes available for similar motor driven projects, namely the Jetson Nano JetBot. The JetBot uses a DC Motor and offers example code for the driving of the motors. While this code may not be exactly what we need, we will be able to use the code as reference for the functionality we need to implement.

8.4 Weather Station and Camera

Data collection is essential to our project. We need to be able to design software that can read the data that is collected by our weather station, and the images captured by our camera. In theory, this should be a simple task. All we need to do is to connect the sensor devices to the microcontroller and read their outputs. In practice, however, it is rarely ever that simple. We will require special adjustments to our software for each of these components, which will allow us to get as much as possible out of them as we can.

Firstly, the weather station we've chosen to use is the Ambient Weather WS-2902 home Wi-Fi weather station. In a typical set-up, the weather station would boot up, then the user connects to the Wi-Fi signal it emits, and using your device you would configure the weather station to connect to the Wi-Fi connection on your network. From there, you can create an account and view the reading on your phone, PC, or on the included LCD display. Unfortunately, we can't read the data from the display on our platform, but fortunately, the Ambient Weather software does give us another option for setting up the weather station. The software gives us the option of using a custom server, meaning that we can configure the station to send the data to our very own private server. This is exactly what we intend to do, we will use the Jetson Nano as a server to receive the data read from the weather station over a Wi-Fi signal. There is only one problem, the Jetson Nano is not Wi-Fi enabled by default. This is a hardware issue, so we won't go in depth here, but suffice to say, we need extra components that will allow the Nano to connect to Wi-Fi. When the custom server has been set up, the weather station will write directly to the Jetson Nano. Then we can perform all of the necessary operations on the file that's been written to. This file will be read and used by the weather prediction system to determine what the probability of incoming rainfall is, which will determine whether the observatory closes or not.

For the camera, we need to be able to manage the frequency of the image captures. The camera we're using is a NexImage solar system imager. Typically, the camera would be managed by the included camera control software. Unfortunately, the included software is only intended for Windows machines. So, we need a different solution for capturing the images. Fortunately, we do have a solution, INDI. INDI, the instrument Neutral Distributed Interface, is an open-source library that is used to control astronomical equipment. This means we can use it to configure and control the NexImage camera. We can use an INDI client to directly control the device. The INDI client will give us a GUI we can use to manage and configure the camera. This will allow us to capture the images on a set timer and store them for future use.

We may need to manipulate the image data collected by the camera. Why? Well, in order to ensure that the Sun is the central focus of the camera we can write another program. We would only do this if we had enough time left to work on this after completing the other major components, but it may be a worthwhile endeavor. This program would simply take the most recent image data, and convert it from a fully colored RGB image, into a black and white contrast image of itself. Then the provided computer vision packages can be used to detect the high contrast white spot left by the sun and tell us if it is in the center of the image or not. This would improve the quality of the imaging significantly because we could detect the contrast and have the platform move the motors to adjust the camera. Then, we would have a centered image of the sun. The telescope on the camera will significantly magnify the image, so that we can get a good quality picture of the sun, so any error in the alignment of the telescope will also be magnified. For this reason, we need a high degree of fine motor control from the motors and the ability to detect whether the sun is centered in the image or not. Typically, this would be achieved by using an autoguiding telescope. Autoguiding is the practice of using a secondary telescope to focus on a specific astronomical object, then the autoguiding telescope moves the motors in the telescope mount to keep the main telescope focused on the correct object. This is typically done for long exposure images of an object, but it can be done any time you want to maintain focus on a specific object for long periods of time. This is similar to what we intend to do, albeit somewhat different. Since we don't have a telescope mount, our platform will have to act as the mount to guide the telescope in the direction of the sun.

So, now we have managed to collect the data from both devices, but now we have run into a new issue. How will we store the data? Well, we can't store all of the data we collect, since that would quickly fill the memory storage on the Jetson Nano. Instead, we will create a memory buffer for the data. We need a memory buffer so that the data collected can be transmitted, and then overwritten. Once the data has been transmitted, at the other end it doesn't matter if the data is stored or deleted.

8.5 Rain Prediction

One of the key features of our system is the ability to predict incoming weather to protect the internal components of our observatory. We need to weatherproof our

observatory in order to protect the sensitive instrumentation inside. We found suitable prediction algorithms in our research on weather forecasting, but now we must discuss the specificities of the software implementation.

To implement a functional weather forecasting system, we decided to try to implement one of two different machine learning algorithms, the logistic regression, and a recurrent neural network. We've chosen these algorithms because they allow us to change the complexity of the program based on our constraints. We will start by implementing the logistic regression, because it is less complex and will require less effort on our part. This gives us a control model to use on our observatory platform. The logistic regression will be a starting point for our weather forecasting efforts. Then, if we have more time once the system's software has been completed and everything has been integrated, we can implement a more advanced neural network model. If all things are equal, we expect the recurrent neural network to be a more accurate weather forecast model. Because the neural network has the ability to consider long-term trends in the data, it should be better able to identify key indicators of incoming rainfall.

Now, regardless of which model we use, we will combine it with what is called fuzzy logic to determine whether the observatory should be open or closed. Fuzzy logic is a kind of logical reasoning that is applied to otherwise vague or imprecise statements. For example, if a person says, "It is hot in here", 'hot' is not a definite concept, and is only relative to the person saying it. Other people may still find the room to be pleasant or even cold. For our project, we want to include questions such as "Is it humid?" and "has atmospheric pressure changed rapidly?" because those conditions are related to the expectation of incoming rainfall. In practice, this means that we check the current value of humidity, and if it is above a certain threshold, we decide that it is too humid to continue operating. We would also store the atmospheric pressures for a certain time frame, say the past 30 minutes, and decide that if there are significant changes, it is best to close the platform in case it might rain. We may even implement fuzzy logic by using both logistic regression and a recurrent neural network, and then seeing if at least one of them predicts incoming rain, we will close the observatory.

When it comes to the implementation of machine learning algorithms, Python offers a large number of different libraries and frameworks. The NVIDIA Jetson Nano includes deep learning libraries such as cuDNN and TensorRT. TensorRT is a software development kit that implements a high-performance machine learning interface. It is designed to work with training frameworks such as TensorFlow, PyTorch and MXNet to run an already-trained network on NVIDIA hardware. Meanwhile, cuDNN is a GPU-accelerated library of primitives for implementing deep neural networks. The inclusion of these libraries may be useful in our software's development, but they're not the only choices available. There are other python libraries used commonly for machine learning such as SciPy, Scikit-learn, TensorFlow, PyTorch and more. These libraries typically implement the most common machine learning algorithms in an easy-to-use manner. The functionality

between them is not very different, so it will be best to choose whichever simplifies our development the most.

We have previously discussed the collection of data from the NCDC's archive of global weather and climate data. Before we can use this data to train any weather forecasting model, we will need to clean the data. Data cleaning, or data cleansing, is a process that fixes or removes incorrect data within a dataset. If we don't ensure that the data is clean, the outcomes of the data and algorithms we develop will be unreliable. For our application, the biggest concern is missing data. If we have a specific variable that hasn't been tracked, hasn't been recorded, or is simply missing, then we need to do something about it. The algorithms we're using cannot work with missing data. Instead, we may consider removing incomplete entries, or collecting data from a different source (a different weather station) that is close to the original. This will ensure the integrity of our system is not compromised by faulty algorithms as a result of unreliable data.

8.6 USB Communications

One of the primary tasks of the software was to transfer the data collected from the weather station's sensors and the images of the sun captured by our camera to an external device. We needed to be able to export all of this data in real time as it is received by our Jetson Nano. For our project, we intended to use a direct USB connection to transfer data. This would offer us various advantages over other common methods. The USB connection offers a fast and stable approach to transfer data. Our weather station's sensors and camera images were captured periodically and instantly transferred to an external device without any delays.

We previously discussed how we could implement USB functionality with the PyUSB library. The advantage of using PyUSB is that the library simplifies the process of setting up and establishing communications between devices. It provides a high-level interface that allows us to set up USB devices, read and write data and manage device-specific operations. So, by using PyUSB, we were able to focus on the data transfer logic instead of focusing on the low-level details of the USB protocol.

There is another library called PySerial that we could also use to establish a potential serial connection over which we could transfer data. Serial connections are typically established over serial ports, but certain USB devices can be recognized as virtual serial ports. In this case, we could implement the PySerial library to establish a serial connection which we could then be used to transfer the required data. However, this approach would be more complicated when compared to using a USB connection established with PyUSB.

Ideally, the USB data transfer program would not need to interface with the rest of the software. Instead, it would act as a child process that is allowed to run autonomously, transferring the available data at specific time intervals. Separating the functions of the data transfer would ensure that the process operates independently of the rest of our software. This design would improve our reliability and the stability of the whole system, as issues with the data transfer process can

be traced and debugged more easily. Additionally, this would allow our computer to make better use of its multiple threads, as the program can run in the background on an unused thread.

Additionally, we needed to write a program on the server or receiver end that would receive the data we transmitted. This program needed to receive and then manage the data it was sent, whether by storing it or deleting it or doing whatever else is needed. By default, we wanted to store the data for historical purposes. In case anyone ever needed to know what the camera had imaged or check that the camera was indeed aiming at the sun. This can then be used to verify the reading and data collected by the smaller telescopes that were provided by CREOL.

8.7 Software Control Flow

The seamless collaboration of our project's various processes was imperative for its successful operation. An illustrative instance of this interconnectedness is evident in the reliance of weather predictions on data from the weather station to furnish accurate forecasts. This crucial interdependence mandated a method for the weather prediction module to interface effectively with the weather station, establishing a harmonious exchange of information. Another noteworthy example revolves around the decision-making process for observatory operations. The weather station's predictions play a pivotal role in determining whether the observatory should remain open or closed. In the event of a forecast indicating rain, it becomes imperative for the motor control system to receive instructions to close the platform, safeguarding sensitive equipment from adverse weather conditions. Given these intricate interdependencies among our processes, a robust framework was essential to manage the flow of programs and facilitate effective communication between them. Inter-process communication (IPC) emerged as a pivotal solution, providing mechanisms through which programs could interact seamlessly. Various approaches exist to enable different processes to communicate, with two widely employed methods being the utilization of shared memory and message passing. Operating systems commonly implement both of these communication methods to ensure efficient coordination between processes. For instance, shared memory allows two processes to access a common region of memory by simply opening or accessing the same file in memory. This shared memory paradigm facilitates the exchange of data in real-time, promoting synergy between interconnected processes and enhancing the overall efficiency of our integrated system. Additionally, the utilization of shared memory not only streamlines communication but also offers a real-time, low-latency data sharing solution. This method enables processes to access and modify shared data with minimal overhead, enhancing the overall responsiveness of our system. Conversely, message passing, another integral facet of our inter-process communication strategy, excels in scenarios where a more controlled and secure exchange of information is paramount. By providing a structured means for processes to send and receive messages, it ensures a clear and organized flow of data, contributing to the overall robustness of our collaborative framework. As our project continues to evolve, these carefully chosen communication mechanisms

lay the foundation for a dynamic and adaptive system that effectively navigates the intricate web of interdependencies between its constituent processes.

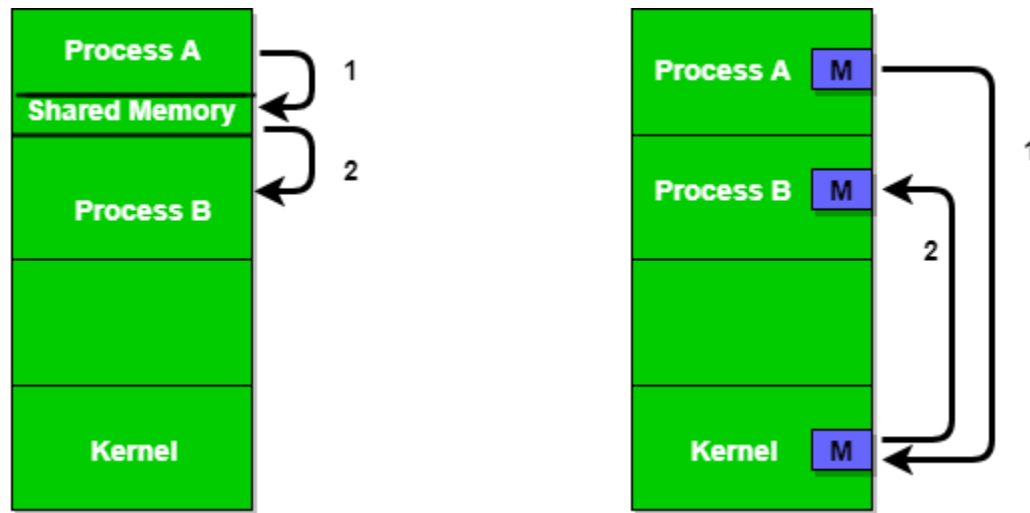


Figure 8.7.1 – Interprocess Communication Models (image from: <https://www.geeksforgeeks.org/inter-process-communication-ipc/#>)

We made a plan to use both mechanisms of Interprocess communication as part of our project. We needed shared memory between the weather station and weather prediction systems and for the USB transmissions. We needed to pass messages between the weather predicting system and our motors to notify them when they need to open or close the observatory.

When we implemented shared memory, we needed to understand how we intended on doing so. The ideal use case for shared memory was for us to write to a file and read from it later. This strategy was used to write the data obtained from the weather station, and the camera to a file. We read the data from the file when we transmitted it over USB to the external system. This data was ideally formatted in a common file format such as JSON. The camera images were sent in common image file formats such as jpg or png. This standardized the formatting for our files, which made it easier for anyone to work with our platform.

To implement message passing in our software, we first needed to understand how it works. The most common implementation of a message passing mechanism is a message queue. A message queue uses a queue, a common data structure, for passing data between two processes. In order to take advantage of message queues in Python, we can make use of the multiprocessing module. The multiprocessing module offers an implementation of a messaging queue that we can use. The main control program is able to run the rest of the processes and establish communication between the programs using a message queue, which allows the processes to communicate with each other.

9.0 System Fabrication & Prototype Construction (Spectrometer and Fabry-Perot Etalon components)

In this chapter, we explain the construction process of each component in our project and their results.

9.1 Optical Fabrication and Prototype Construction

In this section, we discuss the steps we took to build the spectrometer and the Fabry-Perot Etalon.

9.1.1 Spectrometer

The mounting plate is first machined at the UCF machine shop with one quarter inch screw holes whose locations were determined from the SolidWorks analysis of this system. The mounts for the grating and prism were 3-D printed, and the Cannon lens mounts were custom ordered to be machined from aluminum. Upon completing the construction of each part, everything was mounted onto the baseplate with $\frac{1}{4}$ inch cap screws. The single mode fiber was placed into a connector which screwed into a fiber holder at the back focal length of the cannon lens. Because the baseplate and mounts were designed from the Zemax ray trace of the optical system, the system would ideally not require much further alignment. The testing process and results can be seen in section 10.1.1.

9.1.2 Fabry Perot Etalon

The first step to building the etalon was to place the mirrors in the kinematic mirror mounts. One mirror was fixed, and a translation stage was used with the second mirror to precisely adjust the distance between them. The two mirrors were mounted face to face and just nearly touching so that they started parallel to each other.

Before including the broadband source, we needed to align the system with a coherent source. We used a HeNe laser available in the lab as the cavity's input source with a camera at the output. We aligned the system by first measuring the height to match what the mirror height would be and using irises to ensure that the laser was parallel to the optical axis. Then we placed the second mirror into the system and kept an iris in between the laser and the mirror to check the position of the mirror. Seeing the reflection from the mirror, we adjusted the axes until the reflected beam traveled back through the iris. On the camera, a small red beam with rings around it should be detected. Next, we added the first mirror to the system and adjust it in a similar fashion to ensure that the mirrors are parallel to each other. The expected output is shown in Figure 9.1.2.1.



Figure 9.1.2.1 Etalon outputs from (left) red aligned HeNe beam and (right) the collimated LED, utilizing a focusing lens for detection.

From here, we replaced the source with the mounted white LED and added the collimating lens. It was important to find the distance from the lens that gave a parallel beam with the least divergence. This distance was approximately 35.4 mm. Dimensionally, the collimated beam had a diameter of approximately 20 mm and the entirety of the beam was input into the cavity. The broadband source was high in power, but due to the cavity's high Finesse, the light underwent severe loss. The highest output power was 10 micrometers. The proper output achieved here is shown in Figure 9.1.2.1. The similar shapes between the two outputs provide evidence that the etalon has proper alignment for the white LED source.

Once the desired output was achieved, we measured all of the distances that we would use to machine the aluminum sheets in our thermostable design as shown in Figure 9.1.2.3.

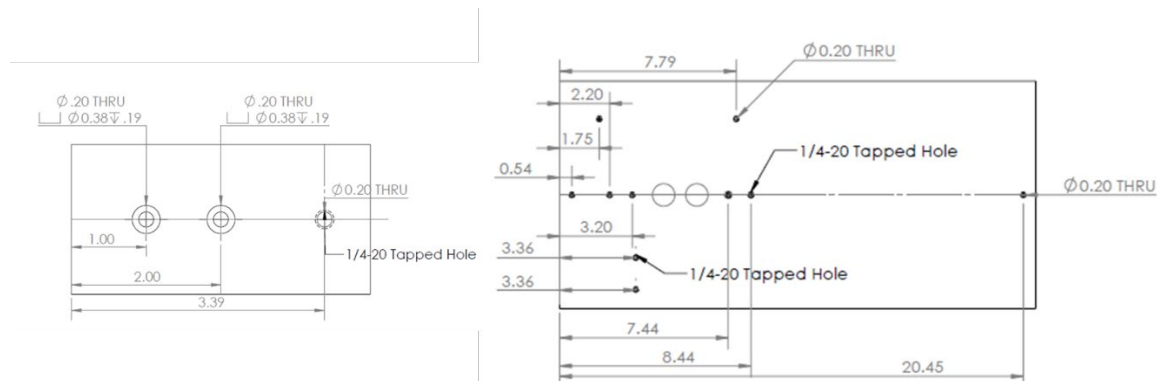


Figure 9.1.2.2 SolidWorks drawings of holes to be machine on (left) the mirror plates and (right) the base plate.

The last step would have been to couple the output of the etalon into a single mode fiber that feeds into the spectrometer. However, with the focus on getting the spectrometer complete and improving the stability of the etalon, we did not have the time to move forward and integrate the optical systems. A visualization of the final system is displayed in schematic in 2.5.4.

10.0 System Testing

10.1 Optical Testing

Although the design calculations and simulations have been completed for the optical system, using the ideal components in a physical working space will also introduce environmental factors such as human error, loss, and non-geometric optics.

10.1.1 Spectrometer Testing and Results

Because the light emitted from the single mode fiber into the spectrometer system is very dim, the spectrometer alignment is first tested with a larger multimode fiber. The multimode fiber is connected to the system, and the other end is aligned with a white LED light source. The light is then traced with a light block throughout the system until the spectrum reaches the last optic. This is so that we can make sure that the spectrometer is correctly aligned, and the light is correctly passing through the system and reaching the sensor. When this step was conducted, we found that there was an error with the prism representation in our Zemax, which resulted in a slight misalignment of the system. It was found that the prism in the Zemax system was much larger than the prism that we were actually using. Upon discovering this, we went back, fixed the Zemax error, and drilled new holes into the base plate for the final cannon lens. After repeating the testing procedure, the correct location for the final cannon lens was determined so that the full spectrum is detected by the ATIK APX60 sensor.

Once the alignment of the system is confirmed, the ATIK sensor is turned on and we observed the resulting bright spectrum from the multimode fiber. With an observable spectrum, the focal lengths and F/# settings of each cannon lens can be adjusted until the spectrum is completely in focus. If these adjustments were made with the single mode fiber, the long exposure time necessary to see the spectrum (at least 30 seconds) would lengthen the process and make it far more difficult to tune the system to the desired accuracy. With the system completely in focus, the multimode fiber is removed and replaced with the single mode fiber that this system was designed for. The single mode fiber is aligned with the white LED to ensure that the system is in focus and to find suitable exposure time and gain settings for the ATIK camera to detect the single mode spectrometer signal.

The next step is to test the specs of the system. This is accomplished by sending light with known emission spectra through the spectrometer. The known wavelengths of the emission spectra are used to measure bandwidth, magnification, and resolution. The system is tested using the emission spectra of Hydrogen and Mercury. Below are the resulting spectra:

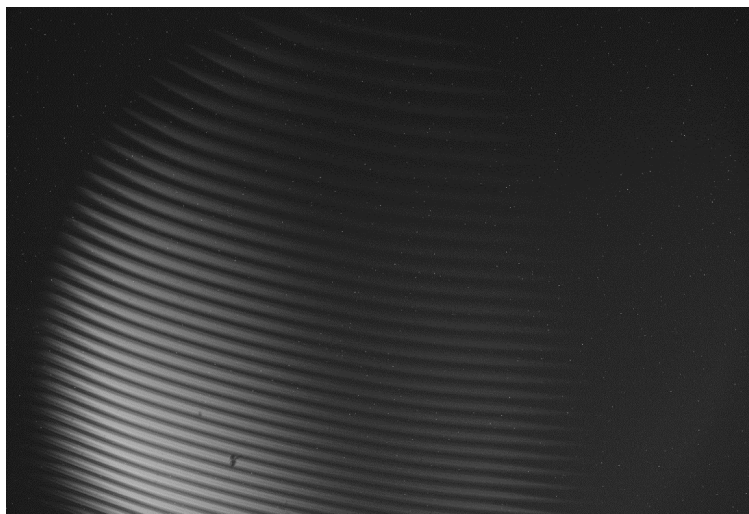


Fig. 10.1.1.1 White LED passed spectrum



Fig. 10.1.1.2 Hydrogen spectrum



Fig. 10.1.1.3 Mercury spectrum

The above images include some noise on the right side of the image. This is not a part of the detected spectrum. The noise does not interfere with the testing of this system. The hydrogen emission spectrum as well as the mercury spectrum allowed us to measure the actual magnification and resolving power of the system. By measuring the number of pixels across a single emission line and multiplying it by the width of a pixel and dividing this by the mode field diameter of the single mode fiber, we can calculate the magnification of the system. The resolving power is measured using the spectrum from mercury. Doublet emission lines which appear in the same diffraction order are used. The width of one line and the distance between them, as well as the known wavelengths of these two emission spectra are used to calculate the resolving power of the system. Upon conducting these two emission spectra are used to calculate the resolving power of the system. Upon conducting the analysis and calculations, the specs for the system were found. It was found that this system roughly has a magnification of 5x, and a resolving power of 98,000. The magnification is slightly over the goal magnification of 3.5x. The resolving power is right within the range we designed the system for, which was 50,000 to 100,000.

10.1.2 Fabry-Perot Etalon Testing

Below is a visualization of the transmission of the transmission spectrum using the chosen mirrors 5 mm apart and an angle of incidence (AOI) of 0 degrees. A zero-degree angle of incidence is ideal, but since the physical system has environmental imperfections, we could test the effect of varying angles on the transmission. A zero-degree angle of incidence is ideal, but since the physical system had environmental imperfections and potentially human error, we could test the effect of varying angles on the transmission.

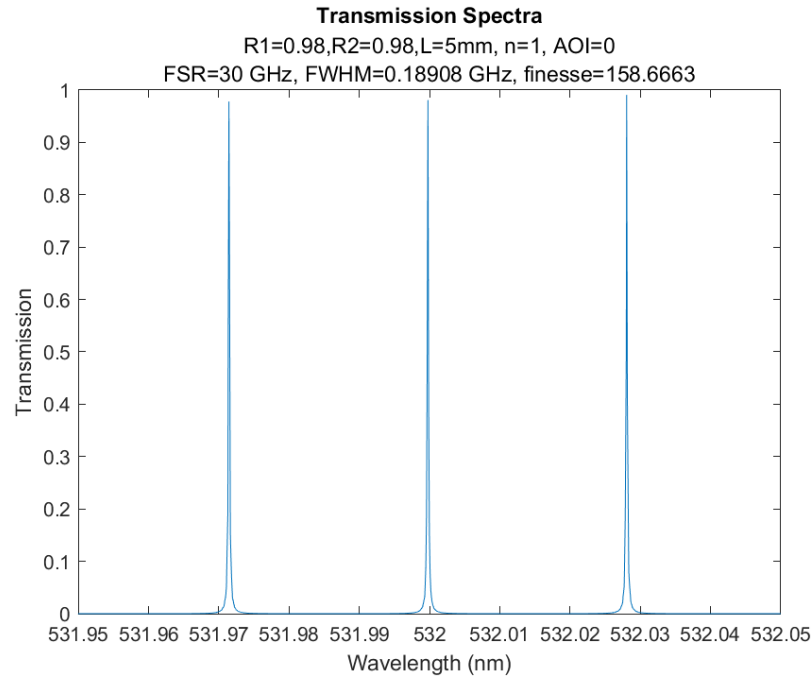


Fig. 10.1.2.1 Transmission spectrum of the etalon with two flat surfaces of reflectance 98%, cavity length 1mm, and 0° angle of incidence.

To see where we had room for error in misalignment of the broadband source, we calculated the FSR and Finesse from zero to one degree with an increment of 0.2 at both possible reflectance of the mirror. The cavity length in the calculations was a constant of 5 mm and the FWHM was unaffected (.09 GHz at this cavity length) at 99% and 0.19 GHz at 98%. We can see from the table below that the FSR increases with increased angle of incidence but remains consistent between the two possible reflectance.

Table 10.1.2.1 Effect of Increasing Angle of Incidence on Free Spectral Range and Finesse

Reflectance	AOI (°)	FSR (GHz)	Finesse
98%	0	30	158.7
	0.2	30.6	161.9
	0.4	32.57	172.3
	0.6	36.35	192.2
	0.8	43.1	227.7
	1	55.5	293.7
99%	0	30	315
	0.2	30.6	322.16
	0.4	32.57	342.8
	0.6	36.35	382.6
	0.8	43.1	453.2
	1	55.5	584.4

From here, we can test the cavity lengths to accommodate for the increased FSR at a one-degree AOI for 98% reflectance. Although we would want to aim for the FSR's range, this information was important to reference when constructing the system. We can see from the plots below that up to a one-degree misalignment can be accounted with a cavity length of 8 – 9 mm to reach the FSR of 30 GHz. Since we've determined that the FSR between 98% and 99% reflectance is consistent, this distance range would be the same as well. However, the lower reflectance also produces a lower finesse.

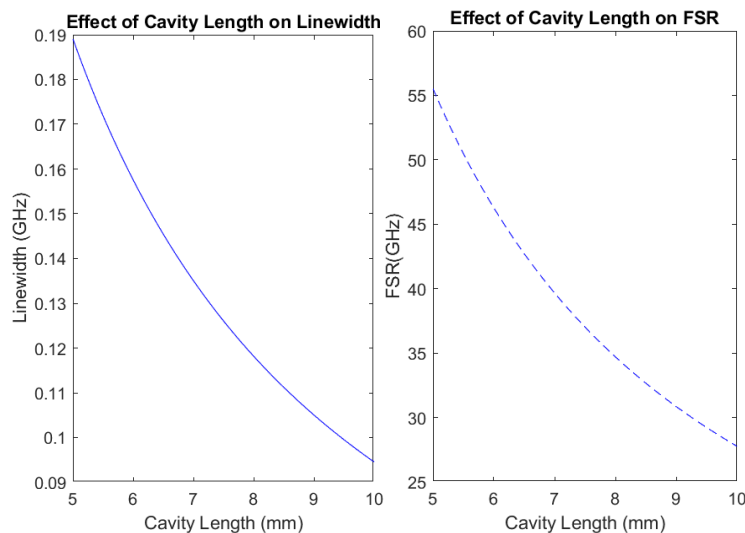


Fig. 10.1.2.2 Visualization of the relationship between the cavity length and full width half maximum (left) and free spectral range (right).

Physical factors affect the characteristics of the Fabry-Perot etalon, so important testing also took place as it was being built. Alignment of the etalon needed to be highly precise for it to work as expected. An issue that we needed to keep in mind is that round-trip cavity loss would be introduced in the etalon, so we needed enough output power from the etalon to be focused and coupled into the single mode fiber of the spectrometer. We measured the power of the broadband source before it was input into the etalon using a power meter. We then measured the output power of the etalon to determine the remaining power and calculate the loss. The ended up being 98-99%, which corresponds to the reflectance of the mirrors and the Finesse.

10.2 Hardware Testing

10.2.1 Electrical Parts for PCBs

For our hardware testing, we used several pieces of equipment available at the UCF, ECE Lab, such as the Oscilloscope (ROHDE & SCHWARZ RTM3004 - 5GSa/s 10-bit ADC), the Function Generator (Tektronix AFG3022B), the Triple Power supply (ROHDE & SCHWARZ NGE100), Breadboards (Global Specialties

Proto-Board). After we received the main components, we proceeded with the electrical test of each one of them to make sure the correct functioning and avoid any issues later.

10.2.2 Power Supply PCB v3 Load

In the process of evaluating our Power Supply PCB v3, which accommodates four distinct voltage lines, a meticulous testing regimen was executed to guarantee its optimal functionality and reliability. Commencing with a thorough visual inspection to identify any visible anomalies or damage, the subsequent steps involved the systematic connection of a multimeter to measure and validate the output of each voltage line, ensuring alignment with specified voltage requirements: 12V, 5V and 3.3V. Stability was scrutinized through continuous monitoring, while load tests, simulating components operation (iOptrom 5A, Jetson Nano 5A, DC Linear Actuator Motor 3A, Light Sensors PCB 1A), were conducted to gauge performance under varying loads. Crucial short-circuit and overload tests were implemented to assess the effectiveness of protective mechanisms. Temperature checks were performed to identify potential thermal issues, with all observations and measurements meticulously documented. Functional tests, involving the connection of the PCB to intended devices, provided insight into operational efficiency.

10.2.3 Wind Speed Sensor – Weather Station – Door-closing

For this part, we made 10 tests to measure how quick the wind sensor works and send signal to weather station hub and later to the Jetson Nano to make the decision of closing the door to protect all the components. We used a hair dryer to simulate high wind speeds. These are the results:

Test #	Timestamp (seconds)
1	35.28
2	41.01
3	36.21
4	37.90
5	40.81
6	36.09
7	37.16
8	39.31
9	40.09
10	34.02
Average	37.78

10.2.4 Rain Sensor – Weather Station – Door-closing

We ran a similar test as the previous one but this time, we pour some water into the rain sensor to measure how quick the weather station sends the signal to the Jetson Nano MCU for processing and then, close the door to protect all the components inside. Results below:

Test #	Timestamp (seconds)
1	40.10
2	45.82
3	43.03
4	30.33
5	34.91
6	33.16
7	38.71
8	40.88
9	39.08
10	41.51
Average	38.75

10.2.5 Linear Actuator DC Motor – Door-opening

On this part of the hardware test, we proceeded to measure the time response of the interaction between the Jetson Nano MCU and the communication with the door DC motor. We measured the time it takes to open the door once the MCU is turn on and checks the weather conditions are good. We placed the weather station outside to get regular readings and proceeded. These are the results:

Test #	Timestamp (seconds)
1	13.24
2	13.89
3	14.12
4	12.03
5	13.11
6	13.78
7	14.87
8	13.22
9	12.91
10	13.11
Average	13.43

10.2.5 Light Sensors PCB v2 Test

For the light sensors test, we simulated the solar light by using an LED light. We started the system and made sure the program for the iOptrom, and Light Sensors was activated. Then, we proceeded to expose the Light Sensors PCB to the LED light and made sure the iOptrom moved at the rate set on our program code.

10.3 Software Testing

Testing our software is an essential step to ensuring the integrity of our observatory. We needed to test the software if we would like to see our project fully functional and prevent potential malfunctions. To do so, we needed to understand the key principles of software testing, and how we could use those principles to

test our programs. There are many approaches to testing your software, but in the field of software development there are three key methods that are typically used to gauge the reliability of a piece of software. These are unit testing, integration testing and system testing. Then, we will take a look at a technique known as test-driven development, and how we will make use of it to improve our application's development.

10.3.1 Unit Testing

Unit testing is the process of running tests that focus on validating the functionality of the smallest testable parts of a program, called units. These units are typically applied to things such as functions. Unit testing is typically carried out during the development process, as the code is being written. This allows a developer to identify any issues early in the development process and ensures the functionality of individual units of code. The other advantages to unit testing are that it allows for bugs to be found before coding even begins, or when it is first written, and it makes refactoring the code later much easier because there is a preexisting test to ensure that the module still works correctly. The biggest disadvantage of unit testing is that it requires discipline to continuously write the tests, and it is of limited practicality for embedded applications.

Unit testing can be broken down into three stages: planning, writing the test cases, and performing the unit test itself. The planning will be done as part of the planning of a specific class or module in the code. When we plan out the functionality that a class should exhibit, we can plan out how we would like to test that functionality to verify that it meets the requirements. Then the test cases are written as the code itself is written. If we finished writing a function that is intended to take a number and square it, then we would want to write a test that would check as many cases as possible (such as negative numbers, zero, small numbers or floating-point numbers, and really big numbers that may cause overflow). Then, after the test has been written out, we can run it and see whether the function gives us an error or if it works exactly as intended. In doing so, we can guarantee that our function will work regardless of what input we give it.

The unit testing process can be done manually, or it can be automated. Manual unit testing will go as expected, the developer will write the tests as they write the code or units they need. Automated testing will typically involve a special testing framework to develop test cases. These frameworks can set special flags and report failed test cases that developers can use to root out any bugs in the code. Unit testing will be an integral part of our development process. Since we needed to guarantee that each piece of our software was reliable and satisfied the engineering requirements, we could not have any bugs in the individual units that made up our code. Python supports unit test, a unit testing framework that has all of the pieces needed to automate the testing of our program. This was used to our advantage, as we could use automated testing to accelerate our development over having to manually write out the test cases.

10.3.2 Integration Testing

Integration testing is the second level of the software testing process. In this step, the individual software modules or components are combined and then tested as a group. It tests the interface between two software modules. Integration testing allows developers to identify any problems that come up when the different units are combined with each other. This allows us to resolve integration issues early in the development cycle. There are many forms of integration testing, but there are four most common approaches that we'll cover here.

The first kind is called Big-bang testing. This is the simplest approach to integration testing, as most of the modules are combined and then tested. This gives us an idea of whether the system functions or not. The advantage is that big-bang testing is easy and fast to implement. It also works well for small systems and systems where there is little interdependence between modules. The issue with the big-bang approach is that it becomes slow for large systems and doesn't give the user an idea of where the issue is located.

The next approach is bottom-up testing. In this method, the lowest modules or components are tested first, and then integrated upwards. This process is repeated until all of the components are functioning together. This approach allows the developer to determine where the issues lie in the program. The disadvantage of the bottom-up testing method is that it requires most of the components to be ready for testing. This makes the method slow and requires a lot of complexity in testing every combination of modules.

After bottom-up testing, there is top-down testing. This technique allows the developer to test the system before the lower-level modules have been integrated. It starts by testing the higher-level modules, and then testing the lower-level modules and integrating them. This will ensure that the high-level system is fully functional. If the lower-level modules have not yet been implemented, a sort of 'placeholder' module can be fit in to test the interface. This method is beneficial because issues in the interfaces can be caught before they come up. The problem with this approach is that it may need many placeholders early-on in the process, and that it may be difficult to gauge functionality from the test's output.

The last major approach for integration testing is called mixed integration testing. This approach is also known as hybrid testing or sandwich testing. This includes a mix of bottom-up and top-down testing. Unlike top-down or bottom-up, the mixed integration method can start testing after some of the higher level or the lower-level modules are ready. The modules that aren't ready can be replaced by placeholders which allow for the testing of the interfaces. The advantage of mixed testing is that it is very effective for large projects and can be performed for lower level and higher-level modules at the same time. The disadvantage of mixed testing is that it can become quite complex as tests are running from the bottom up and from the top down.

These approaches to integration testing are all effective methods for identifying issues with the interfaces between different parts of the program. To test our

program, we used the bottom-up method. Due to its ease of use, and its ability to identify where the bugs are located. It allows us to verify the functionality of our programs.

10.3.3 System Testing

The last key method for testing the functionality of the system is system testing. System testing is the most important step of the whole process. This is because we needed to ensure that the whole system performed as expected. One of the key features of system testing is that it is a 'black box' test. A black box test is one that does not depend on the internal implementation of the system being implemented. So, the tester only needs to know what the output should look like, and then they can use inputs to validate the output.

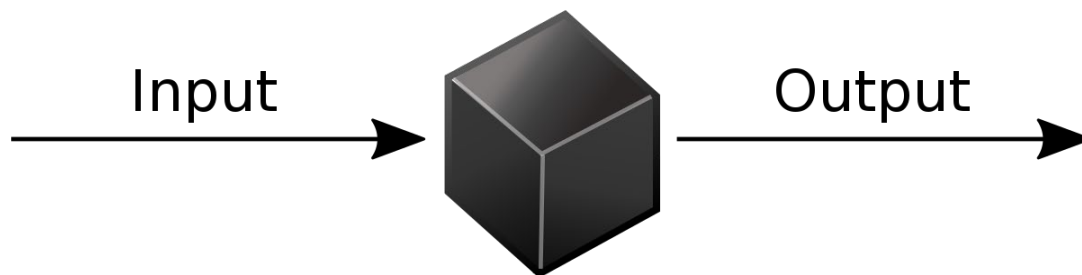


Figure 1 - Black box testing (image from: https://commons.wikimedia.org/wiki/File:Black_box_diagram.svg)

System testing allowed us to determine if our application met the requirements or not. Like unit testing and integration testing, system testing has many approaches, each with their own advantages and disadvantages. Some of the most popular methods of system testing are performance testing, load testing, scalability testing, and regression testing. These tests all seek to determine the effectiveness of an application in some specific domain. Performance testing tries to determine the speed and stability of the software, usually by calculating average load time, response time, etc. Load testing determines how the system performs under an extreme load, maybe running multiple instances at once or by running the software on a resource limited platform. Scalability testing determines how well a software 'scales', that is, how well it performs when the number of requests or instances increases substantially. Finally, regression testing tries to ensure that changes in the application during the system testing or recent updates have not introduced any new bugs or issues with the software. Of these tests, the most relevant to our application were probably performance testing and regression testing. These gave us an indication of how well our software was running, and whether any issues had come up during the testing process.

System testing is a very important step in the development process, but as we have seen, it is not always a simple one. The process of system testing often requires a whole battery of tests to be run, in order to guarantee the functionality of your product. This is one of the disadvantages of system testing, it can be very

time-consuming, complex, and expensive to test every possible feature in every possible way. For these reasons, we primarily focused on testing the functionality of our system first. We needed to ensure that our observatory platform could perform all of the required tasks first before we moved on to checking other properties of the system. If all the functionality required is completed and we are finished with time left, we could move on to testing the performance of the system, seeing how fast the response times are to various stimuli. Then, we could regression test the system, to check whether the program has any new issues or not.

With all of these tests completed, we still had one last test to run. The last test is to actually put our observatory outside to collect data. This was the best test of all, because it gave us an idea of the strengths and weaknesses of our design. We should finish the observatory and its testing with time to spare in order to apply it to the real world. In practice, we should notice any bugs or issues that come up. For example, it may be that due to wind or the general atmosphere, the motors do not move the platform enough. In such a case, we would need to find a way to resolve such an issue, whether it's on the hardware end or the software. If there were major issues that prevented the proper functioning of our platform, then we had to be able to resolve those issues before the project was due. This also helped us prepare for the demonstration we had to do in front of the project review committee.

10.3.4 Test-Driven Development

One last thing we needed to look at is test driven development. Test driven development (TDD) is a software development process that focuses on creating test cases based on the software requirements before the actual code is developed. This allows a developer to iteratively plan tests, write code, test the code, rewrite tests, and refactor their code. In this way, the testing process is what drives the development of the software. This methodology is effective because it makes the developer focus on the requirements before they even think about the code. This way, we could identify the key necessities of our program and then implement them. Ideally, the plan was to use a test-driven development process to write our own software. This not only ensures that the software requirements are met, but also that each piece of code is functional in its own right. Then, we moved on to the next piece of code and worked our way up until the system was complete.

11.0 Administrative Content

In this section, we discuss the estimated budget and provide a bill of materials. To track customer requirements and engineering specifications, a house of quality is included. Milestones throughout the design process have been listed as well as how we split up the work in the group.

11.1 Budget

Our project is being sponsored by the Astrophotonics research group, and they already have spare equipment that we will have access to. The budget is set at \$20,000, and we end up spending a total of approximal \$5000.00 dollars since we used a lot of the material that the department already had.

11.2 Bill of Materials

For the bill of materials, there are several components that we did not have to purchase since our sponsor pointed out that there were parts in the Astrophotonics department available for us to use. Below we include a table that shows the main hardware components that were used in our system as well as PCB#1 and #2 BOM.

Quantity	Description	Price
1	NVIDIA Jetson Nano Developer Kit	149.00
1	NexImage 5 Solar System Imager	19.95
1	Askar FMA180 Pro APO Sextupler Refractor	399.00
1	Linear Actuator DC Motor 12VDC 3A	41.00
1	AC Power Plugs & Receptacles PLUG NEMA 5-15 125V WATERTITE	45.03
1	Edimax 2-in-1 WiFi and Bluetooth 4.0 Adapter	21.50
2	25 mm 400 - 750nm Broadband Mirror	150.00
1	4900 K, 740 mW Mounted LED	171.28
1	Adjustable Collimation adaptor with 1" Lens, 350-700 nm AR coating	309.96
1	T-Cube LED Driver	348.22
1	T-Cube Power Supply, 15V, 2.66A	39.54
2	25.0/25.4mm Optic Dia., Side Flange Direct Mount	63.00
1	MicroSD Card 256 GB	19.99

1	Ambient Weather WS-2000 Home Weather Station with WiFi Remote Monitoring and Alerts & Thermo Hygrometer	299.99
1	ISSDX SUN SENSOR: Digital sensor	381.40
10	NORPS-12 - CDS Photoresistor	24.62
4	Motor cable angled, 2m	121.60
-	Plexiglass sheets by measure	-
1	Fan-4020-PWM-5V for Jetson Nano Developer Kit	8.35

Table 11.2.1: Hardware BOM

Manufacturer Part #	Name	Description	Designator
399-7374-2-ND	0.1 μ F	CAP CER 0.1UF 50V X7R 0603	C1_LS1, C1_LS2
1276-2864-1-ND	10 μ F	CAP CER 10UF 16V X5R 1210	C2
3106685	LTST-C190GKT	LED GREEN CLEAR CHIP SMD	D1, D2
MCP6547T-I/SNCT-ND	MCP6547T-I/SN	IC COMP OPENDRN 1.6V DUAL 8-SOIC	IC1_LS1, IC1_LS2
1725656	1725656	Male Header, Pitch 2.54 mm, 1 x 2 Position, Height 9 mm, Tail Length 3.5 mm	J2, J3, J4, J5, J6, J7, J8_LS1, J8_LS2
P1KBZCT-ND	1 kOhms	RES SMD 1K OHM 5% 1/4W 0603	R1_LS1, R1_LS2, R7_LS1, R7_LS2
311-88.7KHRCT-ND	88.7 kOhms	RES 88.7K OHM 1% 1/10W 0603	R2_LS1, R2_LS2
P100KBYCT-ND	100 kOhms	RES SMD 100K OHM 1% 1/4W 0603	R3_LS1, R3_LS2, R8_LS1, R8_LS2
NSL-19M51-ND	NSL-19M51	PHOTOCELL	R4_LS1, R4_LS2, R5_LS1, R5_LS2
RMCF0603FT113KCT-ND	113 kOhms	RES 113K OHM 1% 1/10W 0603	R6_LS1, R6_LS2
2019-RK73B2BTDD201JCT-ND	RK73B2BTDD201J		R9
65J2575	CRCW1206100RFKEB		R10
MINI-SPDT-SW	MINI-SPDT-SW	Switch	S1, S2

Table 11.2.2: Light Sensors PCB BOM

Manufacturer Part#	Description	Designator
08055C333JAT2A		C1, C7, C14, C20
08051C104KAT2A	General Purpose Ceramic Capacitor, 0805, 100nF, 10%, X7R, 15%, 100V	C2, C3, C6, C8, C9, C12, C13, C15, C18, C19, C21, C24
EEE-1HA221P	Aluminum Electrolytic Capacitor, 220 uF, +/- 20%, 50 V, -40 to 85 degC, 2-Pin SMD, RoHS, Tape and Reel	C4, C10
EEE-FT1H331AP	CAP ALUM 330UF 20% 50V SMD	C5, C11
EEV-TG1H102M	Capacitor Polarised	C17, C22
VEJ471M1HTR-1316	Capacitor Polarised	C23, C16
LTST-C190GKT	LED GREEN CLEAR CHIP SMD	D1, D3, D5, D7, D9
B540C-13-F	DIODE SCHOTTKY 40V 5A SMC	D2, D4, D6, D8
	No Description Available	F1
0685T4000-01	4A 63V AC 63V DC Fuse Board Mount (Cartridge Style Excluded) Surface Mount 1206 (3216 Metric)	F2, F3
0448008.MR	Fuse	F4, F5
529702B02500G	Hardware	H1
691137710003		J1, J2, J3, J4, J5, J7, J8, J9, J14
48405-0003	USB 3.0 F/A STD RA REC CH=4.01 1	J6
691137710002		J10, J11, J12, J13
XL4016E1	Power Supply	PS1, PS2
RC1210FR-071K5L		R1
RC0805FR-0710KL	Chip Resistor, 10 KOhm, +/- 1%, 0.125 W, -55 to 155 degC, 0805 (2012 Metric), RoHS, Tape and Reel	R2
CRCW08055K60JNEA		R3
CRCW1206100RFKEB		R4
3296W-1-254LF	TRIMMER 250K OHM 0.5W PC PIN TOP	R5
CRCW08053K30FKEA	Chip Resistor, 3.3 KOhm, +/- 1%, 0.125 W, -55 to 155 degC, 0805 (2012 Metric), RoHS, Tape and Reel	R6
RK73H2BTDD6800F		R7, R10, R12
CRCW080513K0JNEA	RES Thick Film, 13kΩ, 5%, 0.125W, 200ppm/°C, 0805	R8, R11
RC0805JR-131K5L		R9, R13
CRCW1218200RFKEK	200R 0.75W 1% 1812 (4532 Metric) SMD	R100
L101011ML04Q	No Description Available	SW1, SW2, SW3, SW4, SW5
XL4015	5A 180KHz 36V Buck DC to DC Converter	U1, U2

Table 11.2.3: Power Supply PCB v3 BOM

11.3 Milestones

As a team we came up with set days for us to stay on track while working on our project design. We created some milestones with extra days on each part so that we can have time for fixing any occurrent errors that can come up during the project process. The first week we made sure to form the strong group that we currently

are. For the following week after that was set, we focused on figuring out goals and to work on the division of the paper which went well and was distributed fairly. Since our group is working on collaboration with the optic department one of the milestones included in our table is the initial optic demo for their part. We had a total of four weeks to work on the first portion of the 75 pages that need to be turned in for review the week of June 30th. After turning in our draft to be reviewed by the professors we had 3 weeks to finalize our project with 150-page count. An initial draft was to be ready for review and to upload to our website by July 23rd and have our final paper to be turned in by July 25th. Below is a table depicting the complete milestones of our journey through the project.

Senior Design 1/2		
Milestones	Duration	Dates
Initial Group Formation	1 week	5/15 -5/ 22
Divide and Conquer Document	1 week	5/23-6/2
Modifications for Optics Midterm Demo	1 week	6/24-6/29
60 -75 Page Draft	4 weeks	6/2-6/30
Final 150 Page document	3.5 weeks	6/30-7/25
Final Optics Demo	5 weeks	6/29-8/3
CDR power point	1 week	9/7-9/14
CDR presentation	1 week	9/15-9/22
Midterm Demo	4 weeks	9/26-10/30
Manufacturing	8 weeks	9/26-11/26
EOS final	1 week	11/26-11/30
Live demo	1 week	12/1-12/5
Turn in final documentation and video	2 days	12/5-12/8

Table 11.3: Milestones

11.4 Work Distribution

Our plan since the beginning has been to get all work needed done on a timely basis. With this in mind we divided the workload evenly. The way we did the work distribution was based on the member's experience and field of expertise, as well as the engineering department they are enrolled in. We all been working collaboratively with each other but do have different parts for each member to focused on. Most of the flowcharts and diagrams shown on the Diagrams section have what each member was assigned to work on as well as a table below that shows basic primary and secondary parts that each member was assigned to.

Name	Primary	Secondary
Misael Salazar	Software, MCU	Hardware
Kara Semmen	Spectrometer	Fabry-Perot
Tamara Nelson	Fabry-Perot	Spectrometer
Miguel Daboin	Light Sensors PCB & Power Supply PCB Design / Fabrication / Soldering/ Testing, Light Sensors Analog Signals Processing	WPS Motor, MCU, SolarMEMS
Jarolin Jimenez	WPS Motor & Main Door Mechanism design & implementation, Box Cutting	Hardware

Table 11.4: Work distribution.

12.0 Conclusion

When we began this project, we found it to be fascinating and an interesting system to be working on, and definitely a great story to tell if it works out accordingly. Based on all the requirements that we needed to meet we knew it was going to be challenging and that it would take a lot of our attention and time. This project needed to be precise in order to function the way we want it to work. Before starting the second stage of our project, (Senior Design II), there are several challenges that we are going to need to overcome. One of the challenges will be having all the components we need on time for proper testing before putting together our system. Since we have had to wait for the sponsor to get these components for us it is a bit challenging to get them as soon as we would like to. Another challenging part was putting all the previous ideas together and been able to execute them in a timely manner. Being that SD1 was done during the summer semester, the last part of our designing and writing felt like we had to rush it and crunch out of it. Even so, as the great team that we are, we ended up victorious and managed to get it done and be ready for what there is to come with the second stage of this wonderful experience.

We managed to get the optical design planned out with the guidance of our mentors, which we are grateful for. Throughout the summer we were able to receive appropriate guidance to accomplish the tasks necessary in senior design 1. The challenge in this situation was in regard to the limited availability to meet with mentors to have an in-depth discussion during critical design weeks. This was to be expected because this is the summer semester, and we stayed on top of communication with clear and concise questions to aid in our process of designing our project.

We started super strong, gave ourselves deadlines that we did our best to stick to. Planned online and face to face meetings with each other twice a week, and were able to work productively with one another. Even though the beginning of our design process was looking foggy, eventually we had a clearer vision and understanding of what we needed to accomplish and worked through all the challenges that were placed in our path and strove to get it done.

The results of this project are to be handed off to the Astrophotonics research group, where they will expand on the work we have done here on a PhD level. They will calibrate and optimize the spectrometer, and integrate the systems as needed.

Declaration: We hereby declare that we have not copied more than 7 pages from the Large Language Model (LLM). We have utilized LLM for drafting, outlining, comparing, summarizing, and proofreading purposes.

Appendix A - References

- constraints modelling in product design. (2002).
- contributors, w. (2023). ac power motors. Retrieved June 29 from
- contributors, W. (2023a). Brushed DC electric motor. Retrieved June 29 from
- contributors, W. (2023b). Brushless DC electric motor. Retrieved June 29 from
- contributors, w. (2023). AC power plugs and sockets. wikipedia, the free encyclopedia. Retrieved June 29 from
- contributors, W. (2023). Stepper motor. Wikipedia, The Free Encyclopedia. Retrieved June 29 from
- contributors, W. (7 June 2023). Linear motor. Wikipedia, The Free Encyclopedia . Retrieved June 15 from
- . In.
- . <https://www.nvidia.com/en-us/autonomous-machines/embedded-systems/>
- About us. <https://www.raspberrypi.org/about/>
- akshaybotre203. *System-on-Chip vs Single Board Computers*.
<https://www.geeksforgeeks.org/system-on-chip-vs-single-board-computers/#>
- Akua Opoku, N. *ML-Rainfall prediction using linear regression*.
<https://www.educative.io/answers/ml-rainfall-prediction-using-linear-regression>
- Anuraj, A., & Gandhi, R. R. R. (2014). Solar Tracking System Using Stepper Motor.
- Bauer, F. F., Zechmeister, M., & Reiners, A. (2015). Calibrating echelle spectrographs with Fabry-Pérot etalons. *Astronomy & Astrophysics*, 581, A117. <https://doi.org/10.1051/0004-6361/201526462>
- Bikos, K. (2019). *Altitude & Azimuth: The Horizontal Coordinate System*.
<https://www.timeanddate.com/astronomy/horizontal-coordinate-system.html>
- Chih-Hao, L., Benedick, A. J., Fendel, P., Glenday, A. G., Kaertner, F. X., Phillips, D. F., Sassellov, D., Szentgyorgyi, A., & Walsworth, R. L. (2008). A laser frequency comb that enables radial velocity measurements with a precision of 1 cm s^{-1} . In. Ithaca: Cornell University Library, arXiv.org.
- Climate Data Online*. <https://www.ncei.noaa.gov/cdo-web/>
- Desk, E. T. R. (2021). *Microprocessor vs Microcontroller: What is the difference?*
<https://www.eletimes.com/microprocessor-vs-microcontroller-what-is-the-difference>
- Ferdaus, R., Mohammed, M. A., Rahman, S., Salehin, S., & Mannan, M. (2014). Energy Efficient Hybrid Dual Axis Solar Tracking System. *Journal of Renewable Energy*, 2014.
<https://doi.org/10.1155/2014/629717>
- Forecast Process*. <https://www.weather.gov/about/forecast-process>
- The Forecast Process - Forecasting the Future*.
<https://www.weather.gov/rah/virtualtourforecast>
- Fortier, T., & Baumann, E. (2019). 20 years of developments in optical frequency comb technology and applications. *Communications Physics*, 2(1).
<https://doi.org/10.1038/s42005-019-0249-y>
- The Future of*
- Industrial-Grade Edge AI*. <https://www.nvidia.com/en-us/autonomous-machines/embedded-systems/jetson-orin/>

- Hafez, A. Z., Yousef, A. M., & Harag, N. M. (2018). Solar tracking systems: Technologies and trackers drive types – A review. *Renewable and Sustainable Energy Reviews*, 91, 754-782. <https://doi.org/https://doi.org/10.1016/j.rser.2018.03.094>
- IEC 62471:2006 | IEC Webstore. (2006). <https://webstore.iec.ch/publication/7076>
- Jamroen, C., Komkum, P., Kohsri, S., Himananto, W., Panupintu, S., & Unkat, S. (2020). A low-cost dual-axis solar tracking system based on digital logic design: Design and implementation. *Sustainable Energy Technologies and Assessments*, 37, 100618. <https://doi.org/https://doi.org/10.1016/j.seta.2019.100618>
- Kalogirou, S. A. (1996). Design and construction of a one-axis sun-tracking system. *Solar Energy*, 57(6), 465-469. [https://doi.org/https://doi.org/10.1016/S0038-092X\(96\)00135-1](https://doi.org/https://doi.org/10.1016/S0038-092X(96)00135-1)
- Khalifa, A.-J. N., & Al-Mutawalli, S. S. (1998). Effect of two-axis sun tracking on the performance of compound parabolic concentrators. *Energy Conversion and Management*, 39(10), 1073-1079. [https://doi.org/https://doi.org/10.1016/S0196-8904\(97\)10020-6](https://doi.org/https://doi.org/10.1016/S0196-8904(97)10020-6)
- Lheureux, A. (2023). *Weather forecast using LSTM networks*. <https://blog.paperspace.com/weather-forecast-using-lstm-networks/>
- Lovis, C., & Pepe, F. (2007). A new list of thorium and argon spectral lines in the visible. *Astronomy & Astrophysics*, 468(3), 1115-1121. <https://doi.org/10.1051/0004-6361:20077249>
- Malav, S., & Vadhera, S. (2015, 12-13 June 2015). Hardware implementation of solar tracking system using a stepper motor. 2015 International Conference on Energy, Power and Environment: Towards Sustainable Growth (ICEPE),
- McCracken, R. A., Charsley, J. M., & Reid, D. T. (2017). A decade of astrocombs: recent advances in frequency combs for astronomy [Invited]. *Optics Express*, 25(13), 15058. <https://doi.org/10.1364/oe.25.015058>
- Mpodi, E. K., Tjiparuro, Z., & Matsebe, O. (2019). Review of dual axis solar tracking and development of its functional model. *Procedia Manufacturing*, 35, 580-588. <https://doi.org/https://doi.org/10.1016/j.promfg.2019.05.082>
- Nsengiyumva, W., Chen, S. G., Hu, L., & Chen, X. (2018). Recent advancements and challenges in Solar Tracking Systems (STS): A review. *Renewable and Sustainable Energy Reviews*, 81, 250-279. <https://doi.org/https://doi.org/10.1016/j.rser.2017.06.085>
- NVIDIA Jetson. <https://www.nvidia.com/en-us/autonomous-machines/embedded-systems/>
- Picqué, N., & Hänsch, T. W. (2019). Frequency comb spectroscopy. *Nature Photonics*, 13(3), 146-157. <https://doi.org/10.1038/s41566-018-0347-5>
- Poulek, V. (1994, 5-9 Dec. 1994). Testing the new solar tracker with shape memory alloy actors. Proceedings of 1994 IEEE 1st World Conference on Photovoltaic Energy Conversion - WCPEC (A Joint Conference of PVSC, PVSEC and PSEC),
- Raspberry Pi 4 Tech Specs.** <https://www.raspberrypi.com/products/raspberry-pi-4-model-b/specifications/>
- Raspberry Pi Zero 2 W.** <https://www.raspberrypi.com/products/raspberry-pi-zero-2-w/>
- Rumala, S.-S. N. (1986). A shadow method for automatic tracking. *Solar Energy*, 37(3), 245-247. [https://doi.org/https://doi.org/10.1016/0038-092X\(86\)90081-2](https://doi.org/https://doi.org/10.1016/0038-092X(86)90081-2)
- Sarmiento, L. F., Reiners, A., Huke, P., Bauer, F. F., Guenter, E. W., Seemann, U., & Wolter, U. (2018). Comparing the emission spectra of U and Th hollow cathode lamps and a new U line list. *Astronomy & Astrophysics*, 618, A118. <https://doi.org/10.1051/0004-6361/201832871>

- Saxena, S. (2021). *Learn About Long Short-Term Memory (LSTM) Algorithms*.
<https://www.analyticsvidhya.com/blog/2021/03/introduction-to-long-short-term-memory-lstm/>
- Schroeder, D. V. (2010-2011). *Understanding Astronomy: The Sun and the Seasons (website)*.
<https://physics.weber.edu/schroeder/ua/sunandseasons.html>
- Schwab, C., St, xfc, rmer, J., Gurevich, Y. V., xfc, hrer, T., Lamoreaux, S. K., Walther, T., & Quirrenbach, A. (2015). Stabilizing a Fabry–Perot Etalon Peak to 3 cm s⁻¹ for Spectrograph Calibration. *Publications of the Astronomical Society of the Pacific*, 127(955), 880-889. <https://doi.org/10.1086/682879>
- Sharapov, R. V. (2022). *Using Linear Regression for Weather Prediction 2022 Wave Electronics and its Application in Information and Telecommunication Systems (WECONF)*, St. Petersburg, Russian Federation.
<https://ieeexplore.ieee.org/document/9803493/references#references>
- Singh Chauhan, N.** (2022). Naïve Bayes Algorithm: Everything You Need to Know. In.
- Smith, D. (2023). Calculating the Emission Spectra from Common Light Sources. *COMSOL*.
<https://www.comsol.com/blogs/calculating-the-emission-spectra-from-common-light-sources/>
- System-on-Modules (SOMs): How and Why to Use Them*.
<https://www.xilinx.com/products/som/what-is-a-som.html>
- System on Module VS Single Board Computer. In.
- Understanding Surface Quality Specifications | Edmund Optics*. (2023).
<https://www.edmundoptics.com/knowledge-center/application-notes/lasers/understanding-surface-quality-specifications/>
- What are Naïve Bayes classifiers? <https://www.ibm.com/topics/naive-bayes>
- What are single-board computers? <https://www.baesystems.com/en-us/definition/what-are-single-board-computers>
- What is a Decision Tree? <https://www.ibm.com/topics/decision-trees>
- What is a System on Chip (SoC)? <https://anysilicon.com/what-is-a-system-on-chip-soc/>
- What is linear regression? <https://www.ibm.com/topics/linear-regression>
- What is machine learning? <https://www.ibm.com/topics/machine-learning>
- What is the k-nearest neighbors algorithm? <https://www.ibm.com/topics/knn>
- Wikipedia, T. F. E. (2023). *Position of the Sun*.
https://en.wikipedia.org/w/index.php?title=Position_of_the_Sun&oldid=1148157103
- Zogbi, R., & Laplaze, D. (1984). Design and construction of a sun tracker. *Solar Energy*, 33(3), 369-372. [https://doi.org/https://doi.org/10.1016/0038-092X\(84\)90168-3](https://doi.org/https://doi.org/10.1016/0038-092X(84)90168-3)
-